

**SBORNÍK GEOLOGICKÝCH VĚD
JOURNAL OF GEOLOGICAL SCIENCES**

ANTROPOZOIKUM • ANTHROPOZOIC

25



CZECH GEOLOGICAL SURVEY
PRAGUE 2004

Scientific editor

RNDr. Jaroslav Tyráček, CSc.

The discussion on this volume was held at the advisory committee meeting convened by the scientific editor on November 29, 2002

CONTENTS – OBSAH

DAGMAR MINAŘÍKOVÁ

Quaternary palaeogeography of the northern part of Mesopotamia 5

Paleogeografie kvartéru severní části Mezopotámie 20

JIŘÍ CHLACHULA – GERMAN I. MEDVEDEV – GALINA A. VOROBYOVA

Palaeolithic occupation in the Angara region, East Central Siberia, in the context of Pleistocene climate change 31

Pleistocenní klima a paleolit v údolí Angary ve východní části střední Sibiře 48

Journal of Geological Sciences	Anthropozoic 25	Pages 5–30	17 figs.	8 tabs.	– pl.	Czech Geological Survey Prague 2004	ISBN 80-7075-613-6 ISSN 0036-5270
-----------------------------------	--------------------	---------------	-------------	------------	----------	----------------------------------------	--------------------------------------

Quaternary palaeogeography of the northern part of Mesopotamia

Paleogeografie kvartéru severní části Mezopotámie

DAGMAR MINAŘÍKOVÁ[†]

Received January 24, 2003

Key words: Iraq, Mesopotamian Plain, Quaternary, heavy minerals, stratigraphy, palaeogeography

MINAŘÍKOVÁ, D. (2004): Quaternary palaeogeography of the northern part of Mesopotamia. – Sbor. geol. Věd, Anthropozoikum, 25, 5–30. Praha.

Abstract: The sedimentological research described in this paper was carried out during the years 1978 and 1979. About 300 samples from shallow and deeper boreholes drilled into the sediments of the Adhaim, Diyala, Tigris, and Euphrates rivers, the Zagros Foothill zone, and the Mahmudia Formation were analysed. The analysis of heavy minerals was found to be the most functional method for distinguishing and interpreting the provenance, origin, and age of these sediments. Furthermore, the degree of corrosion of pyroxene and amphibole grains was studied in the interest of defining criteria for relative age determination. The area covered by the sediments of the Tigris, Euphrates, and Diyala rivers experienced complicated development accompanied by considerable hydrographical changes. In deep boreholes (DBH) Nos. 4 and 5, three units of the Tigris River sediments were distinguished: the “young” Tigris (Holocene to Upper Pleistocene), the “older” Tigris (Middle Pleistocene), and the “oldest” Tigris, all of which differ in the degree of corrosion of their pyroxenes and amphiboles. During the Pleistocene, the Diyala River deposited its sediments to the east of its current course. The author supposes that all rivers in the northern part of Mesopotamia migrated west and south-west during the Pleistocene and Holocene. This was probably caused by the uplift of the Zagros Mountains.

Karlovo náměstí 48, 674 01 Třebíč, Czech Republic

Introduction

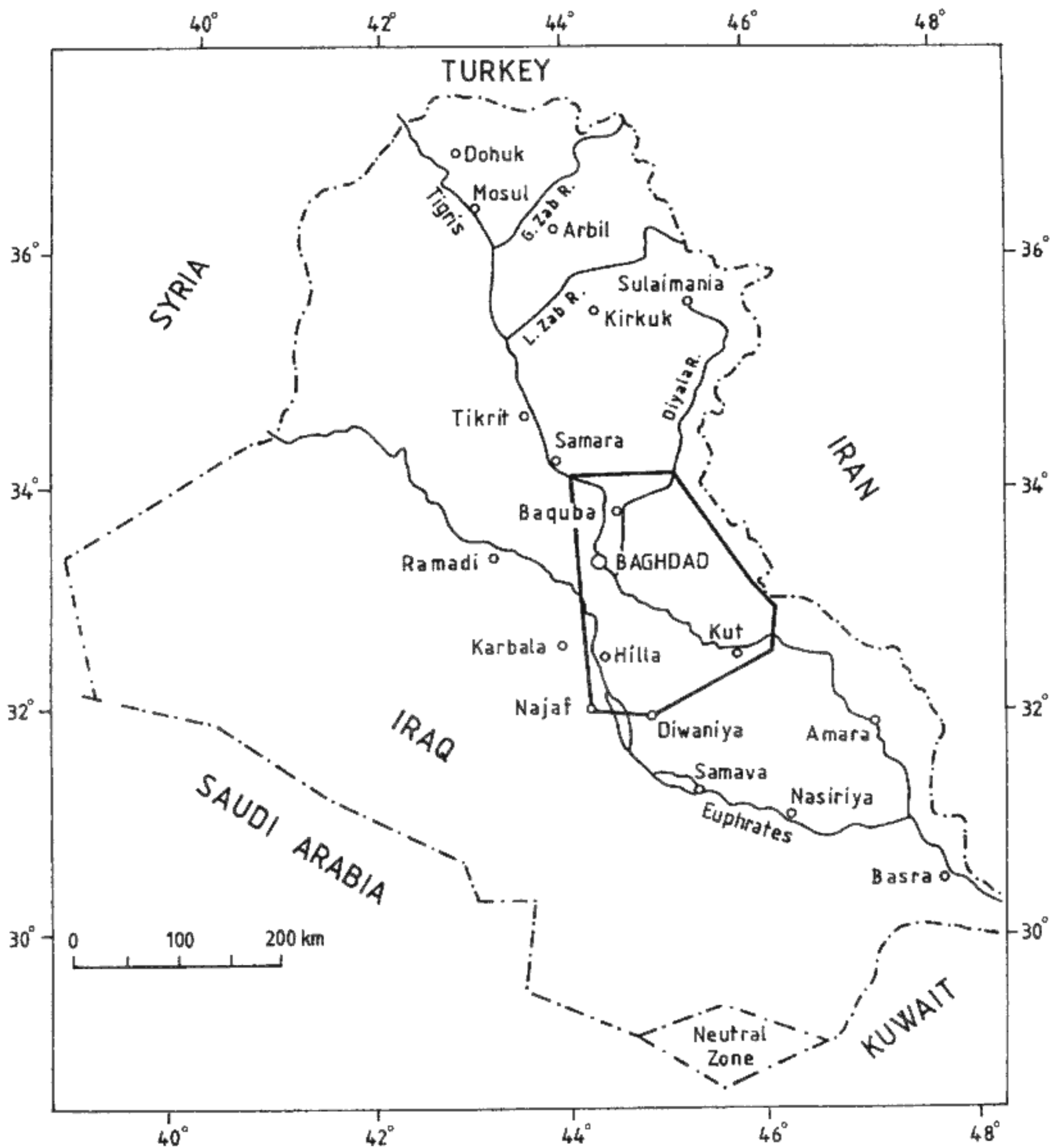
Geological mapping was undertaken during the years 1977 and 1978 in the northern part of the Mesopotamian Plain by the State Organization for Minerals (SOM) in Baghdad. The extent of the area is shown in Figure 1. More than 100 shallow and deeper boreholes were drilled in this area. With few exceptions, the majority of the boreholes were situated on profile lines (see Figure 2).

The sedimentological research was carried out in 1978 and 1979, during which we performed grain-size analysis, and examined the petrology of the sand, gravel, and heavy mineral fractions. The composition of the heavy fraction (about 300 samples) distinguishes the sediments of different provenances. The most important clastic constituents for distinguishing the sediments of the Mesopotamian Plain were found to be the altered minerals, rock fragments, common and brownish amphibole, monoclinic pyroxene (particularly titanite), garnet, and, in some cases, opaque minerals. Furthermore, the degree of corrosion of the pyroxene and amphibole grains was studied. Due to significant differences in the degree of corrosion of these minerals, we were able to define certain criteria for differentiating the Upper Pleistocene, older Quaternary, and pre-Quaternary deposits.

Several authors, especially PHILIP (1968) and ALI (1977), have studied the heavy minerals of the northern part of Mesopotamia. Both of the above-mentioned au-

thors investigated HMs particularly in the recent sediments of the Mesopotamian rivers. More recently, DOMAS, MINAŘÍKOVÁ, and SABAH (1984) presented a “Proposal on the Introduction of the Mahmudia Formation” at the Seventh Iraqi Geological Congress in 1984. According to these studies, a distinct sequence has been recognized in some boreholes in the northern part of Mesopotamia, which differs in heavy mineral content and degree of mineral corrosion from the deposits of the Tigris, Euphrates, and Diyala rivers. With respect to its sedimentological and stratigraphical position, the name Mahmudia Formation was recommended for this sequence. Some beds of finer deposits within this sequence are rich in microfossils, particularly Ostracods (as determined by Wijdan al Haddad, S.O.M.). The main Ostracod genera found in this formation are *Candona*, *Cyprideis*, *Cypronotus*, *Ilyocypris*, *Darwinulla*, and *Lymnocythere*.

Moreover, some Ostracod species typical of Pliocene and Quaternary deposits were recognized. For the Pliocene, these include *Candona* cf. *balatonica* (DADAY), *Darwinulla dadayi* NEMES, *Candona* cf. *elegans* NEMES; while the Quaternary species include *Candona* cf. *neglecta* SARRIS, *Candona* cf. *sucki* HARTWIG, *Candona* cf. *angulata* MÜLLER. It can be concluded from this list that the Tertiary/Quaternary boundary lies within the Mahmudia Formation. The sediments of the Mahmudia Formation were deposited mainly by rivers, and partly in lakes whose salinity oscillated from fresh to brackish. The differences in the heavy mineral content within the



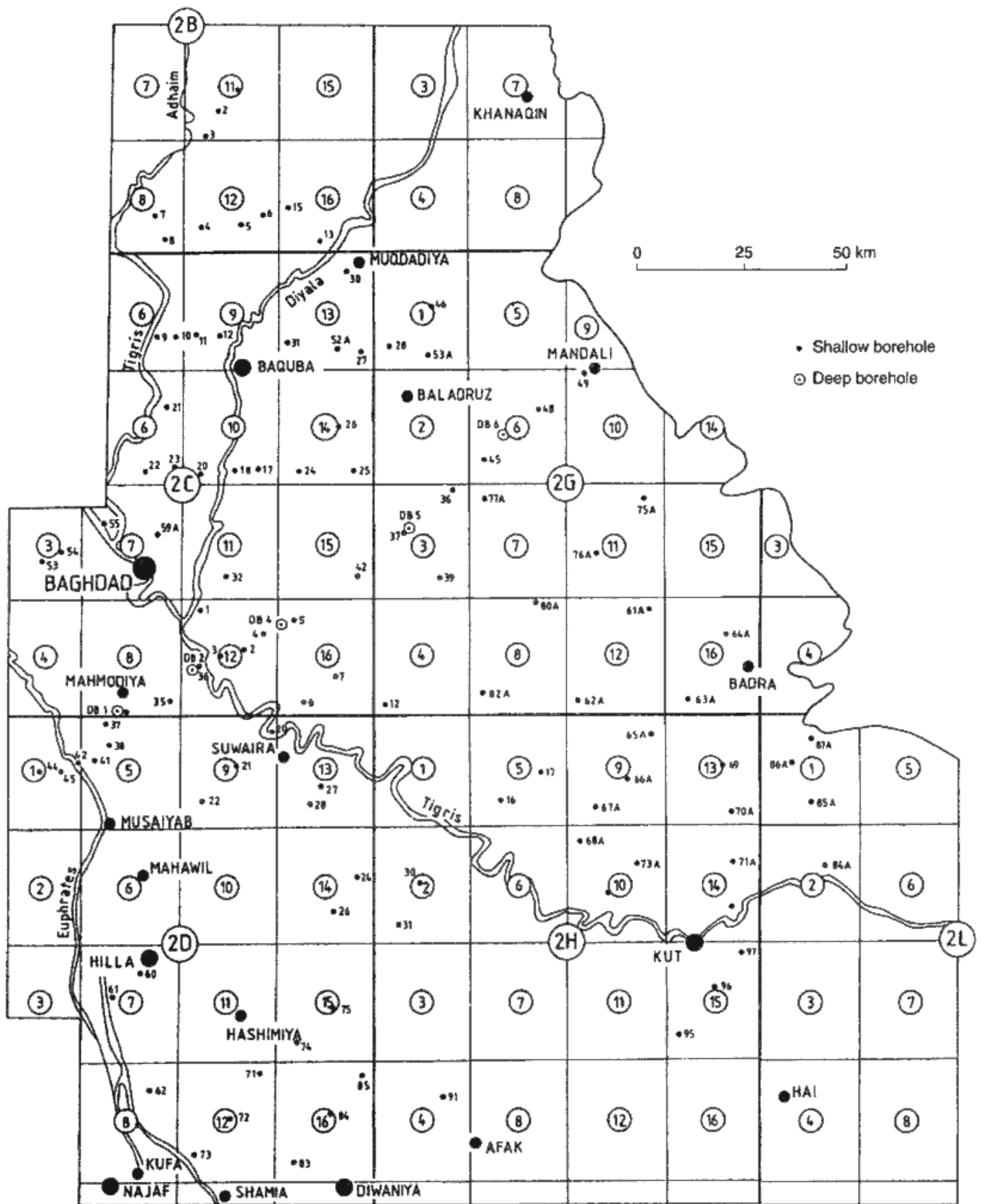
1. Map of the study area.

formation reveal that the influx of desert material was typical for the western part, whereas the clastic material to the eastern part was supplied from the Zagros and younger uplifted structures. The clastic material of the central part was introduced by rivers from more remote areas. The proposed Mahmudia Formation overlies the Pliocene fluvial sediments and underlies the Pleistocene sediments of the Euphrates and Tigris rivers. Its deposition began in an arid Pliocene climate and ended during the first pluvial oscillations of the Pleistocene. Boundaries with the underlying and overlying beds are conformable, and are marked by the specific composition of

the heavy mineral fraction and by the profound corrosion of pyroxenes, amphiboles, and garnets.

Heavy minerals (HM)

For separating the heavy mineral fraction, bromoform and magnetic separation techniques were used. The quantitative composition of the heavy fraction was determined by the study of samples mounted in Canadian Balsam. The total content of the heavy fraction (in weight %) was found to be important for distinguishing



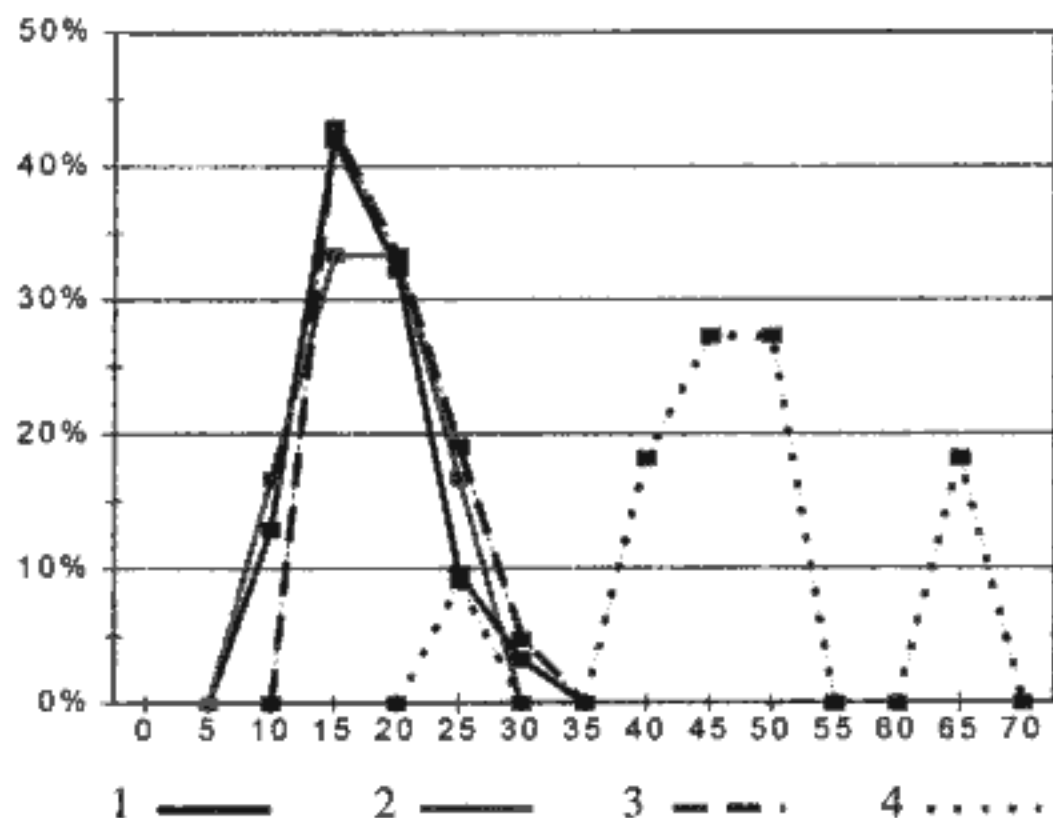
2. Location of boreholes according to coordinates.

between the sediments of the Diyala and Tigris rivers. Low heavy mineral contents were observed in the Zagros foothill sediments and in the Diyala and Adhaim river deposits. The results of these analyses are presented in Tables 1–8 on pages 22–30 (in Tables 1–7 are

shallow boreholes – SBH, and in Table 8 is a deeper borehole – DBH; MINAŘIKOVÁ 1978, 1979).

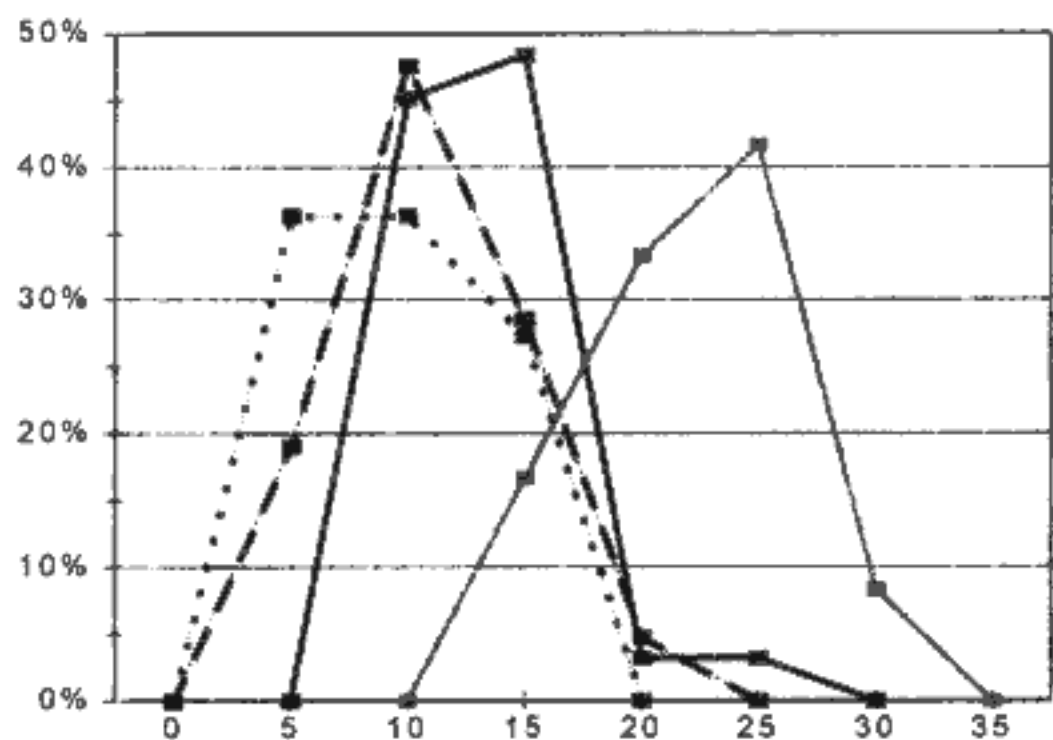
The magnetic fraction is comprised mainly of magnetite, with rare pyrrhotine and titanomagnetite. Relatively higher magnetic fraction contents were found in

opaque minerals



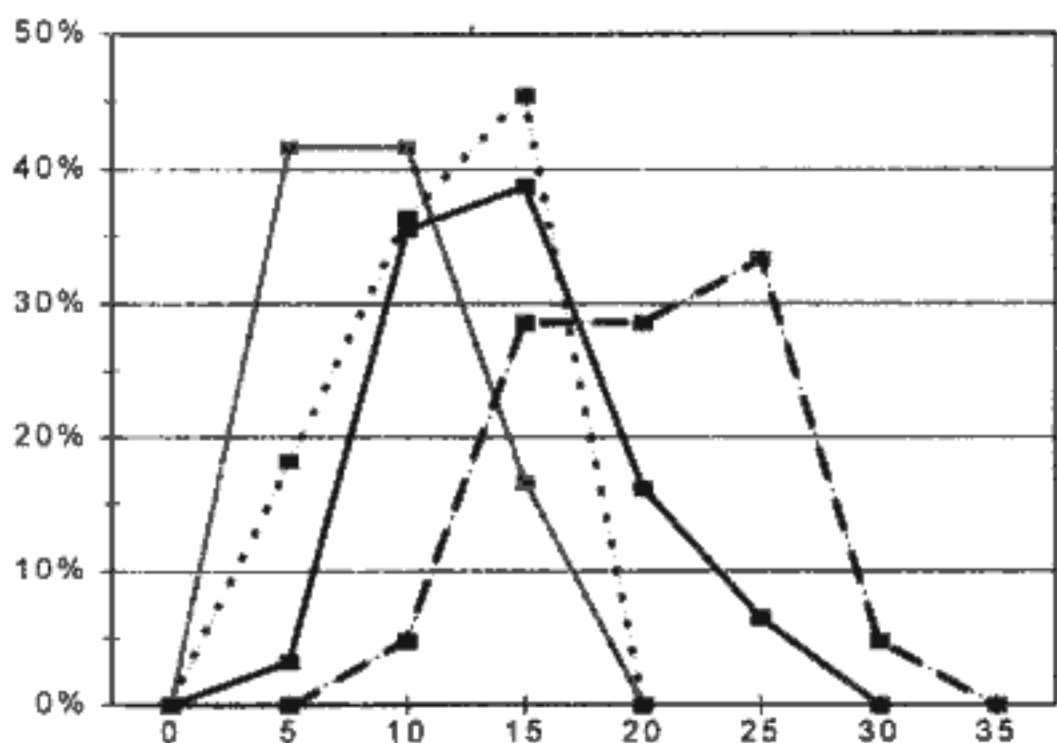
3. Relative frequency of opaque minerals. 1 - Tigris River deposits; 2 - Euphrates River deposits; 3 - Diyala River deposits; 4 - Foothill zone deposits.

clouded minerals



4. Relative frequency of clouded minerals. For explanations see Figure 3.

rock fragments



5. Relative frequency of rock fragments. For explanations see Figure 3.

the Diyala River sediments and the foothill deposits. Opaque minerals are represented mainly by limonite and ilmenite. Limonite usually predominates over ilmenite, while the opposite relation is rather exceptional. In many samples some of the ilmenite grains are covered with leucoxene and limonite. Hematite and pyrite are rare. Opaque minerals are abundant, especially in the foothill sediments, but most of them are authigenic. Figure 3 shows the distribution of opaque minerals in the sediments of the Tigris, Euphrates, and Diyala rivers and the foothill zone.

All minerals that were not amenable to reliable determination are included under clouded minerals. They seem to be strongly weathered minerals of the zoisite-epidote group, with a minor proportion of amphiboles. Their content is important for distinguishing between the sediments of the Tigris and Euphrates rivers (see Figure 4).

Most of the rock fragments found in the heavy fraction contain minerals of the zoisite-epidote group, green schist, amphibolite, and basic igneous rocks. They are usually altered and weathered. Such rock fragments are present mainly in sediments of the Adhaim and the Diyala, less in the Tigris and Foothill zone deposits. The Euphrates River sediments contain a smaller proportion of rock fragments (see Figure 5).

Minerals of the zoisite-epidote group include epidote, clinozoisite, and zoisite; piemontite is rare. They are often partly altered. These minerals are plentiful in the Adhaim River sediments (see Table 1), but occur less frequently in deposits of the other rivers and the Foothill zone (see Figure 6).

Common amphibole includes several varieties that differ in colour and intensity of pleochroism. A greyish-green variety with mild pleochroism is the most common. Varieties of an intense green colour are rare. Amphibole is more abundant in the Tigris sediments than in those of Euphrates and Diyala (see Figure 7), and is rare in the Adhaim and Foothill deposits (see Tables 1-8). The brownish amphibole is mostly basaltic amphibole, but sometimes common amphibole. Tremolite-actinolite is not rare but it is a minor accessory mineral.

Orthopyroxenes include an isomorphous series of enstatite, bronzite, and hypersthene. Their total content is low, but they show significant differences among the different provinces. The highest proportion of orthopyroxenes was found in the Diyala deposits, and somewhat less in the Tigris and Euphrates deposits. The foothill sediments, and especially the Adhaim River sediments, contain a very minor orthopyroxene fraction (see Tables 1-8). Monoclinic pyroxenes found in these sediments include nonpleochroic, light green diopside augite, and smaller proportions of a greener, pleochroic augite. Titanaugite was found particularly in the Diyala River deposits, while in the Tigris and Euphrates sediments it is a common but minor mineral. The Foothill zone and Adhaim River deposits contain very minor

fractions of this mineral(see Tables 1–8). Titanaugite is typically brown-violet and pleochroic. The relative frequency diagram in Figure 8 shows the distribution of augite and titanaugite together. Whitish pyroxenes present in these sediments are grains of diopside.

The garnet found in these sediments is commonly light pink, sometimes colourless, rarely yellow or brown. Most of the grains have irregular shapes, but some idiomorphic crystals do occur. The relative frequency of garnet in the studied sediments is shown in Figure 9.

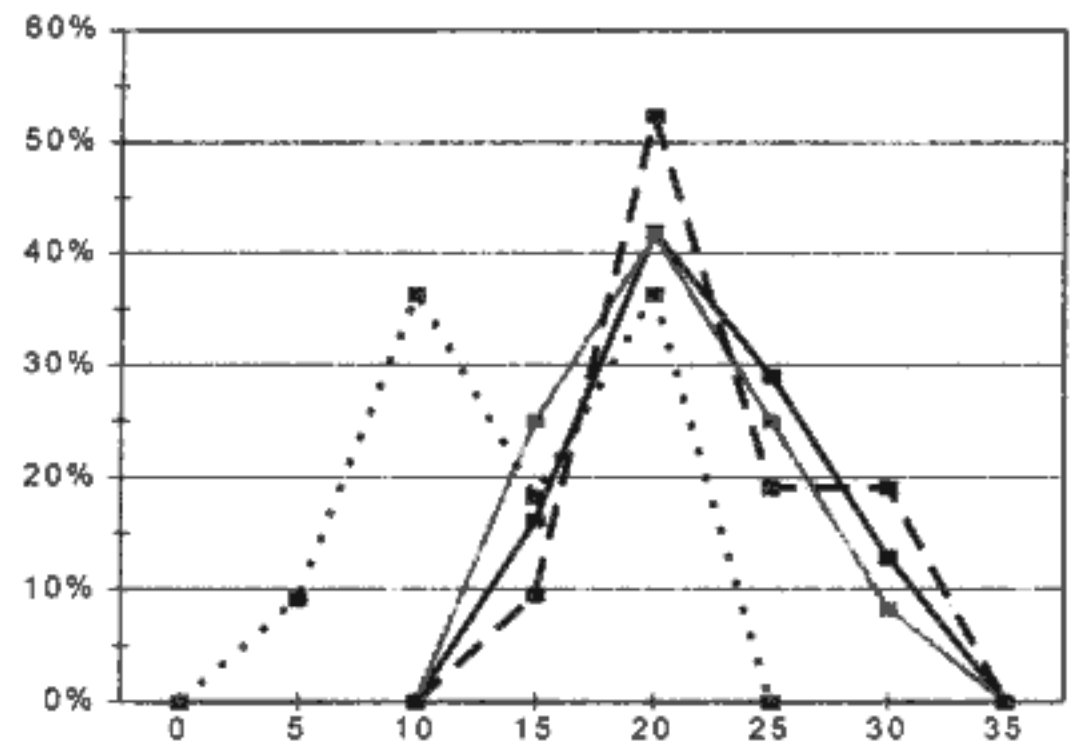
Rare minerals include rutile, zircon, tourmaline, titanite, andalusite, sillimanite, kyanite, staurolite, and chromite. Titanite, chromite, and tourmaline were found mainly in the Diyala River sediments. The Tigris River deposits contain the same rare minerals, with the addition of chromite. The Euphrates River sediments have a slightly higher content of metamorphic minerals than those of the Tigris. The Foothill zone and the Adhaim River deposits contain more rutile, zircon, and chromite, and less sillimanite and staurolite (see Tables 1–8).

The mica minerals of these sediments are mainly chlorite, with less biotite. The quantity of chlorite was found to depend on grain-size distribution, as it is more common in very fine-grained deposits. Minerals of the barite-celestite isomorphous mixture are of authigenic origin, and were found particularly in the Foothill and the Adhaim River sediments, in which they are relatively common (see Tables 1–8). Very rare minerals in these sediments include spinel, monazite, xenotime, corundum, and topaz.

From this review it is clear that the quantity of clouded minerals, rock fragments, common amphibole, monoclinic pyroxenes (including titanaugite) and garnet are very important for distinguishing the sediments of different rivers and formations. To illustrate these differences, a triangle diagram representing clouded minerals, rock fragments, and common amphibole has been constructed (see Figure 10). This diagram shows the relatively poor separation of the fields of the Tigris and Euphrates rivers sediments in contrast to the distinct fields of the Diyala River and Foothill deposits.

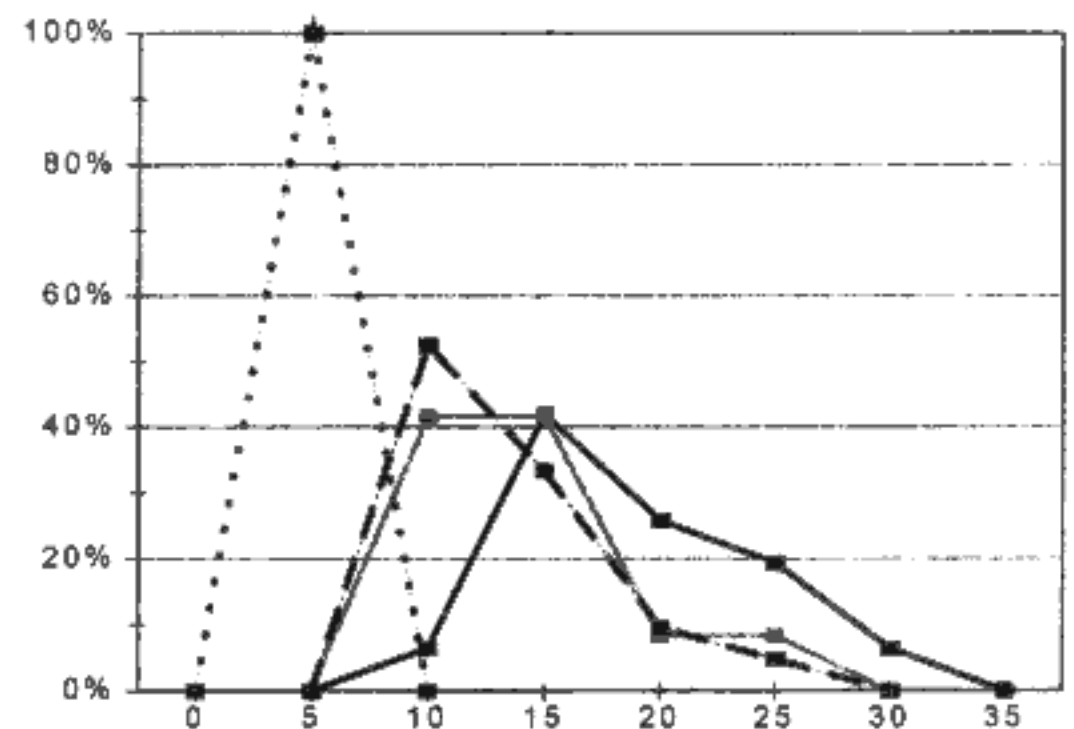
In addition, the degree of corrosion of mineral grains was used for distinguishing sediments of different ages. Corrosion is apparent mainly in pyroxenes, less in amphiboles and garnet. In the Holocene and Upper Pleistocene sediments, only the pyroxene grains are weakly corroded. Stronger pyroxene corrosion, and partial corrosion of amphiboles, was found in the Middle Pleistocene deposits of the Diyala and Tigris rivers. Pyroxenes are strongly corroded in the sediments of the Mahmudia Formation, in which corrosion features on amphibole (common and brownish) and garnet grains is also clearly seen. Mineral corrosion was found to be more extensive in the pre-Quaternary sediments.

zoisite-epidote group



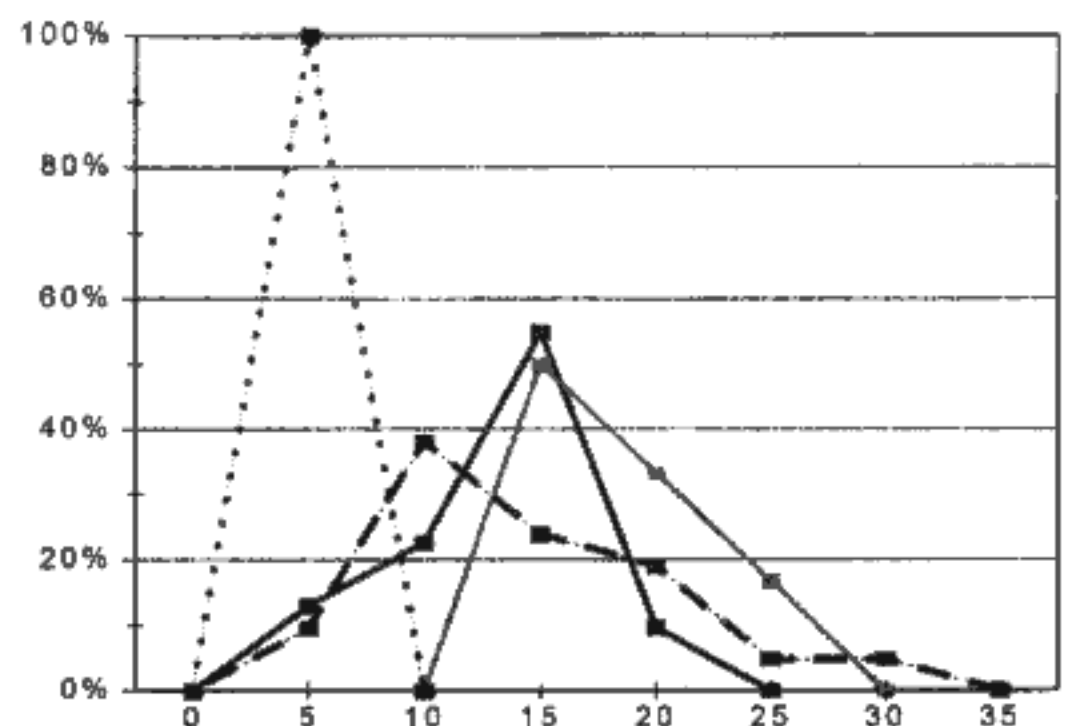
6. Relative frequency of minerals of zoisite-epidote group. For explanations see Figure 3.

common amphibole

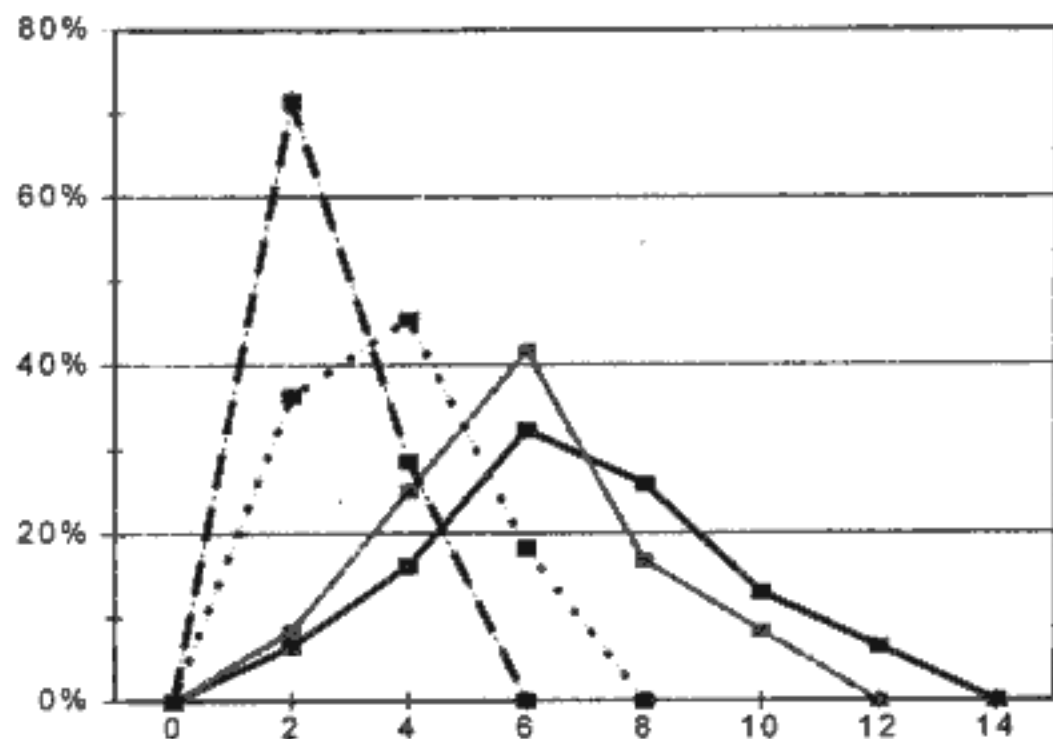


7. Relative frequency of common amphibole. For explanations see Figure 3.

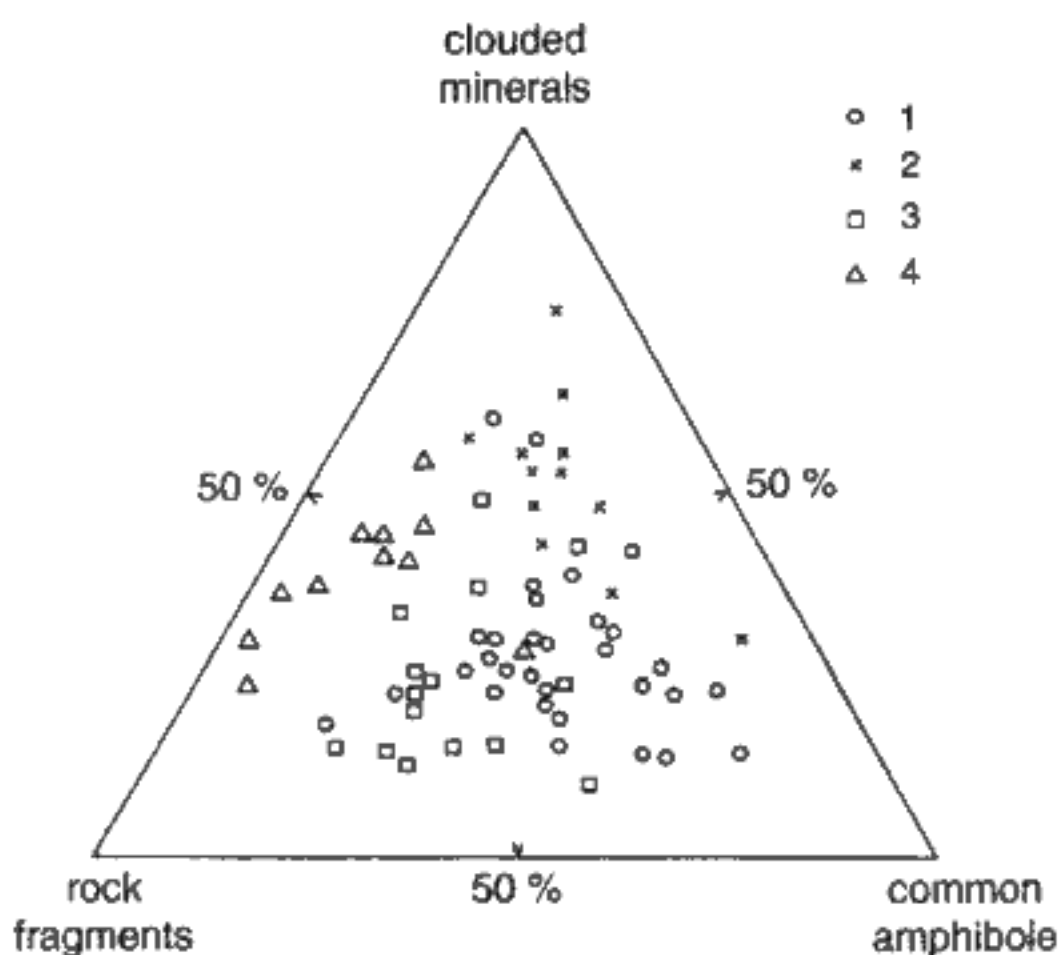
augite + titanaugite



garnet



9. Relative frequency of garnet. For explanations see Figure 3.



10. Triangle diagram showing the contents of clouded minerals, rock fragments and common amphibole. 1 – Tigris River deposits; 2 – Euphrates River deposits; 3 – Diyala River deposits; 4 – Foothill zone deposits.

Description of the sediments from the deeper boreholes (DBH)

In the year 1978, five deeper boreholes were drilled into the Mesopotamian Plain. These boreholes were arranged in a SW-NE trending profile between Mahmudia and Mandali (see Figure 2). The main goals of investigating the DBH sediments were:

1. to locate a boundary between Quaternary and pre-Quaternary deposits;
2. to distinguish between the sediments of individual rivers; and,
3. to determine relative age of the Quaternary deposits.

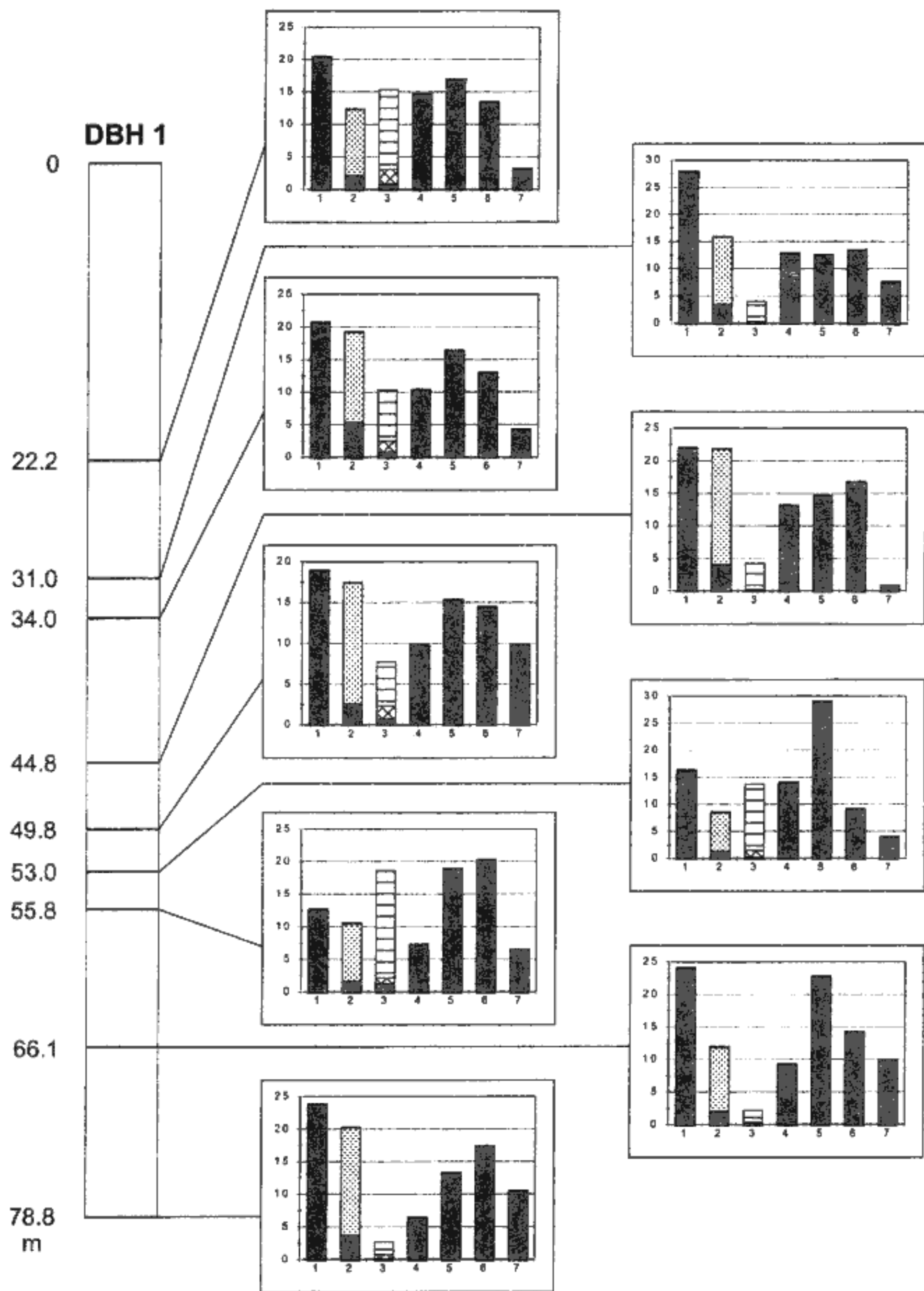
DBH 1 was situated due south of Mahmudia (see Figure 2). The HM composition of these sediments is shown in Table 8 and Figure 11.

Sample No. 1 (22.05–22.20 m) is a fine-grained sand, relatively well sorted and containing only about 5 % of silt and clay particles. Quartz predominates in the < 0.354 mm fraction; rock fragments comprise about 20 %. The coarser fractions are comprised mainly of rock fragments, mostly of chert, with smaller proportions of sandstone, siltstone, carbonates and quartzite. The quartz grains range from being rounded to well rounded in the > 0.5 mm fraction, whereas they are subangular and subrounded in finer fractions. The HM composition shows that the sand is a mixture of Tigris and Euphrates deposits. Sample No. 2 (30.9–31.0 m) contains a significant admixture of silt and clay particles. The composition and degree of roundness of its sandy fraction is similar to that of sample No. 1. The HM fraction of sample No. 2 has a very low pyroxene content, and is of a similar composition to that of the Mahmudia Formation deposits. The author supposes that sample No. 2 represents redeposited sediments of the Mahmudia Formation. In sample No. 3 (33.95–34.05 m) the > 0.354 mm fraction contains mostly mica minerals. Finer fractions are composed of quartz and rock fragments, with minor feldspar. The composition of the heavy mineral fraction shows that it is mixture of the Tigris and Euphrates River deposits. Sample No. 4 is a mixture of sand, silt, and clay, with a small admixture of pebbles, and contains the same rock types as in the overlying beds. It can be concluded that sample No. 4 also represents redeposited sediment from the Mahmudia Formation. The HM composition of sample No. 5 (49.6–49.8 m) indicates that it is a mixture of the Tigris and Euphrates deposits. The heavy mineral fraction of sample No. 6 (52.8–53.0 m) is characterized by a high content of clouded minerals, indicative of the Euphrates River provenance. The heavy mineral fraction of sample No. 7 (55.7–55.8 m) shows that this sediment was deposited by the Euphrates River. However, there are significant differences in the degree of corrosion of some minerals in comparison with those in the overlying beds. The pyroxene grains of sample No. 7 are more strongly corroded, while corrosion textures are also present on amphibole grains. Based on the relative degree of corrosion, it is suggested that these sediments represent an “older Euphrates”.

Samples No. 8 (65.9–66.1 m) and No. 52 (78.75–78.85 m) have the same composition as the sediments of the Mahmudia Formation in this area. Their HMs are weathered, their amphibole and garnet are corroded, and their pyroxene is strongly corroded. All of these features place these sediments in the Mahmudia Formation.

Samples 1–6 correspond to Upper Pleistocene, while sample No. 7 could be of Middle Pleistocene age.

DBH 2 was situated on the right bank of the Tigris River (see Figure 2). Its heavy fraction composition is shown in Table 8, for histograms of the main minerals see Figure 12. The upper part of the sequence is comprised of Tigris River sediments, with local admixtures of Euphrates River deposits (sample No. 6 – 28.1–28.3 m). Euphra-

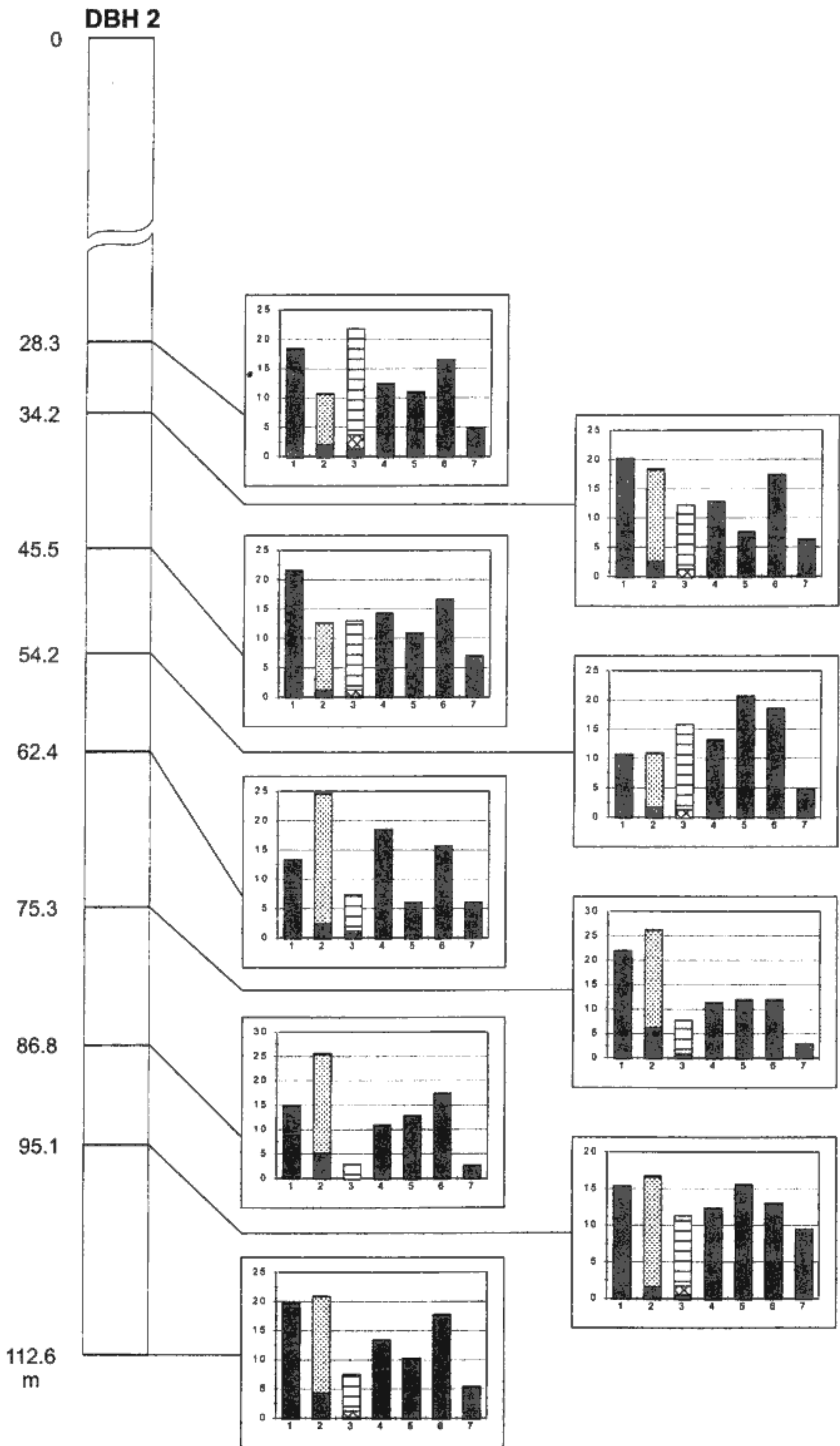


11. Histograms of the main HM in sediments of DBH No. 1. 1 – minerals of the zoisite-epidote group; 2 – amphibole group (lower part of the column – brownish amphibole, upper part – common amphibole); 3 – pyroxene group (lower part – orthopyroxene, middle part – titan-augite, upper part – augite and diopside augite); 4 – rock fragments; 5 – clouded minerals; 6 – opaque minerals; 7 – garnet.

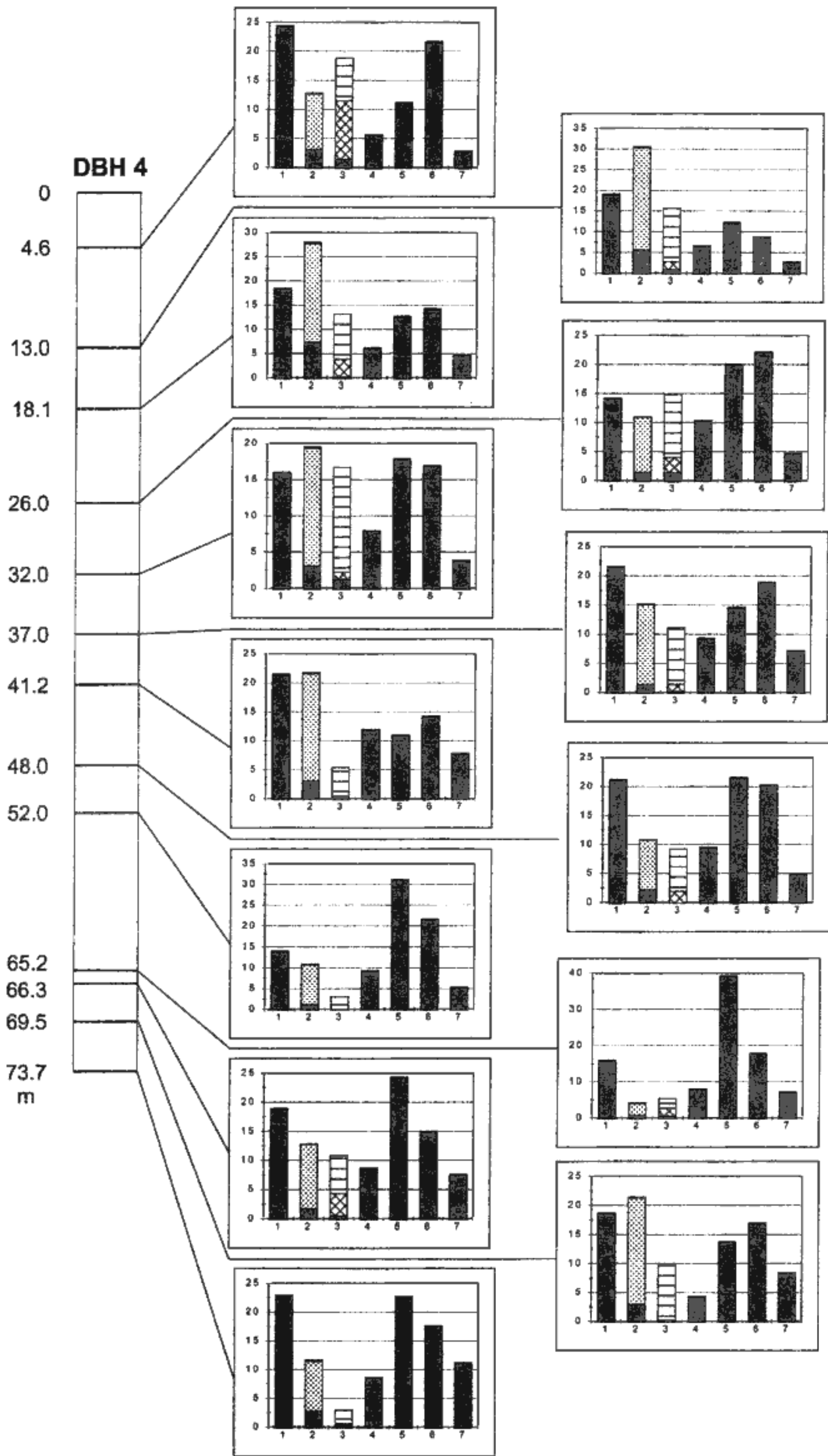
tes River deposits were found at a depth of more than 50 m (sample No. 9), which correspond to those evinced in DBH 1 at a depth of 53 m. In the next two samples (No. 10 – 62.2–62.4 m, and No. 11 – 75.0–75.3 m) the HM composition and the degree of corrosion are similar to those of the Mahmudia Formation deposits. Corroded grains of garnet and amphibole and strongly corroded pyroxenes were found in the last three samples (Nos. 18, 32

and 49). The author supposes that these sediments are pre-Quaternary.

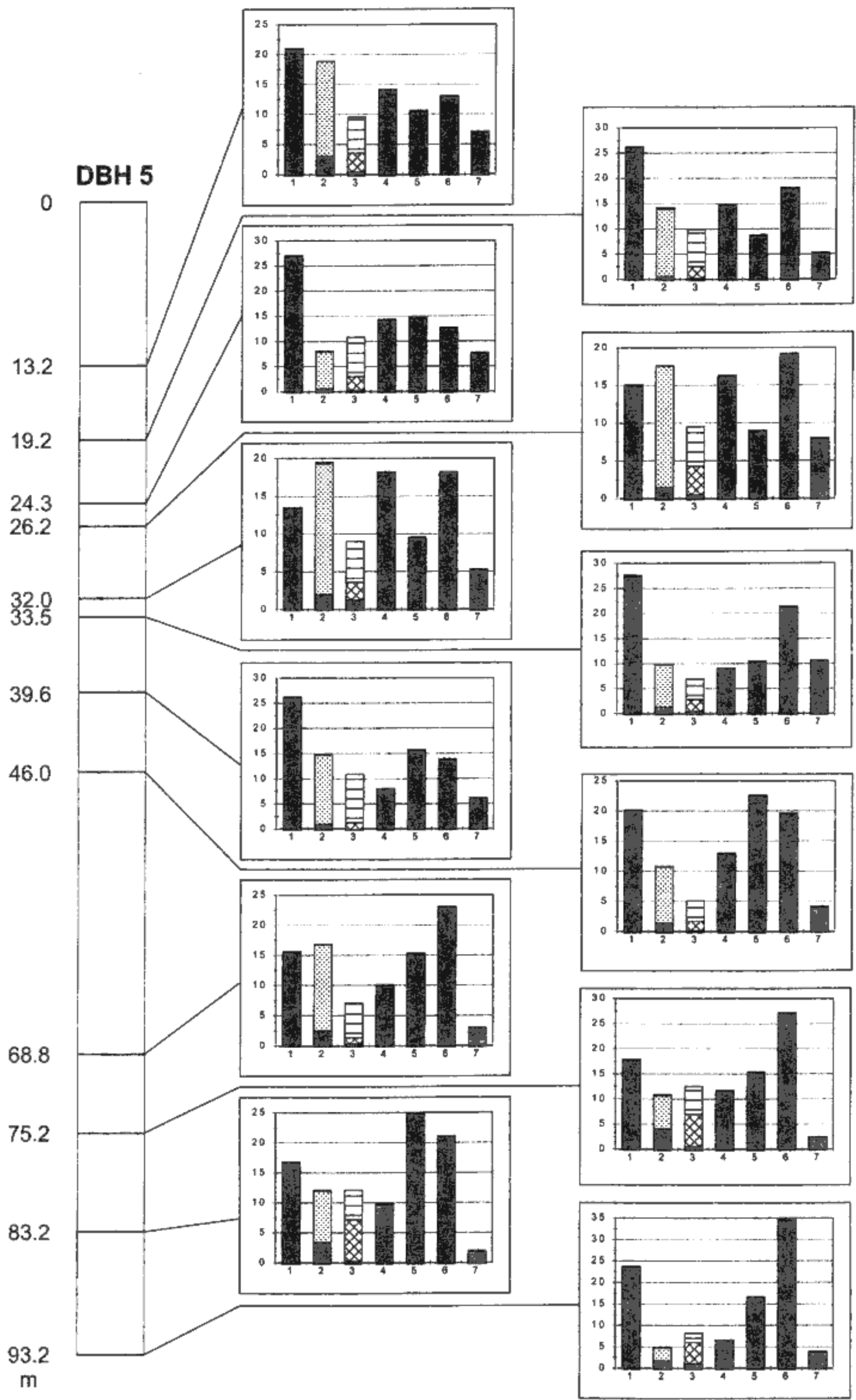
DBH 4 was situated in the NW margin of map sheet 2C16 (see Figure 2). The HM composition of this sample is shown in Table 8 and in the histograms in Figure 13. Sample No. 16 (4.5–4.6 m) represents the typical sediment of the Diyala River. Sample No. 17 (12.9–13.0 m) is a mixture of deposits from the Tigris and the Diyala



12. Histograms of the main HM in sediments of DBH No. 2. For explanations see Figure 11.



13. Histograms of the main HM in sediments of DBH No. 4. For explanations see Figure 11.



14. Histograms of the main HM in sediments of DBH No. 5. For explanations see Figure 11.

ivers. Samples 18, 19, and 20 (from a depth range of 18–32 m) have the same composition as the Tigris River sediments, although the degree of corrosion on pyroxene and amphibole grains is a little higher than in the Upper Pleistocene deposits. These sediments must therefore be older, and are thus referred to as “older” Tigris River sediments. Samples 21, 22, and 23 (from a depth range of 37–48 m) are characterized by pyroxene and amphibole with an even higher degree of corrosion. Their HM composition is similar to that of the Tigris River sediments. It is therefore concluded that these sediments were also deposited by the Tigris River. However, they are clearly older than the overlying beds at depths between 18–32 m, and thus we use the term “oldest Tigris River sediments” with reference to them. The next three samples, Nos. 24, 44, and 46 (in the depth of 52–66 m), represent sediments of the Mahmudia Formation. The last two samples, Nos. 54 and 55 (from a depth range of 69–74 m), correspond to the pre-Quaternary sediments with respect to their composition and degree of corrosion.

DBH 5 was situated near the centre of map sheet 2G3 (see Figure 2). This sample contained the same sediments as in DBH 4 (see Table 8 and Figure 14): i. e., the Upper Pleistocene „young Tigris“, the „older Tigris“ (at a depth of 19–32 m), and the „oldest Tigris“ (at 33–46 m). The age of the last two units of this sample cannot be exactly determined due to the absence of palaeontological evidence. The lower part of the borehole, below 68 m in depth, probably passed through the Mahmudia Formation.

DBH 6 was situated SW of Mandali (see Figure 2). Its HM composition is shown in Table 8. The first three samples (Nos. 8, 9, and 69, from depths between 21.4–49.2 m) represent Zagros Foothill zone deposits. High contents of opaque minerals and low contents of amphibole and pyroxene are typical of these sediments. Authigenic minerals of the barite-celestite group are present in all samples. The HM compositions of the remaining nine samples, from depths of 56.5 to 202.4 m, are very similar to those of the foothill deposits, but their pyroxene and amphibole grains are strongly corroded. We therefore suppose that these sediments are pre-Quaternary in age.

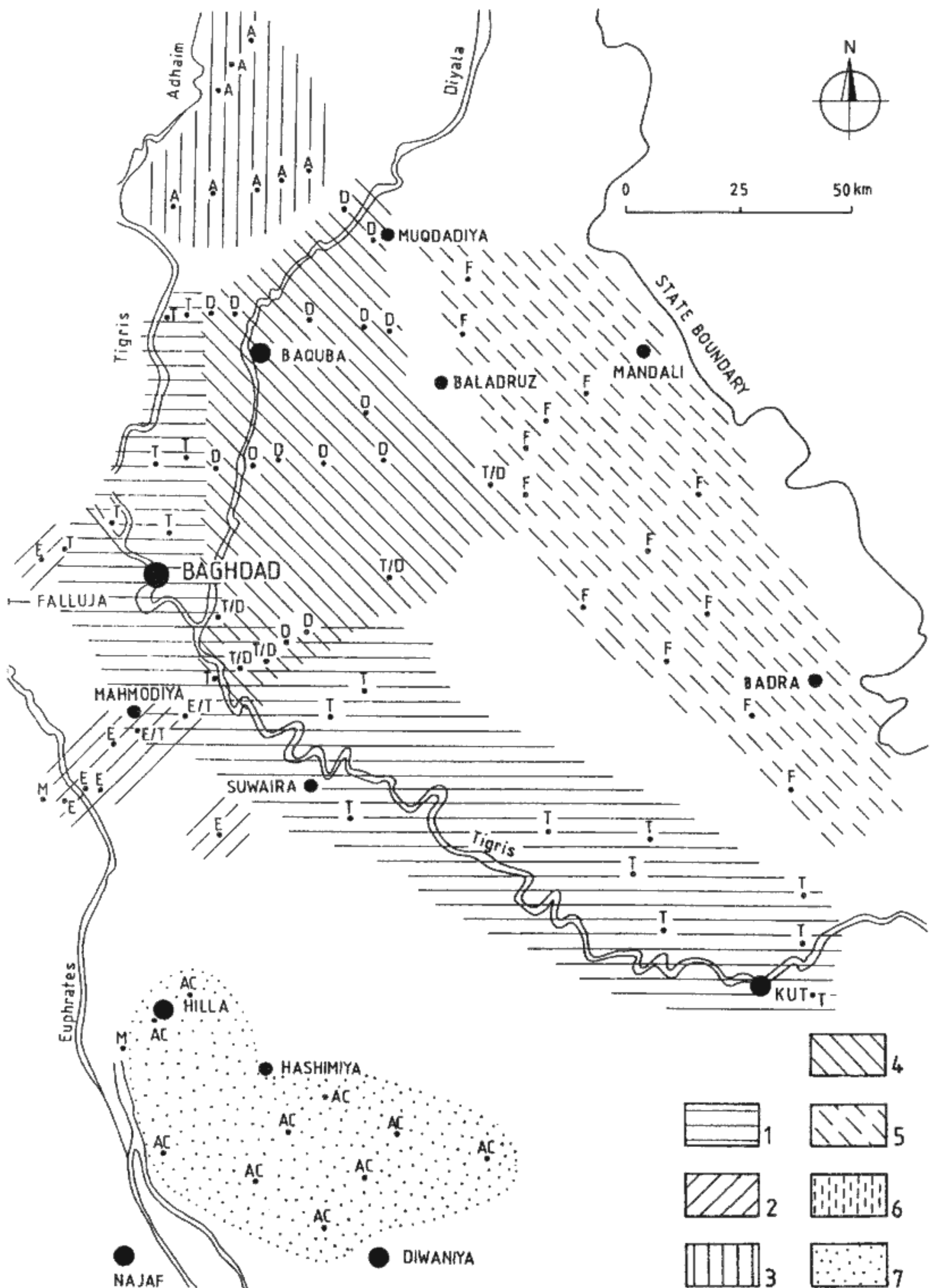
The investigation of sediments from deeper boreholes confirm that the Tigris and Euphrates rivers migrated westward during the Pleistocene and Holocene. The most intense accumulations probably occurred in successive phases during the Upper Pleistocene and the Holocene, within the area between Mahmudia and Salman Pak (DBH Nos. 1 and 2). This massive accumulation could have been caused by subsidence, or by intense denudation in the source areas. The presence of older Tigris River sediments at the same depth and not very far to the east (in the DBH Nos. 4 and 5), supports the latter possibility.

Characteristics and extent of the sediments

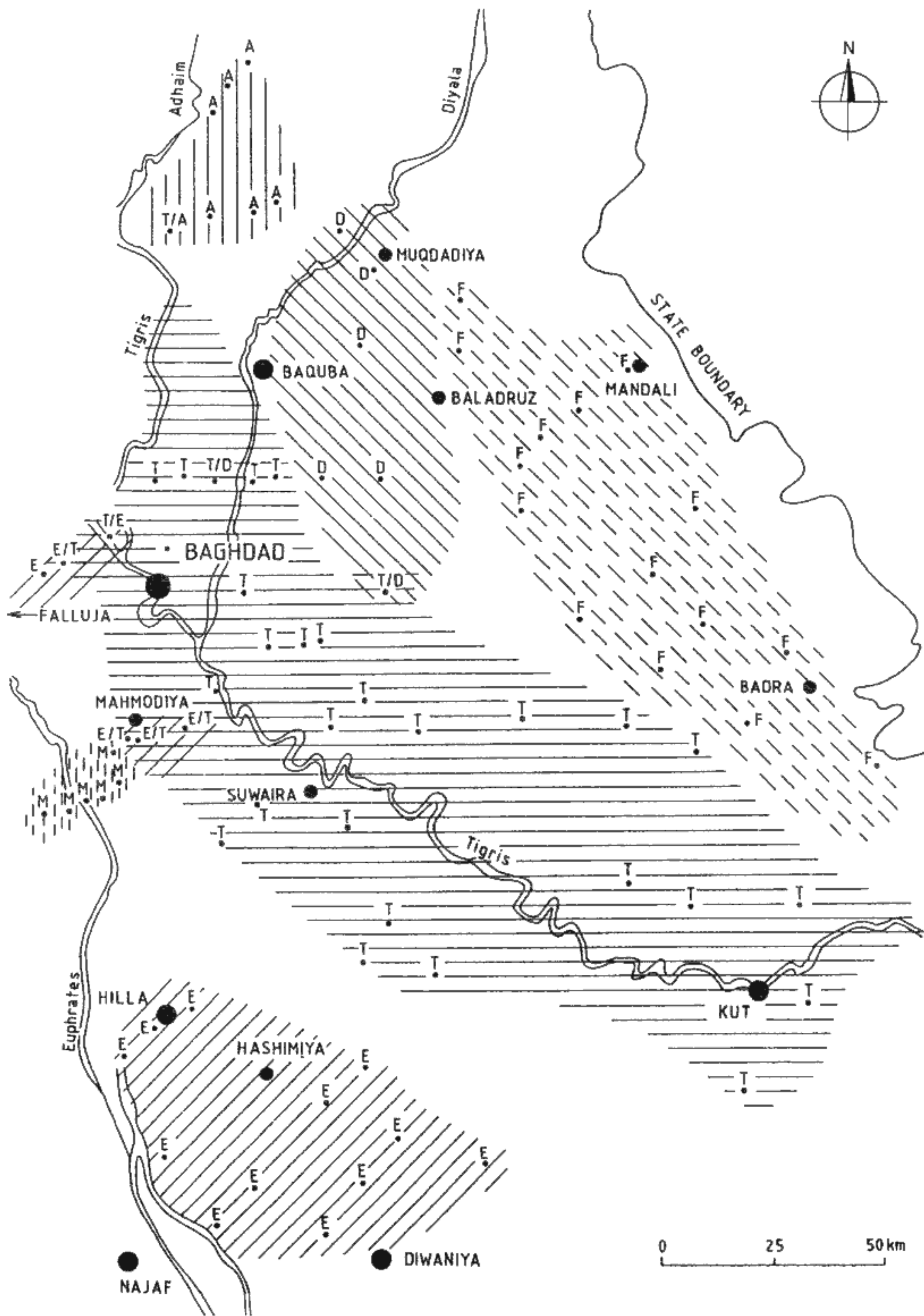
The sediments of the Adhaim River were studied by means of shallow boreholes (SBH) along the river's left bank (see Figure 15). These sediments are characterized by a very high content of minerals from the zoisite-epidote group, relatively high rock fragment contents, very low amphibole contents, and an extremely low pyroxene contents (see Table 1). The composition is vertically and horizontally constant, which confirms that the source of the clastic material must be sought for in the older sedimentary formations to the north.

The young (probably Holocene) Diyala River sediments border this river's present course up to its confluence with the Tigris River. To the S and SE they are often enriched with material from the Tigris River, repositioned from underlying beds (see Figure 15). Rock fragments prevail over clouded minerals in these sediments. The quantities of minerals from the zoisite-epidote, amphibole, and pyroxene groups are similar to those of the Tigris and the Euphrates sediments; the Diyala deposits, however, contain more orthopyroxene and significantly more titanite. The garnet content is very low. Metamorphic minerals are almost completely absent (see Tables 1, 2, and 4). The Upper Pleistocene deposits of the Diyala seem to occur only on the left bank (southward of Baquba) of the present Diyala River (see Figure 16). Older Diyala River sediments were found below the depth of 12–14 m. They differ from the younger deposits by being significantly higher in titanite, and by higher degrees of pyroxene and amphibole corrosion. These sediments occur on the left bank of the Diyala River to the south of Muqdadia (see Figure 17), and are possibly of Middle Pleistocene age. The HM fraction of the Diyala River deposits indicate that the source of the clastics is to be sought in the basic igneous rocks of the Walash Series, along the border between Iraq and Iran.

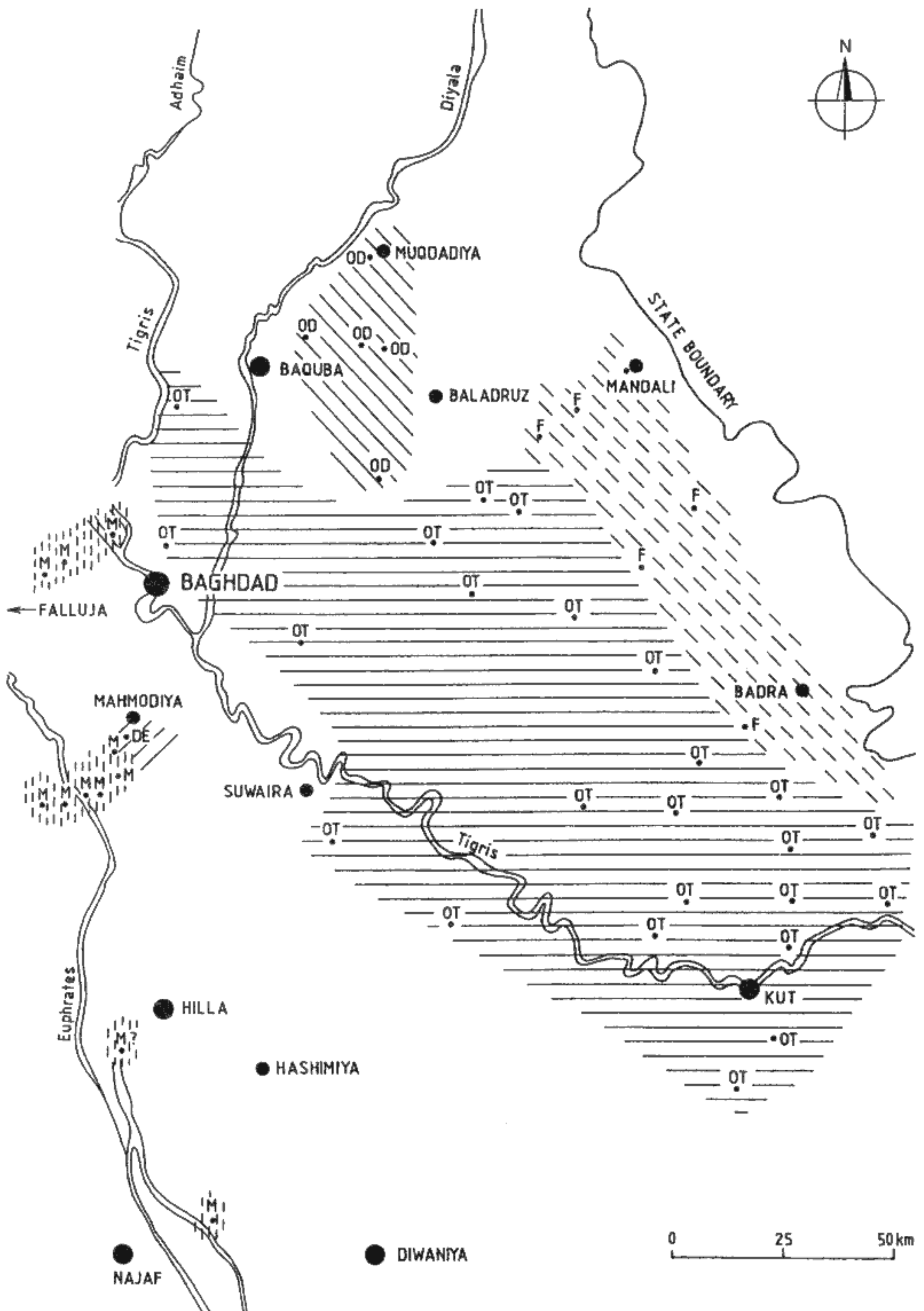
The Holocene sediments of the Tigris River border its present course. To the north of Baghdad the boundary between the sediments of the Tigris and Diyala rivers is sharp; while the mixing of their deposits appears in the vicinity of their confluence (see Figure 15). The Tigris River sediments that constitute a wide belt reaching many kilometres to the east of the river's present course (see Figure 16) are probably of Upper Pleistocene age. In the western part, they are covered by Holocene sediments from the Diyala River (compare Figures 15 and 16). The medium content of clouded minerals and rock fragments, and the presence of titanite downstream from the mouth of the Diyala River, are typical characteristics of the HM fraction. The Tigris River deposits contain much more garnet than those of the Diyala River (see Tables 2–8). Sediments that must be older than Upper Pleistocene were found in DBHs Nos. 4 and 5, and in several SBHs in the NE margin of the Plain (between Baladruz and Kut; see Figure 17). The composition of their heavy fraction does not differ significantly, though



15. Extent of the Tigris, Euphrates, Adhaim, Diyala, and Foothill zone sediments, and the Mahmudia Formation. 1 – Tigris River deposits; 2 – Euphrates River deposits; 3 – Adhaim River deposits; 4 – Diyala River deposits; 5 – Foothill zone deposits; 6 – Mahmudia Formation; 7 – deposits from artificial canals.



16. Extent of the Upper Pleistocene deposits. For explanations see Figure 15.



17. Extent of the Middle Pleistocene deposits. For explanations see Figure 15.

amphibole grains are corroded and the pyroxene corrosion a little stronger than in the Upper Pleistocene deposits. These sediments lie below a depth of 18 m, and are about 15 m in thickness. Unfortunately, there is no paleontological evidence for determining their age. They appear to be of Middle Pleistocene age, and thus the term "older" Tigris River sediments is used for them. Another older unit of the Tigris River deposits was found in the same DBHs (Nos. 4 and 5). This unit occupies a depth range from 33 m to about 50 m, and contains less pyroxene, though the quantity of other heavy minerals is similar (see Table 8). The corrosion of pyroxene and amphibole grains is evidently stronger than in the Upper Pleistocene and the "older Tigris" sediments. The "oldest Tigris River sediments" is the provisional term for this unit.

The Holocene sediments of the Euphrates River border its present course (see Figure 15). This river's older sediments have been located in the area between the present courses of the Euphrates and Tigris rivers (see Figure 16). The HM assemblage of the Euphrates deposits is very similar to that of the Tigris River sediments. Significant differences were found only in the contents of pyroxene, clouded minerals, and rock fragments. The Euphrates River sediments contain a slightly larger amount of metamorphic minerals (see Tables 1-8). The surface of the area between Hilla and Diwaniya is covered by recent deposits from artificial canals (see Figure 15). The composition of their heavy fraction differs from the typical Euphrates River sediments in that the former contain great amount of amphibole and very minor garnet. Chlorite and biotite are commonly present (see Tables 5 and 7). These canal deposits are usually fine-grained. It is supposed that the differences in HM content are mostly caused by the differences in grain-size distribution. In DBH No. 1 and SBH Nos. 53, 54, 34, and 35 (see Figure 2) the mixed sediments of the Euphrates and Tigris rivers are present to a depth of about 50 m. These deposits do not show a higher degree of amphibole and pyroxene corrosion, and must therefore be young, probably of Upper Pleistocene age. The oldest sediments of the Euphrates River were hitherto found close to Mahmudia in DBH No. 1, at a depth of more than 50 m. Considering the corrosion of amphibole and pyroxene, these deposits seem to correspond to sediments of the "older Tigris," and could therefore be of Middle Pleistocene age.

The NE part of the Mesopotamian Plain is covered by large alluvial fans preserved in the foothill zone of the Zagros Mountains. The HM contents of these sediments consist mainly of opaque minerals (partly of authigenic origin), minerals of the zoisite-epidote group, and authigenic minerals of the barite-celestite group (see Tables 1, 5, 6, and 8). This HM composition indicates that the Zagros Foothill zone deposits were derived from the neighbouring mountains, which were built-up from the Bakhtiari and Fars sedimentary formations. In the area between Mandali and Badra, the Foothill zone deposits overlap sediments of the "older Tigris" (compare Figures 16 and 17).

The sediments of the Mahmudia Formation (DOMAS et al. 1984) in the western part of the study area were investigated in shallow and deeper boreholes (see and compare Figures 15, 16, and 17). The HM content of these sediments differs from those of the Euphrates and Tigris by having a higher brownish amphibole content and a lower pyroxene content (see Tables 2, 3, and 8). Grains of pyroxene, amphibole, and garnet show strong corrosion. There was a marked change in the paleoclimate during the deposition of the Mahmudia Formation, which began in an arid Pliocene climate and ended during the first (oldest) pluvial oscillations of the Pleistocene.

Palaeogeographical conclusions

The N and NE parts of the territory under consideration are covered by sediments from the Adhaim River and by Zagros Foothill zone deposits. It seems that no substantial changes took place in this area during the Upper Pleistocene and Holocene. Only in the area between Mandali and Badra, where the foothill deposits overlie the sediments of the "older" Tigris. These covering sediments reach far to the west during this period of time (compare Figures 17 and 15, 16).

The remaining part of the area, covered by sediments from the Tigris, Euphrates, and Diyala rivers, experienced complex development accompanied by substantial hydrographical changes.

The Tigris River deposited its sediments more than 100 km to the east of its present course during the Upper, Middle, and perhaps even the Lower Pleistocene. At that time, the Tigris River sediments extended as far as the NE part of the Mesopotamian Plain, where they came into contact with Foothill zone deposits. To the north of Baghdad, the course of the Tigris River turned to the east, toward Baquba, to the area of the contemporary course of the Diyala River (compare Figures 15 and 16). During Upper Pleistocene, the Tigris River gradually shifted its course increasingly to the W and SW. During the Holocene, the Tigris River accumulated sediments along its present course (see Figure 15).

Pleistocene accumulations of the Diyala River were deposited to the E of its present course. During the Holocene, or perhaps even towards the end of the Upper Pleistocene, when the Tigris River migrated westward, the course of the Diyala River must have undergone large scale changes. The whole NE part of the Mesopotamian Plain is built up by sediments of the Diyala River, which overlie Upper Pleistocene and older sediments of the Tigris River. The confluence of the Diyala with the Tigris River shifted downstream from the Baquba area toward Baghdad, and the course of the Diyala River gradually migrated to the W (compare Figures 15 and 16).

The older sediments of the Euphrates River, possibly of Middle Pleistocene age, and its Upper Pleistocene

equivalents, also occur eastward of its present course. During the Upper Pleistocene, mixing of the Euphrates and Tigris rivers sediments took place in the Falluja and Mahmudia areas. The Euphrates River seems to have migrated westward by the end of Upper Pleistocene and during the Holocene. SW of Mahmudia, for example, the Holocene sediments of the Euphrates River rest immediately upon the Mahmudia Formation (compare Figures 15, 16, and 17).

The courses of all rivers in the N part of the Mesopotamian Plain migrated due W and SW during the Pleistocene and Holocene. Among the controlling factors of this migration, tectonics and climate changes were of major importance. The author concludes that the main cause was the gradual uplift of the Zagros Mountains. The progress of the Foothill zone sediments into the Mesopotamian Plain during the Upper Pleistocene and Holocene further supports this view.

The most intense accumulation from what seems to be a younger phase of the Upper Pleistocene and Holocene occurs in the area between Mahmudia and Salman Pak, where younger sediments of great thickness occur. This massive accumulation could have been controlled either by subsidence or by strong erosion and denudation at the source area. The presence of older sediments from the Tigris River at the same depth, and not far to the E (in DBH Nos. 4 and 5), favours the second possibility.

Acknowledgements

I wish to express my thanks to the Directorate of The State Organization for Minerals (S.O.M.) in Baghdad for permission to publish the results of the petrographical research that I carried out during my stay there. At the same time, I would like to thank my Iraqi colleagues

Hisham Al-Hashimi, Wissam Al-Hashimi, Nuri Hamza, and Nazaar Hassani, and my Czech colleagues Jaroslav Tyráček and Jaroslav Domas for cooperation, fruitful discussions, and valuable comments.

Translated by the author

Recommended for print by J. Petránek

References

- ALI, J. A. (1977): Heavy mineral provinces of the recent sediments of the Euphrates-Tigris basin. – *J. Geol. Soc. Iraq*, 10., 33–46. Baghdad.
- DOMAS, J. – MINAŘÍKOVÁ, D. – SABAH, Y. Y. (1984): Proposal on the introduction of the Mahmudia Formation. – Lecture on the 7th Iraqi Geological Congress in Baghdad. Baghdad.
- MINAŘÍKOVÁ, D. (1978): Preliminary study of the heavy minerals of the Quaternary sediments and Upper Fars Formation in northern part of Mesopotamia. Sketch of paleogeographical development. – MS, S.O.M. Baghdad.
- (1979): Heavy minerals of Quaternary and pre-Quaternary sediments in the deep boreholes between Mahmudia and Mandali (Mesopotamian Plain). – MS, S.O.M. Baghdad.
- (1979): The results of the Quaternary sediments investigation in the northern part of the Mesopotamian Plain. – MS, S.O.M. Baghdad.
- PHILIP, G. (1968): Mineralogy of recent sediments of Tigris and Euphrates rivers and some older detrital deposits. – *J. sed. Petrology*, 38, 35–44. Tulsa.

Paleogeografie kvartéru severní části Mezopotámie

(Résumé anglického textu)

DAGMAR MINAŘÍKOVÁ

Předloženo 24. ledna 2003

V letech 1978 a 1979 pracovala autorka pro State Organization for Minerals (S.O.M.) v Bagdádu na výzkumu kvartéru severní části Mezopotámie. Tamní kvartérní sedimenty jsou reprezentovány převážně jemnozrnnými písky, silty a jíly. Bylo zjištěno, že analýzy těžkých minerálů jsou jedinou vhodnou metodou pro rozlišení různých typů sedimentů. Proto bylo prostudováno více než 300 vzorků z mělkých i hlubších vrtů (jejich lokalizace je uvedena na obr. 2) ze sedimentů řek Adhaimu, Diyaly, Tigridu a Eufratu, dále z příúpatních uloženin pohoří Zagrosu, ze sedimentů formace Mahmudia a z předkvartérních sedimentů (výsledky analýz jsou uvedeny v tabulkách 1–8 a na obr. 13 a 14).

Vůdčími minerály pro rozlišení různých typů sedimentů jsou zakalené minerály, horninové úlomky, obecný a čedičový amfibol, augit, titanogit a granát. Vedle složení byla velká pozornost věnována i stupni koroze zrn pyroxenů a amfibolů, případně granátu. Pozorovatelné rozdíly v korozi zrn těchto minerálů závisí na stáří sedimentu. Pomocí koroze byly v hlubších vrtech rozlišeny tři různě staré jednotky sedimentů Tigridu – svrchnopleistocenní, starší, pravděpodobně středopleistocenní („older Tigris“) a nejstarší („oldest Tigris“), které nelze zatím přesněji stratigraficky zařadit.

Výsledky studia těžké frakce poskytly základní data potřebná pro úvahy o paleogeografickém vývoji území. Na obrázcích 15–17 je schematicky znázorněno rozšíření studovaných sedimentů v holocénu a ve svrchním a středním pleistocénu. Severní část území, které je pokryto sedimenty řeky Adhaimu, neprodělala během holocénu a svrchního pleistocénu žádné podstatné změny. Rozšíření příúpatních sedimentů v území mezi Mandali a Badrou se výrazně měnilo: nejmenší rozsah mělo během středního pleistocénu, zatímco v průběhu svrchního pleistocénu a holocénu se nápadně rozšiřují směrem k jihozápadu a jihu, takže překrývají středopleistocenní sedimenty Tigridu. Ty zasahovaly ve středním pleistocénu více než 100 km od dnešního toku směrem k východu a severovýchodu. Sledujeme-li rozšíření sedimentů Tigridu, vidíme, že se od středního pleistocénu posunují setrvale k západu a jihozápadu. Řeka Diyala ukládala své sedimenty ve svrchním pleistocénu a pravděpodobně i dříve východně od dnešního toku a její ústí do Tigridu leželo jv. od Baquby. V holocénu se Diyala posunula směrem k západu, její ústí do Tigridu leží na jih od Bagdádu a její sedimenty tvoří povrch velké části severní Mezopotámie, kde překrývají svrchnopleistocenní sedimenty Tigridu. Rovněž sedimenty Eufratu se posunují od východu k západu. Svrchnopleistocenní uloženiny Eufratu pokrývají území na východ od dnešního toku. V oblasti Mahmudie došlo k přemístění toku Eufratu k západu až v historické době.

Z tohoto přehledu je patrné, že všechny řeky v severní části Mezopotámie přesouvaly své toky v průběhu pleistocénu a holocénu směrem k západu a jihozápadu. Příčinou tohoto stěhování je pravděpodobně postupné zdvihání pohoří Zagros na hranicích mezi Irákem a Iránem. Pro tento předpoklad svědčí i rozšiřování příúpatních sedimentů.

K nejintenzivnější akumulaci dochází v mladší fázi svrchního pleistocénu a v holocénu v oblasti Mahmudie, kde byly zjištěny smíšené sedimenty Tigridu a Eufratu tohoto stáří až do hloubky kolem 50 m. Tato mohutná akumulace mohla být podmíněna buď subsidencí, nebo zvýšenou dotací klastického materiálu, vyvolanou silnou erozí a denudací ve zdrojové oblasti.

Vysvětlivky k obrázkům

1. Vymezení studovaného území.
2. Lokalizace studovaných mělkých (SBH) a hlubších (DBH) vrtů.
3. Relativní četnost opakních minerálů. 1 – sedimenty Tigridu; 2 – sedimenty Eufratu; 3 – sedimenty Diyaly; 4 – sedimenty příúpatní zóny.
4. Relativní četnost zakalených minerálů. Vysvětlivky viz obr. 3.
5. Relativní četnost horninových úlomků. Vysvětlivky viz obr. 3.
6. Relativní četnost minerálů zoisit-epidotové skupiny. Vysvětlivky viz obr. 3.
7. Relativní četnost obecného amfibolu. Vysvětlivky viz obr. 3.
8. Relativní četnost augitu a titanaugitu. Vysvětlivky viz obr. 3.
9. Relativní četnost granátu. Vysvětlivky viz obr. 3.
10. Trojúhelníkový diagram ukazující zastoupení zakalených minerálů, horninových úlomků a obecného amfibolu. 1 – sedimenty Tigridu; 2 – sedimenty Eufratu; 3 – sedimenty Diyaly; 4 – sedimenty příúpatní zóny.
11. Histogramy hlavních těžkých minerálů (TM) v sedimentech DBH 1. 1 – minerály zoisit-epidotové skupiny; 2 – skupina amfibolů (*spodní část sloupce* hnědý amfibol, *svrchní část sloupce* zelený obecný amfibol); 3 – skupina pyroxenů (*spodní část sloupce* ortopyroxeny, *střední část sloupce* titanaugit, *spodní část sloupce* augit a diops. augit); 4 – horninové úlomky; 5 – zakalené minerály; 6 – opakní minerály; 7 – granát.
12. Histogramy hlavních TM v sedimentech DBH 2. Vysvětlivky viz obr. 11.
13. Histogramy hlavních TM v sedimentech DBH 4. Vysvětlivky viz obr. 11.
14. Histogramy hlavních TM v sedimentech DBH 5. Vysvětlivky viz obr. 11.
15. Rozšíření holocenních sedimentů Tigridu, Eufratu, Adhaimu, Diyaly, sedimentů příúpatní zóny a uloženin formace Mahmudia. 1 – sedimenty Tigridu; 2 – sedimenty Eufratu; 3 – sedimenty Adhaimu; 4 – sedimenty Diyaly; 5 – sedimenty příúpatní zóny; 6 – sedimenty formace Mahmudia; 7 – sedimenty umělých kanálů.
16. Rozšíření svrchnopleistocenních sedimentů. Vysvětlivky viz obr. 15.
17. Rozšíření středopleistocenních sedimentů. Vysvětlivky viz obr. 15.

Vysvětlivky k tabulkám

- Tabulka 1. TM v sedimentech oblasti Muqdadie a Baquby.
 Tabulka 2. TM v sedimentech oblasti Bagdadu a Baladruzu.
 Tabulka 3. TM v sedimentech oblasti Mahmudie.
 Tabulka 4. TM v sedimentech mezi Mahmudí a Mandali.
 Tabulka 5. TM v sedimentech mezi Hillou a Mandali.
 Tabulka 6. TM v sedimentech oblasti Kutu a Badry.
 Tabulka 7. TM v sedimentech oblasti Hashimie a Badry.
 Tabulka 8. TM v sedimentech hlubších vrtů mezi Mahmudí a Mandali.

Table 1. Heavy minerals in the sediments of the Muqadadiya and Baquba area

No. of borehole	map sheet	depth (m)	opaque minerals	clouded minerals	rock fragments	zoisite-epidote group	amphibole common	amphibole brownish	glaucophanane	tremolite-actinolite	orthopyroxene	augite dips augite	titanaugite	pyroxene whitish	rutile	zircon	apatite	tourmaline	titanite	garnet	andalusite	sillimanite	kyanite	staurolite	chromite	chlorite	biotite	barite-celestite	origin of sediments
1	2B11	6.8-7.4	25.7	26.1	17.4	16.2	2.8	0.4	0.4			0.8	0.4	0.4	0.4	0.4		0.4	1.2	3.2			0.4		0.4	3.2		Adhaim R.	
1	2B11	14.0-14.4	26.0	13.5	19.6	22.1	5.6	0.3				1.3		0.5	0.3	0.2	0.4		0.3	5.6			0.2		3.8		0.5	Adhaim R.	
2	2B11	10.0-11.0	15.4	11.2	24.0	37.5	5.0	0.9	0.3			0.6			0.3	0.3	0.3		0.3	2.1				0.3	1.2		0.3	Adhaim R.	
3	2B11	15.0-15.5	16.1	15.6	27.1	31.7	2.0	0.5				0.5				0.5				4.5		0.5		0.5	0.5			Adhaim R.	
3	2B11	18.0-19.0	23.1	13.9	19.2	25.7	4.7	2.4	0.3	0.5	0.3	2.1	0.3	0.3	0.3	0.3		0.3	0.5	4.5			0.3	1.0	0.3			Adhaim R.	
8	2B8	3.7-3.9	12.3	8.5	7.2	61.1	5.5					0.7				0.3			1.4	1.7			0.3	0.3	0.3			Adhaim R.	
8	2B8	16.5-17.2	16.3	11.1	14.8	25.9	13.3	0.7			0.7	6.7	0.7					0.7		5.2					3.7			Tigris+Adhaim R.	
4	2B12	9.2-9.5	20.8	15.3	19.0	33.6	1.8	0.4		0.4		0.4	0.4	0.4	0.4	0.4			0.4	5.1				0.7	0.7		0.4	Adhaim R.	
5	2B12	2.3-2.6	14.2	14.2	8.5	50.1	3.0	0.9				1.2		0.3	0.3	0.3		0.3	0.6	2.1			0.3	0.3	2.4	0.3	0.9	Adhaim R.	
5	2B12	10.7-11.0	11.8	12.4	21.3	42.9	2.9	1.0	0.3	0.3		1.0				0.3			0.6	2.5			0.2	0.6	1.3		0.6	Adhaim R.	
6	2B12	13.0-13.5	21.2	15.0	20.2	31.9	1.0	1.3			0.3	0.8	0.3		0.3	0.3	0.2		0.3	2.6			0.2	0.5	2.6		1.0	Adhaim R.	
15	2B16	4.7-5.0	17.8	19.3	24.9	25.5	2.4	0.9			0.3	0.3		0.3	0.3	0.3		0.3	0.6	3.0			0.3	0.9	2.1		0.6	Adhaim R.	
13	2B16	11.8-11.9	11.7	10.9	21.2	18.3	11.7	3.6	0.7		3.9	7.3	7.3	1.5					0.4	0.7					0.7	1.5		0.6	Diyala R.
9	2C5	19.5-20.0	14.1	9.1	22.8	22.5	10.6	1.9	0.3	0.3	0.3	4.1	0.3	1.9	0.3	0.3	0.3		0.3	9.4			0.3	0.3	0.3			Tigris R.	
10	2C5	18.5-19.5	19.2	8.0	15.3	26.4	10.4	1.5		0.2	0.5	3.4	0.5	0.5	0.5			0.2	0.3	9.2				0.5	2.7	0.5		Tigris R.	
11	2C9	7.2-7.4	18.1	6.2	20.1	18.1	13.5	3.5		0.4	2.3	5.4	3.9	0.8					0.4	0.4		0.4			5.0		1.2	Diyala R.	
12	2C9	10.0-10.4	17.3	8.8	18.4	20.5	10.1	3.0		0.5	1.6	4.9	7.4	0.5	0.3	0.3	0.3		0.3	1.4			0.2	0.5	1.9		1.6	Diyala R.	
30	2C13	8.8-9.5	40.8	7.6	11.6	13.5	7.2	2.2	0.2	0.2	0.2	2.4	1.8	0.2	0.2	0.4	0.4		0.2	6.8			0.2	0.4	1.1		2.0	aeol.sand	
30	2C13	12.4-13.4	15.9	13.2	23.4	13.6	9.0	7.5		0.6		3.3	6.6	0.9	0.3	0.3			0.3	1.8				0.3	0.9			"older" Diyala R.	
31	2C13	11.0-12.5	31.7	5.7	20.8	9.2	5.4	2.0		0.3	1.0	4.0	15.6			0.3		0.3	0.5	2.2			0.7	0.3	0.3			"older" Diyala R.	
52A	2C13	5.4-5.7	14.7	8.1	21.8	19.8	10.9	5.1		0.5	1.5	4.6	3.6	1.5			0.2		0.5	1.8			0.3	3.3	1.5	0.3	0.3	Diyala R.	
52A	2C13	10.0-10.2	20.0	7.9	18.3	27.9	8.2	2.2		0.5	0.7	4.1	1.2	1.2		0.2		0.2	0.7	1.4				0.2	4.6		0.5	Diyala R.	
52A	2C13	11.3-11.7	15.6	5.0	22.0	27.3	9.8	3.9	0.3	0.6	0.3	5.9	1.1	0.3		0.3		0.3	0.9	2.5			0.3	2.5	0.3			"older" Diyala R.	
52A	2C13	24.0-24.5	12.5	8.7	17.2	17.0	17.3	7.3	0.2	1.2	1.2	10.1	4.9	0.2		0.2			0.7	0.2			0.2	1.2				"older" Diyala R.	
27	2C13	2.1-2.4	23.8	15.2	12.5	18.0	7.6	1.7	0.3			4.2	6.6	1.4	0.3	0.3			0.3	5.5				0.4	1.4			aeol.sand	
27	2C13	18.2-18.5	24.9	13.2	14.3	15.9	5.4	3.5	0.3	0.5	0.3	4.1	11.9	0.5		0.3			0.8	3.5			0.3	0.2	0.7	0.3		"older" Diyala R.	
28	2G1	13.5-13.6	36.3	10.4	16.5	14.7	5.2	0.5	0.2	0.2	1.1	1.6	2.7	1.1	0.2	0.2	0.2	0.2	0.5	6.7			0.2	0.2	0.7			aeol.sand	
46	2G1	0.6-0.9	49.0	8.1	9.6	18.4	2.6	1.7	0.3					0.3	0.3	0.3			0.3	3.5				0.3	3.2		2.3	foothill	
46	2G1	10.8-11.0	38.3	10.9	11.7	19.4	1.9	1.9	0.3	0.3		0.3			0.3		0.5	0.3	0.8	4.0				0.5	2.4		6.6	foothill	
53A	2G1	5.3-5.4	47.1	8.4	14.2	10.6	0.9	0.9				0.4							0.4	5.3				0.4	3.1		7.6	foothill	
53A	2G1	12.2-12.5	49.8	4.4	13.0	8.9	1.2	1.2	0.4			0.4				0.4	0.4	0.4	0.4	3.2				0.4	3.6		11.3	foothill	
21	2C6	18.5-19.0	14.5	8.4	12.7	24.8	15.3	1.7		0.6	0.3	4.9	0.3	1.2	0.6	0.6	0.3	0.3	0.3	10.7			0.3	0.3	2.0			"older" Tigris R.	

Table 2. Heavy minerals in the sediments of the Baghdad and Baladriz area

No. of borehole	map sheet	depth (m)	opaque minerals	clouded minerals	rock fragments	zoisite-epidote group	amphibole common	amphibole brownish	glauco-phane	temo-likite-actinolite	orthopyroxene	augite dlops. augite	titanaugite	pyroxene whitish	rutile	zircon	apatite	tourmaline	titanite	garnet	andalusite	sillimanite	kyanite	staurolite	chromite	chlorite	biotite	barite-celestite	origin of sediments
53	2C3	9.5-10.0	12.6	15.8	9.9	16.7	12.1	2.7		0.3	1.5	16.3	2.2	0.2		0.2		0.2	0.3	7.4	0.2	0.2			0.5	0.5		Euphrates R.	
53	2C3	16.7-17.0	13.6	19.3	8.0	21.8	9.5	1.5		1.3	1.8	14.9	2.3	1.0		0.3			0.3	3.8		0.3	0.3					Euphrates R.	
53	2C3	20.8-20.9	11.8	12.6	12.6	24.0	17.4	3.1		0.3		11.5	1.0	0.3		0.3		0.3		4.1			0.3	0.3				Euphrates R.	
53	2C3	29.7-29.8	25.9	10.9	8.1	23.4	5.0	0.8		0.8	0.3	1.9		0.3	0.3	0.8		0.3	1.7	18.4			0.3	0.3	0.3	0.6		Mahmudia F.	
54	2C3	4.5-4.7	21.1	11.7	12.4	22.8	7.0	1.5	0.2	0.5	0.3	9.0	0.3	0.5	0.2	0.2		0.3		11.2	0.2	0.2	0.5		0.2			res. Mahmudia F.	
54	2C3	7.6-7.7	9.3	9.0	8.3	28.2	23.9	2.3		1.0	1.0	12.1	5.0	0.7				0.3		2.8			0.2	0.3	1.0			Tigris R.	
54	2C3	12.1-12.2	10.0	19.5	7.5	25.2	14.5	1.8		1.4	1.8	12.1	2.3	0.5	0.2	0.2			0.2	1.8		0.2	0.2	0.7				Euphrates R.	
54	2C3	19.0-19.1	16.8	11.4	14.3	16.6	13.6	2.7		1.0	0.7	13.6	2.5	0.5	0.2	0.2			0.3	4.6			0.5	0.2	0.5			Euphr. + Tigris	
54	2C3	21.4-21.5	13.9	7.6	12.4	21.8	19.0	1.8	0.3	1.0	1.8	10.4	1.8	0.5					0.5	5.6	0.3		0.3					Euphr. + Tigris	
54	2C3	36.8-37.0	24.6	12.6	13.8	20.7	4.8	0.9		0.2	0.2	8.7	0.9		0.2				10.3			0.2	0.2	0.7	0.5	0.2		Mahmudia F.	
55	2C7	6.6-6.7	11.3	6.5	7.9	13.9	30.1	5.2		0.5		3.4	0.5	0.5	0.3			0.3	1.0	3.7				0.5	14.1		0.3	Tigris R.	
55	2C7	9.5-9.6	10.4	8.5	6.5	26.1	24.4	2.0	0.3	1.3	1.6	10.7	2.3					0.3	0.3	1.6				0.3	3.3			Tigris R.	
55	2C7	16.7-17.0	21.4	5.9	11.1	18.1	14.1	1.4		0.7	2.4	12.0	1.8		0.5	0.2			0.5	8.9	0.2		0.2		0.5			Tigris R.	
55	2C7	25.9-26.0	15.6	15.9	11.1	22.6	7.3	1.0		1.3	1.0	15.3	1.3	1.0		0.3			0.3	5.1				0.3	0.6			Tigris+Euphr.	
55	2C7	32.7-33.0	19.1	10.4	14.1	19.3	11.6	1.7		0.7	0.2	6.7	1.2	1.0		0.2		0.2	0.2	11.3	0.5	0.2	0.2	0.2	0.5			Mahmudia F.	
22	2C6	3.3-3.7	23.0	11.8	4.8	14.0	12.1	2.5		1.2	4.2	11.1	1.0		0.3		0.9			10.9					0.3	1.5	0.3		Tigris R.
22	2C6	17.6-17.8	9.1	11.4	8.4	23.4	14.7	2.3	0.3	3.6	3.6	13.7	0.6		0.6		0.3	0.6	1.0	6.1				0.3	0.3	0.3		Tigris R.	
23	2C6	6.5-6.8	14.3	5.8	20.1	14.2	5.8	1.4		1.1	0.4	5.2	0.4																Tigris R.
23	2C6	17.7-18.0	28.1	15.8	6.4	12.4	4.5	0.8		0.3	4.2	15.3	0.3			0.5		0.3	0.3	10.1	2.6			1.1	1.1	1.1	25.0	Tigris R.	
59A	2C7	3.4-3.6	13.7	5.9	11.6	18.8	23.3	1.8		0.9	0.3	2.1	1.8		0.3	0.3		0.3	0.3	5.7				0.3	0.3	0.3			Tigris R.
59A	2C7	14.1-14.2	8.8	10.7	17.1	15.8	20.1	2.7		0.6	1.8	12.8	1.2	0.6	0.3	0.3		0.3	0.3	5.2			0.3	0.3	0.3	2.4	0.3		Tigris R.
59A	2C7	20.2-20.5	11.8	14.8	14.8	20.4	12.5	2.3		0.3	0.3	8.9	0.7	0.7				0.3	0.3	9.9	0.3		0.3	0.3	0.3	0.3	0.3		Tigris R.
59A	2C7	26.0-27.0	17.3	11.2	15.6	17.8	10.0	1.6		1.4	0.5	4.9	1.4	0.3		0.3		0.3	0.8	11.2			0.3	0.3	0.3	0.3	0.3		"older" Tigris R.
20	2C10	6.7-7.0	16.9	4.6	13.3	22.7	11.7	4.2			5.2	16.2	2.0				0.3		1.0	0.6			0.3	0.3	0.3	4.4			"older" Tigris R.
20	2C10	16.3-16.6	7.8	7.6	10.8	16.0	25.2	2.0		1.7	1.0	14.7	5.4	1.2		0.2	0.2		1.0	3.2			0.3	0.3	0.5	1.0			Diyala R.
18	2C10	10.0-10.2	10.1	14.6	20.1	17.5	8.2	3.9			2.3	15.5	3.0						2.0	1.6						0.3			Tigris+Diyala
18	2C10	18.8-19.0	14.8	8.4	7.9	24.6	18.3	2.5			3.2	7.7	0.2		0.2	0.2		0.5	2.2	5.6			0.2	0.7	0.2	1.2	0.9		Diyala R.
17	2C10	4.6-4.9	10.5	3.8	14.2	23.8	7.0	3.5			6.7	18.2	5.0					0.6	1.6	1.2			0.3		0.3	1.9	1.6		Tigris R.
17	2C10	15.7-16.0	19.2	11.5	8.2	19.5	17.2	2.7	0.2	1.3	0.4	7.9	1.6	0.4		0.2			0.7	6.6		0.2	0.2	0.5	1.4			Diyala R.	
24	2C14	11.7-11.9	10.1	8.6	12.8	27.2	15.9	2.3			3.5	14.3			0.4				1.6	1.1						0.8			Diyala R.
24	2C14	15.3-15.5	13.3	7.7	33.4	16.1	11.3	1.7		0.3	2.5	8.1	0.3						0.7	0.7						3.8			Diyala R.
26	2C14	5.8-6.0	17.3	4.2	19.8	26.5	10.9	2.2		0.6	0.6	6.1	3.6	0.6		0.3		0.3	0.8	2.8		0.3		0.3	2.8	0.3			Diyala R.
25	2C14	4.2-4.4	10.3	4.6	17.7	15.1	26.2	4.0		0.8	0.6	3.7	1.1	0.6	0.6	0.3			1.1	1.7			0.3	0.3	9.4	1.4			Diyala R.
25	2C14	17.0-17.2	22.1	8.3	18.5	18.8	6.9	1.7		0.7	1.1	5.6	10.6	0.3				0.3	1.0	2.3				0.7	0.7	0.3			"older" Diyala

Table 3. Heavy minerals in the sediments of the Mahmudiya area

No. of borehole	map sheet	depth (m)	opaque minerals	clouded minerals	rock fragments	zoisite-epidote group	amphibole common	amphibole brownish	glaucophanane	tremolite-actinolite	orthopyroxene	augite dlops. augite	titanagite	pyroxene whitish	rutile	zircon	apatite	tourmaline	titanite	garnet	andalusite	sillimanite	kyanite	staurolite	chromite	chlorite	biotite	barite-celestite	origin of sediments
44	2D1	5.5-5.6	18.4	9.9	8.2	20.2	19.9	4.6		0.7	1.2	6	0	0.7			0	0	0	6		0		1		2		Mahmudia F.	
44	2D1	20.0-20.1	17.4	22.8	4.6	18.9	14.3	4.1		0.4		6.5		0.7	0	0	0	0	1	5		0	0	1	0	2	0	Mahmudia F.	
45	2D1	0.8-3.3	20.1	17	8.3	11.6	10	4.4		0.2	1.2	19.4	1	1.2	0	0				3			0	1	1	0		Euphrates R.	
45	2D1	5.6-5.7	18.6	21.4	4.6	15.7	7.7	3.6		1	0.8	14.2	0	0.8		0	0	0	0	8		0	1		0	1		Euphrates R.	
45	2D1	12.2-12.3	21.1	22.2	6.5	21.4	7.9	4.8			0.3	4.2		0.3	1	0	0	0	0	8		0	1	1		0		Mahmudia F.	
45	2D1	16.1-16.2	14.3	30	8.2	21	8.8	3.4	0	0.3	0.8	4.5		0.3			1	1	4	4		1	1	1	2			Mahmudia F.	
42	2D1	9.3-9.4	6.1	11.7	3.5	22.8	24.8	3.2		0.6	1.2	16.3	1			1			1	4		0	0		2			Euphrates R.	
42	2D1	12.4-12.5	9.1	16.2	6.9	27.6	17.5	2.9	0	0.8	0.4	6.4	0	0.8		0	0	0	0	3		0		0	5			Mahmudia F.	
42	2D1	15.5-15.6	18	22.4	6.3	19.9	11.4	4.7		0.3		4.1	0		0	1		1	1	6		1	0	1	0	3		Mahmudia F.	
42	2D1	19.6-19.7	24.1	20.8	5	11.8	11.9	3		0.3	0.3	5.3		0.3		0		0	1	9		1	1	1	2			Mahmudia F.	
42	2D1	19.9-20.0	22.2	18.3	6.9	15.9	10.8	3.9		0.3	1.5	14.4	0	0.9		0			4	4					1			Mahmudia F.	
42	2D1	24.9-25.0m	8.1	12.2	8.4	19.5	5.1	2.7				2.2	0	0.3	0	0	0	0	0	1	4		1	2	1	0	33.0	pre-Quaternary	
41	2D1	4.5-4.6	18.2	21.1	6.4	15.4	10.1	2.7		0.5	1	11.5		0.7	1	0	0	0	0	8		0	1	1	0	2		Euphrates R.	
41	2D1	8.5-8.6	15.6	24.2	15.9	16.6	8	4.2				7.3		0.4			0	0	1	3		0		1	2	0		Mahmudia F.	
41	2D1	16.1-16.2	16.8	14.9	7	17.7	11.1	6.1		0.9	0.7	9.6		1.4	0	0	0	0	0	9			0	0	0	2	0.2	Mahmudia F.	
41	2D1	17.2-17.3	25.3	14	5.4	24.3	8	5		0.3	0.3	3		1.4			0	1	9	9		0	0	0	3			Mahmudia F.	
38	2D5	7.7-7.8	25.1	13.1	4.7	19.9	12.9	2.3	0.2			8.7	0.2	1.2	0.2	0.5			0.7	8.0		0.2	0.2	0.5	1.2			Mahmudia F.	
38	2D5	11.4-11.5	18.9	26.2	7.6	17.9	12.3	3.6	0.4		1.1	5.1							0.4	2.2		0.4	1.1	1.1	0.4	0.4		Mahmudia F.	
38	2D5	25.8-26.6	8.7	21.4	9.6	18.9	14.4	3.6		1.7	0.4	13.6		0.7	0.2	0.2			0.2	4.9		0.2	0.2	0.2	0.2	0.4		Mahmudia F.	
37	2D5	2.5-3.2	23.2	24.3	2.7	12.0	5.1	2.9		0.3	2.1	17.9	1.3	1.1				0.3	5.3	5.3		0.3	0.5	0.3	0.5			Euphrates R.	
37	2D5	18.0-19.0	27.6	15.2	5.5	17.6	15.5	3.6	0.3	0.3	0.3	3.0	0.3			0.3		0.3	5.1	0.3		0.3	0.3	0.3	3.9			Mahmudia F.	
34	2C8	6.5-6.6	5.6	4.6	11.6	19.0	38.4	2.8		1.8	0.7	9.5	0.3						1.4	1.4					0.3	3.2	0.7	Euphr. + Tigris	
34	2C8	10.6-10.7	13.1	9.3	10.0	17.9	24.4	1.7		0.3	0.3	17.2	1.4	0.3	0.3				0.3	1.3					2.1			Euphr. + Tigris	
34	2C8	12.6-12.7	9.7	18.8	5.7	17.0	19.7	1.6		1.1	1.8	16.1	2.0	1.4				0.2	2.2	2.5		0.2	0.2	0.5	0.5	0.9		Euphr. + Tigris	
35	2C8	5.6-5.8	10.2	7.8	2.9	23.3	23.3	2.2	0.4	2.2	2.7	16.0	3.6	1.3	0.2	0.2	0.2	0.2	0.2	1.3				0.2	0.2	1.3	0.2		Euphr. + Tigris
35	2C8	7.5-7.6	11.3	18.3	13.7	15.4	17.1	2.9			1.3	14.2	0.8	1.3				0.4	0.4	1.7					1.3			Euphr. + Tigris	
35	2C8	15.5-15.6	12.6	22.0	7.4	23.4	11.0	2.2		2.0	1.0	10.0	0.2	1.0	0.2				0.6	4.8		0.4		0.2	0.6	0.4		Euphrates R.	
35	2C8	20.0-22.4	13.0	19.2	10.8	17.5	11.4	0.8		0.8	1.1	17.8	0.8	1.1		0.3			0.3	4.6		0.3	0.3					Euphr. + Tigris	
36	2C12	14.5-15.1	9.6	11.6	9.1	19.9	24.5	2.0		1.4	0.3	8.8	1.4	2.6		0.3		0.3	0.6	1.4		0.3	0.3	0.6	4.8			Tigris R.	
22	2D9	8.1-11.3	15.8	14.5	7.6	18.1	17.1	3.3		1.3	0.6	13.5	1.3	1.0			0.3	0.3	0.3	4.2		0.3	0.3	0.3	0.3			Euphrates R.	
22	2D9	15.1-15.2	17.5	10.7	16.0	19.3	13.6	1.8	0.3	0.9	0.6	8.6	2.4	0.9	0.3	0.3		0.3	0.3	3.8			0.6	0.3	0.3	1.5		Tigris R.	
21	2D9	13.6-13.7	21.7	5.4	10.8	19.6	25.0	3.9	0.3	0.3		6.0	0.3	0.3		0.3			0.6	2.7			0.3		2.4			Tigris R.	

Table 4. Heavy minerals in the sediments of the area between Mahmodiya and Mandalji

No. of borehole	map sheet	depth (m)	opaque minerals	clouded minerals	rock fragments	Zoisite-epidote group	amphibole common	amphibole brownish	glaucophanite	temolite-actinolite	orthopyroxene	augite diops. augite	tranaugite	pyroxene whitish	rutile	zircon	apatite	tourmaline	titaniaite	garnet	andalusite	sillimanite	kyanite	staurolite	chromite	chlorite	biotite	barite-celestite	origin of sediments	
32	2C11	2.7-3.0	14.6	10.2	10.7	10.6	7.3	3.2		1.5	0.3	36.0	2.0		0.5	0.2				0.5	1.2		0.2		0.5		0.2	0.2	Diyala R.	
32	2C11	15.8-16.0	11.4	13.2	10.8	15.5	12.6	3.2	0.3	1.6	2.0	19.0								0.6	7.9		0.3		0.3		0.3	0.3	Tigris R.	
1	2C12	13.0-13.2	17.4	13.2	7.7	19.5	11.3	2.7		2.2	3.9	11.6	3.6	1.1	0.3	0.3		0.3	0.8	3.0	3.0	0.3			0.3	0.3	0.3	0.3	Tigris+Diyala R.	
3	2C12	10.8-11.0	10.9	12.2	12.4	16.2	16.5	2.3	0.2	3.5	2.0	17.5	0.8	1.5					0.3	1.3	1.3	0.2	0.2	0.2	0.2	1.3	0.2		Tigris+Diyala R.	
3	2C12	13.7-14.0	11.6	12.6	6.4	21.5	13.4	3.0		1.5	1.3	17.9	1.8	3.3	0.2		0.2		0.2	4.3	4.3			0.2	0.2	0.5			Tigris+Diyala R.	
2	2C12	7.0-7.1	21.9	9.8	4.8	19.6	19.8	3.6		2.3	0.5	5.2	0.9	1.1		0.2		0.2	0.7	3.9	3.9	0.2		0.7	3.9	0.2			Tigris+Diyala R.	
2	2C12	13.1-13.2	15.4	11.1	15.1	19.6	12.0	1.2		3.3	3.0	11.4	1.8	2.4		0.3			0.3	2.1	2.1				0.3	0.3	0.3	0.3	Tigris+Diyala R.	
2	2C12	14.9-15.0	19.2	11.3	3.7	22.6	13.0	1.1	0.3	2.0	1.7	13.6	2.3	0.8		0.3		0.3	0.6	4.8	4.8		0.3	0.3	0.6	1.7			Tigris+Diyala R.	
4	2C12	3.9-4.0	16.6	16.9	11.0	17.9	7.8	1.9		1.6	0.9	7.8	11.6	2.3			0.3			1.6	1.6				0.6	0.3	0.3	0.3	Diyala R.	
4	2C12	7.8-8.0	20.0	5.2	16.2	22.7	12.1	3.1			0.3	7.2	1.0	1.0					1.7	4.1	4.1				3.4	0.7	0.7	0.7	Tigris+Diyala R.	
4	2C12	17.3-17.4	13.9	11.4	12.6	20.0	13.4	2.3	0.2	2.3	1.0	10.9	2.3	1.5	0.3	0.2			0.5	6.0	6.0			0.5	0.3				Tigris R.	
5	2C16	10.0-11.0	16.2	13.0	10.5	16.1	11.2	2.5	0.2	1.8	0.7	11.4	3.2	2.7		0.2		0.2	0.5	9.0	9.0		0.2		0.5	0.2			Tigris R.	
5	2C16	13.6-14.0	19.8	10.6	8.3	15.9	16.4	4.3		2.3	0.3	6.3	2.9	2.6	0.3	0.6		0.6		6.0	6.0		0.6	0.3	0.3	1.7			Tigris R.	
5	2C16	18.3-18.4	13.8	5.1	13.8	24.5	17.1	1.4			1.4	11.2	2.2	0.8	0.3		0.3		0.3	4.8	4.8		0.8	0.6	1.4	0.3			Tigris R.	
42	2C15	4.0-4.2	17.5	13.6	9.6	22.1	7.7	3.1		0.8	1.3	16.0	2.0						1.0	3.3	3.3		0.3		0.5	0.5	1.0	1.0	Tigris+Diyala R.	
42	2C15	10.4-11.0	10.2	5.8	8.7	17.3	30.7	3.5	0.3	0.9	1.2	5.5	0.3	0.6		0.3				1.2	1.2			0.3	11.0	2.3			Tigris+Diyala R.	
42	2C15	15.0-15.3	11.9	7.6	8.1	15.5	17.3	2.3		3.0	2.5	23.4	2.0			0.3		0.5	0.3	2.5	2.5		0.3	0.3	0.3	0.8	0.3	0.5	Tigris+Diyala R.	
37	2G3	15.7-16.0	13.8	5.8	12.7	32.6	12.4	1.2			2.2	9.6	0.3		0.8	0.3		0.5	2.2	3.3	3.3		0.5	0.3	0.3	0.8		1.4	Tigris+Diyala R.	
37	2G3	19.8-20.0	18.5	10.8	7.5	15.3	14.4	3.3	0.3	3.0	1.4	13.6	0.3		0.3				1.7	7.5	7.5			0.3	0.3	0.8		1.1	"older" Tigris R.	
36	2G3	4.7-4.8	16.7	14.5	7.9	18.4	6.3	2.1			4.8	19.6	4.0			0.3			0.3	3.0	3.0		0.3		0.6	0.6			Tigris+Diyala R.	
36	2G3	18.0-18.2	21.7	8.8	11.4	18.9	9.8	2.1		2.3	2.1	8.5	0.8		0.8	0.2	0.2	0.2	0.5	10.9	10.9			0.2	0.5	0.5	0.5			"older" Tigris R.
45	2G6	18.4-18.5	45.6	6.2	9.3	13.6	1.0	1.0		0.7	0.2	1.2			0.2		0.5		1.2	1.5	1.5		0.2		0.2				foothill	
48	2G6	19.2-19.5	72.6	3.4	4.2	5.6	4.2	1.1	0.2	1.1	0.8	3.1			0.2	0.2		0.2	0.2	0.6	0.6			0.3	1.3	0.5			foothill	
49	2G10	6.7-6.9	20.5	5.1	4.5	6.3	1.8	0.7	0.1	1.8	0.8	3.3			0.2	0.2		0.3	0.3	0.3	0.3	0.2	0.2	1.0		0.3	0.3	53.8	foothill	
49	2G10	16.3-16.5	48.4	4.6	10.2	18.8	0.3	0.3			0.6	1.4			1.0	0.7	0.7	0.3	2.1	3.2	3.2		1.4	1.0				5.0	foothill	
20	2D9	15.3-15.4	14.8	13.4	18.2	15.1	13.1	3.1		1.4	0.6	9.4	2.0	0.3	0.6	0.6			0.3	5.1	5.1		0.3		0.8	1.1			Tigris R.	
20	2D9	19.8-19.9	17.9	9.2	18.2	15.3	15.0	2.3	0.3	0.6	1.4	10.4	2.3	0.9		0.3		0.3	0.3	4.0	4.0			0.3	0.3	0.3			Tigris R.	
6	2C16	7.2-8.0	12.7	13.7	8.2	20.8	13.5	2.1	0.3	0.5	2.9	12.7	2.1	2.1		0.3		0.3	0.3	6.9	6.9		0.3		0.3				Tigris R.	
6	2C16	15.5-16.7	17.8	10.9	11.6	14.2	14.6	4.7	0.2	2.0	0.2	9.9	1.5	3.5		0.5		0.2	0.5	5.9	5.9		0.5		0.7	0.5			Tigris R.	
7	2C16	10.4-10.5	11.6	26.5	8.9	15.0	10.6	1.0		1.7	1.7	11.6	2.0	1.7	0.3	0.3		0.3	0.3	4.6	4.6		0.3	0.3	0.3	2.0			Tigris R.	
39	2G3	19.5-19.7	23.7	4.0	12.7	11.9	18.2	3.0		1.3	1.3	7.5	2.5	0.7		0.3		0.3	0.3	10.7	10.7		0.2	0.2	0.5	2.0			"older" Tigris R.	

Table 5. Heavy minerals in the sediments of the area between Hilla and Mandali

No. of borehole	map sheet	depth (m)	opaque minerals	clouded minerals	rock fragments	zoisite-epidote group	amphibole common	amphibole brownish	glaucophanes	tremolite-actinolite	orthopyroxene	augite dops. augite	titanite	pyroxene whitish	rutile	zircon	apatite	tourmaline	trianite	garnet	andalusite	sillimanite	kyanite	staurolite	chromite	chlorite	biotite	barite-celestite	origin of sediments	
61 2D7	8.1-8.2	19.6	13.2	6.7	15.9	20.2	4.4				0.3	5.3	0.3			0.3		0.3	0.6	5.9						6.4	0.6		res. Mahmudia F.	
61 2D7	10.3-10.4	10.0	19.2	7.3	19.7	14.6	1.8			0.6	3.0	16.7	2.4	0.3					0.6	2.4					1.2			Euphrates R.		
61 2D7	17.3-17.5	22.9	14.4	7.9	24.4	14.1	2.3			0.3	1.6	2.3			0.3	0.6		0.3	0.3	8.2	0.3		0.3	0.3	0.8				Mahmudia F.	
60 2D7	4.2-4.3	6.9	9.3	5.9	20.6	34.3	3.7			0.3	1.6	10.0	1.6	0.3					0.3	1.6	3.1	0.3			2.5	0.3	0.6	art. canal		
60 2D7	9.1-9.2	16.1	13.6	7.3	19.0	13.0	2.2			0.3	1.6	18.4	3.2	0.3		0.3			0.3	4.1	2.7	0.3			0.3				Euphrates R.	
60 2D7	12.7-12.8	10.7	11.9	6.1	19.8	24.7	3.4			0.3	1.2	12.5	0.9	0.6					0.6	2.7	4.0	0.6			2.7	1.5			Euphrates R.	
60 2D7	14.2-14.3	13.0	13.6	7.7	18.9	20.7	2.2			0.3	0.6	13.6	1.6	0.3	0.3	0.3	0.3	0.3	0.6	4.0	3.1	0.6		0.3	0.6				Euphrates R.	
60 2D7	19.5-19.6	19.3	17.7	7.0	22.0	8.6	2.5			0.3	0.3	16.8	0.6	0.3	0.3	0.3			0.3	2.1	3.1	0.3		0.3	0.6				Euphrates R.	
59 2D7	3.0-3.1	10.8	11.1	8.7	17.1	24.9	4.8			0.3	2.4	11.4	1.2	0.6	0.3				0.3	1.8	12.2			0.3	0.3	0.3				art. canal
59 2D7	6.9-7.0	14.4	17.7	9.0	18.0	22.8	3.0			0.6	1.2	9.3	1.5						0.3	1.8	12.2			0.3	0.3	0.3				art. canal
59 2D7	17.4-17.5	26.9	19.4	5.9	22.5	3.4	1.6			0.3	0.3	0.6		0.3	0.6	3.4		0.3	1.6	12.2	0.3	0.3	0.3	0.3	0.3	0.4				res. Mahmudia F.
59 2D7	21.0-21.1	7.9	33.8	9.4	16.9	10.5	0.8			0.4	0.4	12.8	1.1	0.8					0.7	2.3	7.4	0.7		0.3	0.3	0.4			Euphrates R.	
28 2D13	19.1-19.2	16.2	10.5	10.8	15.3	22.9	3.4	0.3	0.3	0.3	0.3	5.9	0.3	0.3	0.3	0.3	0.3	0.6	0.3	7.4	0.3	0.3	0.3	0.3	0.3	3.7			"older" Tigris R.	
27 2D13	13.0-13.2	13.5	14.1	16.2	24.3	10.5	1.2	0.3	0.6	0.9	8.1	0.6		1.2	0.3	0.3		0.3	0.6	4.5	0.3	0.6	0.3	0.6	0.6	0.6				Tigris R.
27 2D13	17.6-17.7	16.1	8.3	12.2	15.9	16.7	2.6			1.3	1.0	13.5	1.6	1.6		0.5	0.3	0.3	0.3	6.0	6.0			0.3	0.8	0.5	0.5			Tigris R.
12 2G4	18.6-18.8	18.3	12.2	12.2	25.1	15.9	1.5			0.9	1.2	3.4	0.9			0.3		0.6	0.6	5.2	5.2	0.3	0.3	0.3	0.5	0.3				Tigris R.
77A 2G7	14.4-14.5	59.1	3.7	9.4	10.0	0.7	0.3					0.7							0.3	4.4	4.4	0.3		0.7	1.0			9.4	foothill	
77A 2G7	19.8-20.0	15.3	7.7	6.5	27.5	15.9	3.1	0.3	0.3	0.3	1.1	7.9	1.1		0.6	0.6		0.3	0.6	6.8	0.3	0.3	0.3	0.3	0.9	2.3	0.3			"older" Tigris R.
62 2D8	6.3-6.4	6.5	9.8	8.2	14.8	32.0	2.0			0.3	0.7	12.4	1.0			0.3			0.6	0.3	0.3				8.2	2.9				art. canal
62 2D8	12.2-12.3	10.2	2.7	5.1	13.0	25.6	4.1				0.3	7.2	0.3		0.3	0.3			0.3	0.3	0.3				22.2	7.9				art. canal
62 2D8	15.0-15.1	17.4	10.6	7.6	19.7	18.5	3.2			0.9	2.1	13.5	1.5			0.3	0.3	0.3	0.3	2.6	0.6			0.6	0.3	0.3		0.6		Euphrates R.
26 2D14	10.7-10.8	8.5	6.6	16.8	20.1	20.9	1.7			1.4	1.7	13.8	0.6	0.6				0.6	0.3	0.6	2.5	0.3		0.3	1.1	1.7	0.3			Tigris R.
24 2D14	10.7-10.8	10.8	11.3	14.8	22.3	19.3	3.0			0.5	1.5	8.3	1.5	0.3	0.3	0.3		0.3	0.3	3.6	3.6			0.3	0.3	1.0				Tigris R.
82A 2G8	12.6-12.7	8.4	14.4	10.5	23.1	21.7	3.4	0.3	0.3	1.0	1.0	8.9	0.3	0.3	0.3	0.5		0.3	0.3	2.8	2.8		0.2		2.9					Tigris R.
82A 2G8	17.6-17.7	14.4	19.7	7.5	29.5	7.9	2.5			0.6	0.3	7.9	0.3	0.3				0.3	0.3	7.2	7.2				1.6					Tigris R.
80A 2G8	5.0-5.1	78.3	2.8	6.8	5.3	1.4	0.4					0.4							0.3	0.7	0.7			0.7	1.1			1.8	foothill	
80A 2G8	16.0-16.1	19.2	4.8	9.9	19.2	17.8	2.5	0.3	0.3	0.3	1.1	2.8	0.6	0.6	0.3		0.5	0.3	0.3	3.4	3.4	0.3		0.3	12.7	3.1				"older" Tigris R.
76A 2G11	1.4-1.5	74.4	4.0	6.2	4.9	1.5	0.6	0.3				0.3			0.3	1.2			0.3	0.9	0.9			0.3	1.5			4.4	foothill	
76A 2G11	14.8-15.2	63.1	8.0	7.4	9.7	0.6	0.9					0.9			0.3				0.3	1.2	2.0			0.2	1.7	1.8			0.6	foothill
76A 2G11	18.2-18.5	76.1	4.4	5.5	3.2	0.3	0.3				0.3	0.6				0.6	0.3	0.3	0.3	1.2	1.2			0.6	1.2			4.9	foothill	
75A 2G11	1.7-2.0	71.4	4.5	2.2	4.9	1.8	0.4					0.4		0.4		0.9			0.4	0.4	3.6			1.4	1.4	0.9			4.9	foothill
75A 2G11	12.5-13.0	70.0	3.5	5.0	12.4	1.2	0.8	0.4				0.4				1.6			0.4	1.6	1.6			0.8	0.8			1.2	foothill	
75A 2G11	19.7-20.0	79.0	2.3	3.9	3.1	1.8	1.0				0.3	0.3			0.3				0.3	1.0	1.0			0.8	2.3			3.9	foothill	

Table 6. Heavy minerals in the sediments of the Kut and Badra area

No. of borehole	map sheet	depth (m)	opaque minerals	clouded minerals	rock fragments	zoisite-epidote group	amphibole common	amphibole brownish	glaucophanes	tremolite-actinolite	orthopyroxene	augite dlops. augite	titanite	tourmaline	zircon	apatite	andalusite	sillimanite	kyanite	staurolite	chromite	chlorite	biotite	barite-celestite	origin of sediments	
68A	2H10	2.1-2.2	16.5	11.1	13.9	19.0	16.1	1.6		0.6	0.9	8.9	1.9	0.6	0.3						0.6	5.7			Tigris R.	
68A	2H10	9.1-9.2	15.3	6.8	11.2	20.7	19.2	3.2		0.9	2.0	7.4	1.2	0.3	0.3	0.3		0.3		0.3	0.3	4.1	0.3		Tigris R.	
68A	2H10	13.4-13.5	16.5	9.1	14.6	20.6	14.3	3.0		1.1	0.5	6.3	2.2	0.3				0.3				2.5	0.5		Tigris R.	
68A	2H10	16.4-16.5	20.1	10.5	12.6	21.3	11.7	1.8		0.6		6.6	2.1	0.3	0.3		0.3			0.3	0.9	2.1			Tigris R.	
67A	2H9	3.6-3.7	14.9	6.7	13.6	20.3	19.4	3.9			0.9	3.9	3.3	0.3	0.3	0.6				0.6	0.3	4.9			Tigris R.	
66A	2H9	12.1-12.2	14.2	11.1	13.1	27.6	12.2	3.4		0.6	0.6	4.3	1.1	0.3	0.6	0.3						3.4	0.3		"older" Tigris R.	
65A	2H9	13.9-14.0	11.5	8.5	15.1	16.3	25.1	1.8		0.9	1.2	7.3	2.1	0.3		0.3						6.0	1.8		Tigris R.	
65A	2H9	18.5-18.6	13.1	14.2	14.8	20.7	10.7	1.9		0.5	1.1	10.9	3.0	0.3	0.3		0.3				0.5	1.4			"older" Tigris R.	
63A	2G16	15.7-15.8	67.6	2.9	8.6	8.9	1.7	0.3				0.3	0.5	0.3							0.3	7.1			foothill	
63A	2G16	23.8-23.9	57.0	5.9	7.6	12.4	3.1	0.6				1.7	0.3	0.3				0.3			0.3	2.2	0.8	5.3	foothill	
64A	2G16	1.5-1.7	52.5	4.0	2.5	6.9	2.9	1.4				0.4		0.4								5.4	0.4	21.0	foothill	
64A	2G16	4.8-5.0	32.2	7.8	4.3	18.4	8.3	0.6	0.6			2.0	0.3	0.3							0.9	5.7		15.5	foothill	
74A	2H10	5.5-5.6	15.9	13.8	10.9	20.6	9.7	0.6			1.2	11.5	2.3	0.3		0.3			0.3	0.3	0.3	0.9	1.2	0.3		Tigris R.
74A	2H10	13.2-13.5	12.0	16.1	11.4	20.5	15.5	2.6			1.7	6.7	0.6	0.6		0.3				0.3	0.6	0.6				"older" Tigris R.
73A	2H10	15.8-16.0	12.5	19.2	16.4	25.4	8.1	0.3	0.3	0.3	0.8	4.4	2.2	0.3	0.3	0.3			0.3		0.3	1.7			Tigris R.	
73A	2H10	18.5-18.7	12.5	7.0	12.5	28.3	13.4	3.4		0.6	0.9	7.9	1.5	0.3	0.3				0.6	0.9		0.6				"older" Tigris R.
69A	2H13	6.9-7.2	55.0	2.9	10.8	9.9	2.6	1.8				0.4		0.7							0.4	5.9	1.1	6.1		foothill
68A	2H13	18.8-19.0	17.0	3.9	12.6	17.8	20.7	1.0		0.5	1.0	7.1	1.6	0.3		0.3			0.3			6.8	1.3			"older" Tigris R.
70A	2H13	9.8-10.0	15.4	10.8	13.0	18.2	12.3	2.8	0.3		0.9	9.9	1.2	0.3					0.3			3.4				"older" Tigris R.
70A	2H13	15.7-15.9	22.5	11.0	11.3	16.8	11.0	2.6	0.3	0.3	0.3	6.6	3.2	0.3	0.9	0.3				0.3	0.3	1.7				"older" Tigris R.
71A	2H14	12.6-12.7	11.3	8.4	11.5	20.2	26.5	5.3		0.3	1.7	6.5	1.7	0.3		0.3			0.3			3.4				Tigris R.
71A	2H14	14.7-14.8	20.4	11.0	11.6	21.6	13.4	2.1	0.3	0.3	1.8	3.7	1.2	0.3		0.6					0.3	1.5				Tigris R.
71A	2H14	18.7-18.9	21.5	9.8	14.2	17.9	13.0	1.6			1.6	6.9	1.6								0.4	0.4				"older" Tigris R.
72A	2H14	4.7-4.9	19.6	10.8	13.2	17.9	13.9	1.0		0.7	1.4	6.1	0.7	0.7								5.1				Tigris R.
72A	2H14	20.4-20.8	19.7	16.8	9.8	21.2	7.8	0.6		0.3	0.6	8.1	2.3	0.3	0.3	0.3				0.3	0.3	1.7				"older" Tigris R.
97	2H15	7.9-8.0	11.8	14.2	13.9	18.5	13.3	2.0		0.3	1.5	12.4	2.0	0.3							0.3	2.6				Tigris R.
96	2H15	21.3-21.4	7.5	11.1	11.1	19.0	22.2	4.3		0.7	2.2	12.2	1.1	0.4		0.3				0.3	0.3	3.6				"older" Tigris R.
96	2H15	22.3-22.4	10.9	27.1	6.2	15.4	11.8	2.3			2.7	9.4	2.3	0.9	0.3	0.3				0.3	0.3	0.6				"older" Tigris R.
95	2H15	16.1-16.2	13.5	17.3	10.7	22.0	13.8	1.9	0.3			8.8	1.6		0.3						0.3	2.2				Tigris R.
95	2H15	20.1-20.2	26.1	9.0	9.0	9.0	15.6	3.0		0.3	1.2	9.0	1.5	0.3	0.6	0.3			0.3		1.5	2.4				"older" Tigris R.
84A	2L2	19.7-20.0	11.0	19.0	8.1	19.1	23.9	1.3			1.3	7.1	1.0	1.0	0.3				0.3		0.3	1.6				"older" Tigris R.
85A	2L1	5.4-5.6	50.2	5.1	21.9	9.5	2.7	0.7				0.7			0.3						0.7	2.3	0.3	4.0		foothill
85A	2L1	14.8-15.0	14.9	7.5	8.2	22.8	18.9	2.5		1.1	1.4	9.6	0.3	1.1								3.2				"older" Tigris R.
86A	2L1	19.3-19.5	11.5	7.1	12.0	30.3	16.8	1.9			1.5	7.6		1.2						0.2	1.0	4.4				pre-Quaternary
87A	2L1	14.8-14.9	57.3	6.8	7.1	13.3	0.6	0.9			0.3	0.6			0.9					0.3	0.3	0.3				foothill

Table 7. Heavy minerals in the sediments of the Hasmimiya and Badra area

No. of borehole	map sheet	depth (m)	opaque minerals	clouded minerals	rock fragments	zoisite-epidote group	amphibole common	amphibole brownish	glaucophane	tremolite-actinolite	orthopyroxene	augite dlops. augite	titanaugite	pyroxene whitish	rutile	zircon	apatite	tourmaline	titanite	garnet	andalusite	sillimanite	kyanite	staurolite	chromite	chlorite	biotite	bartite-celestite	origin of sediments
73	2D12	15.5-15.6	11.0	7.0	10.6	18.9	25.9	1.7		0.3	1.7	14.6	1.0	0.7	0.3	0.3		0.3	0.3	3.7				1.0	0.7			Euphrates R.	
73	2D12	23.8-23.9	8.0	19.6	12.2	26.8	12.2	5.1	0.3		0.6	5.6	0.3			0.9			0.6	5.1	0.3	0.6	0.6		0.6			Mahmudia F.	
72	2D12	8.9-9.0	8.3	6.2	10.2	25.2	22.3	3.0		0.3	3.0	13.4	1.6	1.1				0.3	0.3	1.6					3.2			art. canal	
72	2D12	17.5-17.6	9.8	13.9	9.0	23.7	15.1	0.9		1.2	1.4	13.6	1.2	1.2	0.3	0.3			0.3	6.4			0.3	0.3	1.1	0.3		Euphrates R.	
72	2D12	21.4-21.5	13.2	10.4	7.9	25.0	12.6	0.6		0.5	1.1	18.0	2.5	0.3					0.3	5.6				0.2	1.7			Euphrates R.	
71	2D12	9.2-9.4	6.7	9.1	6.7	16.3	41.2	1.2		0.9	1.5	8.2	0.6	0.3						0.3			0.3	0.3	5.2	1.5		art. canal	
74	2D15	6.2-6.4	9.2	6.9	8.7	18.8	30.1	3.6		0.3	0.9	12.8	1.2							1.8			0.3	0.3	4.2	0.6		art. canal	
74	2D15	12.7-12.9	7.8	19.1	19.4	11.3	19.7	2.5		0.3	2.5	10.3	1.6	1.2						2.2		0.3	0.3		1.2			Euphrates R.	
74	2D15	18.4-18.6	9.3	9.0	9.0	28.2	15.8	3.1		0.6	2.8	15.2	1.2	0.3			0.3	0.3	0.6	2.8			0.3	0.3	0.6		0.3	Euphrates R.	
75	2D15	17.3-17.5	8.8	14.0	10.0	21.1	13.1	3.1	0.3	0.3	2.0	19.9	1.4	0.8	0.3				0.3	2.6			0.3	0.3	1.4			Euphrates R.	
31	2H2	10.1-10.2	15.1	2.3	18.5	16.6	24.9	1.5		0.4	0.4	2.6	0.8						0.4	2.7				0.8	18.5	1.1	2.6	Tigris R.	
31	2H2	16.3-16.4	11.8	12.1	16.2	17.5	9.4	3.0		0.7	0.7	15.2	3.0	0.7		0.3	0.3		0.7	6.0	0.3	0.3	0.3		1.3			Tigris R.	
30	2H2	19.1-19.3	18.0	16.2	7.2	18.6	12.6	5.4	0.3	0.3	0.6	9.6	1.2		0.3	0.3		0.3	0.6	6.6			0.3	0.3	1.2			"older" Tigris R.	
16	2H5	7.9-8.0	18.6	9.1	6.3	22.1	18.6	0.9			0.6	7.6	1.6						1.3	8.5				0.9	8.8			Tigris R.	
17	2H5	23.2-23.4	13.4	8.1	6.8	19.2	24.1	1.6		0.3	2.3	9.4	2.0						0.7	9.1				0.7	1.3			"older" Tigris R.	
62A	2G12	14.9-15.0	16.8	7.2	10.5	21.0	22.3	2.1		0.3	0.3	6.0	0.6	0.3				0.3	0.6	5.4		0.3	0.3		5.7			Tigris R.	
60A	2G12	14.0-14.1	19.4	1.2	10.1	6.6	8.9	3.1		0.4		1.9	0.4			0.4				2.3					31.0	13.4	0.8		foothill
60A	2G12	21.0-21.1	14.1	16.6	12.4	26.6	8.6	0.6		0.3	1.1	5.5	0.8		0.3		0.3	0.3	0.6	8.9			0.3	0.5	1.1	0.3	0.3	0.5	"older" Tigris R.
61A	2G12	3.1-3.2	62.4	6.3	4.4	7.5	1.5			0.3					0.6	0.6	0.3	0.9	0.6	3.5				2.2	4.7	0.3	3.8	foothill	
61A	2G12	19.4-19.5	73.7	4.3	2.7	7.3		1.7				0.3				0.3		0.3	0.3	0.7				0.3	0.7		7.0	foothill	
83	2D16		7.4	9.6	8.9	21.5	26.3	2.6		0.4	1.5	16.7	1.7	0.4					0.4	1.1			0.4	0.4	0.7				art. canal
83	2D16		13.3	12.0	11.0	23.0	17.1	2.3		1.0	1.9	9.7	1.3	0.6				0.3	0.3	3.6					2.6				Euphrates R.
83	2D16		15.6	11.4	8.0	27.5	17.4	1.8		0.3	1.2	8.4	0.9	0.3		0.6				4.8			0.3	0.3	1.5				Euphrates R.
84	2D16	3.2-3.4	6.4	5.5	9.4	21.6	31.3	2.2			1.4	15.8	2.2						0.3	1.7					2.2				art. canal
84	2D16	19.3-19.5	6.3	16.4	10.1	32.4	13.0	3.3			2.3	9.7	1.3	0.3		0.3				4.0			0.3	0.3					Euphrates R.
85	2D16	3.2-3.4	5.9	2.2	12.4	15.2	37.5	3.4			1.2	7.1	0.3		0.3				0.3	0.9					11.8	1.2			art. canal
85	2D16	12.0-12.2	12.9	1.8	11.4	14.2	19.9	1.5			0.3	5.5								0.9					23.6	8.0			art. canal
85	2D16	19.5-20.0	13.1	14.3	9.8	25.6	16.1	3.6		0.3	0.9	9.8	0.9	0.3					0.3	3.6					0.9				Euphrates R.
91	2H4	9.3-9.6	13.7	9.2	13.1	20.3	20.3	4.6				3.9	0.6			0.6			0.6	0.6					9.2	2.0	1.3		art. canal
91	2H4	20.0-20.5	7.2	16.1	6.6	15.8	15.6	3.7		0.6	2.9	21.3	1.7	0.9		0.3			0.3	4.6		0.3	0.6	0.6	0.6				Euphrates R.

Table 8. Heavy minerals in the sediments of the deep boreholes between Mahmudiya and Mandali

No. of borehole	map sheet	no. of sample	depth (m)	opaque minerals	clouded minerals	rock fragments	zoisite-epidote group	amphibole common	amphibole brownish	glaucophane	tremolite-actinolite	orthopyroxene	angle dops. augite	titanaugite	pyroxene whitish	rutile	Zircon	apatite	tourmaline	titanite	garnet	andalusite	sillimanite	kyanite	staurolite	chromite	chlorite	biotite	barite-celestite	origin of sediments
DBH 1	2C8	1	22.1-22.2	13.5	17.0	14.7	20.5	10.1	2.3		0.9	0.9	12.1	2.3	1.2							3.2		0.3	0.3	0.3	0.3		Tig.+Euphr. R.	
DBH 1		2	30.9-31.0	13.5	12.6	12.9	28.0	12.3	3.6		0.3	0.3	3.4	0.3	1.1	0.8	0.3		0.3	1.1	7.6	0.3	0.3	0.3	0.3	0.6		res.Mahmudia F.		
DBH 1		3	33.9-34.0	13.0	16.4	10.4	20.7	13.8	5.5		1.2	0.9	7.7	1.7	0.9	0.3			0.3	0.6	4.3		0.3	0.3	0.3	1.7		Tig.+Euphr. R.		
DBH 1		4	44.6-44.8	16.8	14.7	13.2	22.0	17.7	4.2		0.3	0.3	3.9		0.3				0.3	0.6	0.9	0.3	0.3	0.3	4.2	0.3		res.Mahmudia F.		
DBH 1		5	49.6-49.8	14.5	15.4	9.8	19.0	14.8	2.7	0.3	1.2	0.9	5.3	1.5	0.3	0.3	0.3			0.6	9.8	0.3	0.6	0.6	0.3	0.9	0.9		Tig.+Euphr. R.	
DBH 1		6	52.8-53.0	9.2	29.1	14.1	16.4	7.2	1.4		1.2	0.3	12.1	1.3	0.3		0.3				4.0	0.9	0.3	0.3	0.9	0.3	0.9		Euphrates R.	
DBH 1		7	55.7-55.8	20.3	18.9	7.3	12.7	8.7	1.9	0.2	0.7	1.4	16.3	0.9	1.7	0.2	0.2			0.2	6.6			0.2	0.5	0.2	0.7		"older"Euphr. R.	
DBH 1		8	65.9-66.1	14.3	22.8	9.3	24.1	9.8	2.2		0.5	0.3	1.7	0.2	0.5	0.2	0.5			0.2	10.0	0.2		0.8	1.7	0.2			Mahmudia F.	
DBH 1		52	78.7-78.8	17.4	13.3	6.5	23.9	16.5	3.8			0.3	1.8	0.6	0.6	0.3	0.3			0.3	10.6	0.3			0.3	0.3	2.4		Mahmudia F.	
DBH 2	2C12	6	28.1-28.3	16.5	11.0	12.4	18.4	8.5	2.2	0.3	0.8	1.4	17.9	2.5	0.5					0.5	4.9	0.3	0.3	0.3	0.5	0.5			Tig.+Euphr. R.	
DBH 2		7	34.0-31.2	17.4	7.6	12.8	20.2	15.6	2.8		0.3		10.8	1.4	1.0	0.3	0.3			0.3	6.3		0.3	0.3	0.3	0.3	1.7		Tigris R.	
DBH 2		8	45.3-45.5	16.6	10.9	14.3	21.6	11.4	1.3		0.8	0.3	11.7	1.0	0.5	0.3	0.8			0.3	7.0					0.5	0.8		Tigris R.	
DBH 2		9	54.0-54.2	18.6	20.7	13.2	10.7	9.1	1.9		1.1		14.5	1.3	0.8	0.3				0.3	4.8		0.3	0.3	0.3	0.8	1.1		Euphrates R.	
DBH 2		10	62.2-62.4	15.7	6.1	18.5	13.4	22.0	2.6		0.6	1.0	6.1	0.3	0.3		0.3			0.6	6.1	0.3		0.3		5.1	0.3		Mahmudia F.	
DBH 2		11	75.0-75.3	12.0	12.0	11.4	22.0	19.9	6.4		0.3	0.8	6.6	0.3	0.8				0.3	0.3	2.9			0.3	0.3	0.5	2.7		Mahmudia F.	
DBH 2		12	86.6-86.8	17.4	12.8	10.9	14.8	20.3	5.3	0.2	0.5		2.9		0.5	0.2				0.2	2.7		0.2	0.2		9.7	0.2		pre-Quaternary	
DBH 2		32	95.0-95.1	13.0	15.6	12.4	15.4	15.0	1.7			0.6	9.5	1.2	0.9	0.6	0.3				9.5					0.3	3.8		pre-Quaternary	
DBH 2		49	112.4-112.6	17.8	10.3	13.4	19.8	16.4	4.5			0.3	6.2	1.0	1.4				0.3	0.3	5.4			0.3		2.1			pre-Quaternary	
DBH 4	2C16	16	4.5-4.6	21.6	11.2	5.6	24.4	9.6	3.2			1.6	7.2	10.0	0.4	0.4	0.4				2.8					1.2	0.4		Diyala R.	
DBH 4		17	12.9-13.0	8.8	12.3	6.6	19.1	24.8	5.7		2.0	1.1	12.5	2.0		0.3	0.3	0.3			2.8		0.3	0.3		1.1			Tig.+Diyala R.	
DBH 4		18	18.0-18.1	14.2	12.7	6.2	18.5	20.4	7.6		0.4	0.4	9.1	3.6		0.4	0.4			0.4	4.7			0.4	0.4	0.7			"older"Tigris R.	
DBH 4		19	25.8-26.0	22.2	20.1	10.4	14.2	9.5	1.5	0.3		1.5	10.7	2.7	0.3						4.7	0.3	0.3			1.5			"older"Tigris R.	
DBH 4		20	31.8-32.0	16.9	17.9	7.9	16.0	16.3	3.2			1.3	14.4	1.0	0.3						3.8					1.0			"older"Tigris R.	
DBH 4		21	36.8-37.0	18.9	14.6	9.3	21.6	13.6	1.5			0.3	9.6	1.2							7.2					0.3	1.2		"oldest"Tigris R.	
DBH 4		22	41.0-41.2	14.3	11.0	11.9	21.5	18.5	3.3			0.6	4.8							0.6	7.8				0.3	4.5			"oldest"Tigris R.	
DBH 4		23	47.8-48.0	20.3	21.6	9.5	21.2	8.5	2.3		0.3		7.2	2.0						0.3	4.9	0.3		0.3		1.3			"oldest"Tigris R.	
DBH 4		24	51.8-52.0	21.6	31.2	9.3	14.0	9.6	1.3		0.3		2.7	0.3	0.3					0.3	5.3	0.3		0.4	0.4	2.3			Mahmudia F.	
DBH 4		44	65.0-65.2	17.8	39.2	8.6	15.9	3.2	1.0		0.3	0.7	2.3	2.3	0.3	0.3					7.1	0.3	0.3	0.3	0.3	0.7			Mahmudia F.	
DBH 4		45	66.2-66.3	15.0	24.3	8.6	18.9	10.9	1.9			0.6	6.4	3.8							7.6			0.3	0.3	0.9			Mahmudia F.	
DBH 4		54	69.3-69.5	17.0	13.7	4.3	18.7	18.4	3.0		0.3		9.7	0.3	0.7	0.3	0.3			0.3	8.4	0.3		0.3	0.3	0.3	2.7		pre-Quaternary	
DBH 4		55	73.6-73.7	17.6	22.7	8.6	22.9	8.8	2.9	0.3		0.5	2.1	0.3		0.3	0.3	0.3		0.5	11.2	0.3		0.3	0.3	0.3	0.8		pre-Quaternary	

Journal of Geological Sciences	Anthropozoic 25	Pages 31–49	10 figs.	1 tab.	2 pls.	Czech Geological Survey Prague 2004	ISBN 80-7075-613-6 ISSN 0036-5270
-----------------------------------	--------------------	----------------	-------------	-----------	-----------	----------------------------------------	--------------------------------------

Palaeolithic occupation in the Angara region, East Central Siberia, in the context of Pleistocene climate change

Pleistocenní klima a paleolit v údolí Angary ve východní části střední Sibiře

Jiří Chlachula¹ – German I. Medvedev² – Galina A. Vorobyova²

Received January 24, 2003

Key words: Pleistocene, Angara Basin, geoarchaeology, palaeoenvironments

CHLACHULA, J. – MEDVEDEV, G. I. – VOROBYOVA, G. A. (2004): Palaeolithic occupation in the Angara region, East Central Siberia, in the context of Pleistocene climate change. – Sbor. geol. Věd, Antropozoikum, 25, 31–49. Praha.

Abstract: Systematic geoarchaeological investigations at palaeolithic sites in the upper Angara River basin have provided evidence of several stages of early human occupation, with the earliest dating to the late Middle Pleistocene. Besides the cultural and historical implications, the multidisciplinary Quaternary studies have produced information on the past climate variations, the dominant geomorphic processes, the landscape development, and palaeoenvironmental conditions during the Pleistocene of Central Siberia. Palynological and palaeontological records, combined with early cultural data, bear witness to strongly fluctuating Late Pleistocene climatic changes, controlling the territory's habitation potential for early human populations. Reconstruction of the evolutionary pathways and dominant processes in the natural environments, knowledge of the specific material and technological conditions and production levels of the Middle and Late Palaeolithic communities, as well as documentation of climatic events stored in the geological record, are the principal objectives of the current studies.

¹Laboratory for Palaeoecology, University Zlín, 762 02 Zlín, Czech Republic

²Department of Archaeology, Irkutsk State University, 664 000 Irkutsk, Siberia, Russia

Introduction

The history of the palaeolithic occupation of Siberia is emerging as one of the main issues in the study of human prehistory. The upper Angara, Lena, and Yenisei River basins are the principal areas of palaeolithic site distribution, and the related Pleistocene-age geoarchaeological records (e. g., VOROBYOVA and MEDVEDEV 1985, DROZDOV et al. 1990, 1999, MEDVEDEV et al. 1990, DE-REVIANKO et al. 1992, GAI and ANTOSCHENKO-OLENEV 1993, CHLACHULA 2001a, b, CHLACHULA et al. 1994, 2003). The higher density of documented archaeological finds, and the enhanced site visibility along the upper Angara and Yenisei rivers, is due to the large scale erosion of Quaternary sections exposed along the valley slopes of these dammed rivers. Because of the continuity of the erosional processes, the amount of new contextual and chronological data is steadily increasing.

The current geoarchaeological studies in the broader Angara area are aimed at the chronological refinement and the micro-stratigraphical documentation of each of the palaeolithic sites, and the reconstruction of Quaternary environments during particular stages of early human occupation. Multidisciplinary investigations at specific localities include detailed mapping of the local geomorphology, ascertaining the stratigraphical context of archeological records, the spatial-temporal correlation of the deposits, documentation of sedimentary envi-

ronments and dynamics, taphonomic analyses of the associated palaeontological remains, and palaeoclimatic and palaeoenvironmental reconstruction. Detailed studies are the most feasible at the more geologically recent sites, including sections dated to the second half of the late Pleistocene and Holocene, whereas the earlier records are more fragmentary because of their poorer preservation and/or insufficiently dated geological context.

Long-term geoarchaeological research objectives at key palaeolithic sites in this region include the establishment of a uniform methodological framework, and a detailed database recording the Quaternary history of the geological and geomorphological processes and their corresponding sedimentary environments.

The main priorities of the ongoing investigations are focused on reconstructing the past climate changes and the related Quaternary environments, and on the early adaptation and cultural history of the palaeolithic people of north-central Asia. These priorities particularly concern the following:

- (1) The present imbalance of documented geoarchaeological sites located near densely populated industrial centres, along railway corridors, and around large River dams (all of which are areas where the surface cover has been intensely disturbed and surveyed), as opposed to the less documented sites in more remote areas.

- (2) The disproportion between well- and poorly-dated sites. The majority of the latter belong to the final stages of the Late Pleistocene. This must be compensated for by searching for new sites, especially those representing the insufficiently known Middle Pleistocene occupations. The cultural complexes of the early-mid glacial period (Middle and early Late Palaeolithic) also need further investigation.
- (3) The differential preservation of cultural finds within particular, mostly disturbed, geological contexts, and orienting studies toward multi-stratified open-air sites and cave sites.

The aim of this contribution is to summarize the current status and perspectives of the geoarchaeological research at palaeolithic sites in the upper Angara region and the adjacent part of the northern Baikal area, east Central Siberia.

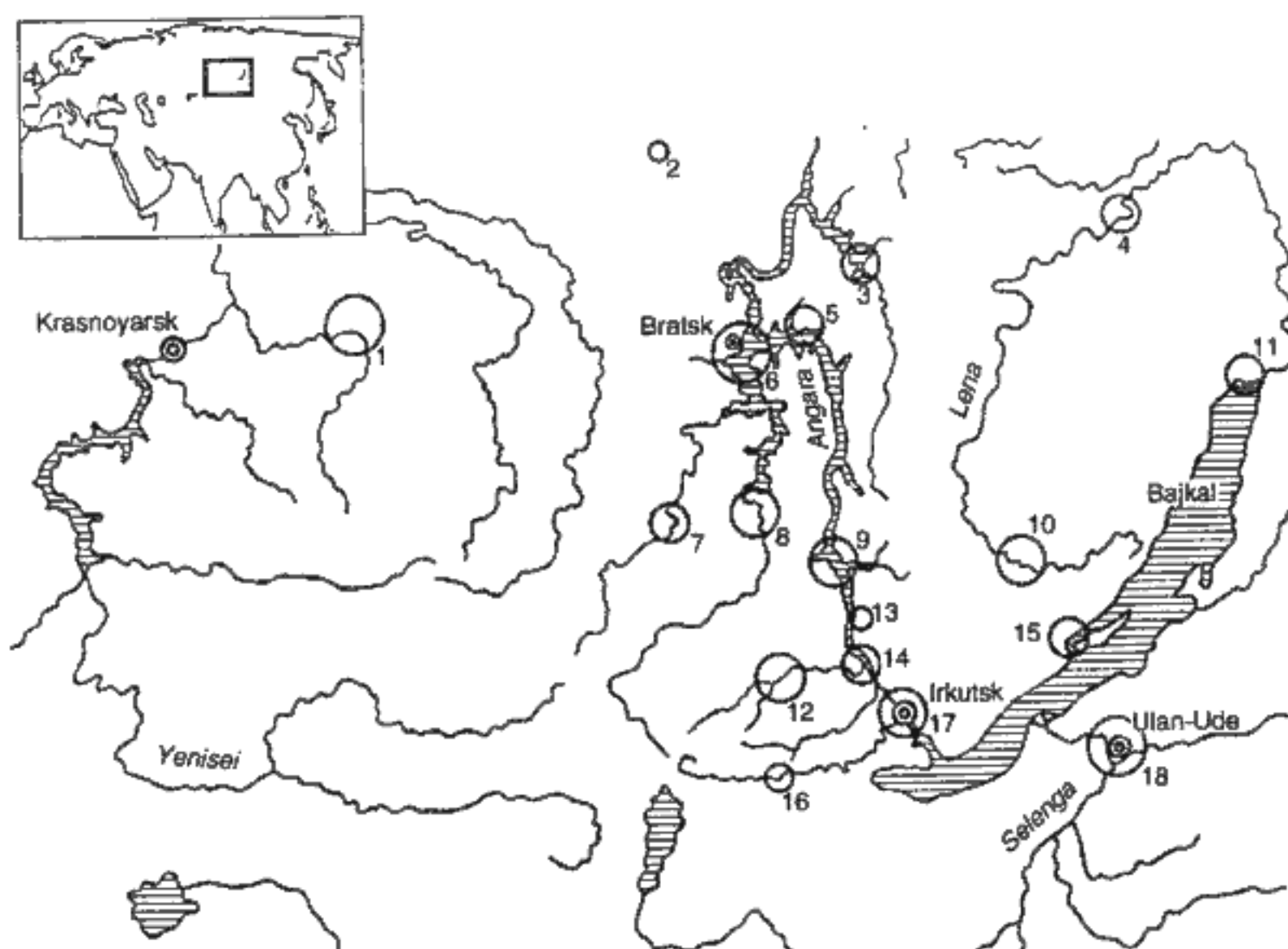
Natural setting*

The study area, located in the eastern part of Central Siberia, is characterized by a combination of major tectonic structures: the Siberian Platform and the adjacent mountain massifs. The southern part of the platform is formed by the Irkutsk Depression, which is geographically confined by the Eastern Sayan Mountains to the

south-southwest, and by the Pribaikal Range (with maximum elevations of 2500–3000 m above sea level) to the east. The central area of the depression contains the Angara-Lena Plateau, with altitudes of 800–1200 m above sea level rising northward toward the Lena River basin (Figure 1).

The base of the Irkutsk Depression consists of igneous and metamorphic rocks overlain by partly lithified sedimentary deposits. Lower Cambrian dolomites and the Upper Cambrian limestones and siltstones are locally exposed along the most active denudation zones. The most distinct pre-Quaternary geological formations are relics of the Palaeogene relief preserved in the form of elevated plateaus, 300–500 m asl, raised by a subsequent orogenic event to about 900 m asl. Apart of these high denudation surfaces, thick Tertiary deposits are buried in old fluvial basins.

Neotectonic activity during the Oligocene and Miocene along the marginal regions of the Irkutsk Basin created a system of depressions that subsequently became filled by palaeolakes (REZANOV 1988, 1994). Renewed tectonic movements in the Pribaikal and West Transbaikal area around the time of the Pliocene/Pleistocene boundary opened the Baikal rift zone (the Baikal Orogenic Phase, lasting from 3 Ma to the present). Deepening of the basin promoted the formation of new drainage systems for the major east Siberian rivers (Angara, Lena, Selenga). This tectonic activity contrib-



1. Geographical location of Central Siberia. Distribution of the principal palaeolithic site areas (polygons) in the Angara Basin, the adjacent part of Lake Baikal, and the Yenisei Basin. 1 – Kanskiy, 2 – Kovinskiy, 3 – Ilinskiy, 4 – Balyshovskiy, 5 – Zajarskiy, 6 – Angaro-Okinskiy, 7 – Tulunskiy, 8 – Sredneokinskiy, 9 – Angaro-Okinskiy, 10 – Kachurgskiy, 11 – Severo-baykalskiy, 12 – Mischelevskiy, 13 – Angaro-Idinskiy, 14 – Mal'tinsko-Buret'skiy, 15 – Olkhenskiy, 16 – Zangisanskiy, 17 – Irkutskiy, 18 – Nizhne-selengiyskiy.

* Editorial note: Because this article refers to Russian territory, the original Russian terms 'Early', 'Middle', and 'Late' Pleistocene were left without change, even though 'Lower', 'Middle', and 'Upper' Pleistocene would be used in accordance with the Czechoslovak Stratigraphical Commission. Czech archaeology employs the term 'Upper' Palaeolithic instead of the Russian 'Late', as well as the 'Late' Palaeolithic instead of the Russian 'Final.'

uted to complex geomorphic processes, which resulted in solifluction and massive alluvial, eolian, and other clastic deposition (MATS et al. 1982). Quaternary deposits fill the broad river basins and valleys, with alluvial, colluvial, and sub-aerial formations being the most extensive (BAZAROV 1986).

The progressive tectonic uplift of the East Siberian mountain massifs, providing lateral support to Lake Baikal's water masses, triggered several catastrophic discharge events. During the Early and Middle Pleistocene, lake water discharge followed a passage through the Irkut River valley, emptying into the Yenisei basin. Reactivation of the orogenic activity during the late Middle Pleistocene resulted in a major Lake Baikal transgression into the Angara River watersheds (REZANOV 1994).

A system of 40–50 m-high river and lake terraces, and adjacent alluvial fans, formed during the Tobolsk (OIS 9) interglacial period, and continued in the following Samarovo (OIS 8) glacial period. The present conditions were established during the Late Pleistocene, as a result of neotectonic movement, which opened an outlet into the Angara River drainage system (KONONOV and MATS 1986).

Tectonics has been a major factor during the entire Quaternary, which, in conjunction with the mountain glaciations, has shaped the geomorphic relief of the broader area. The earliest Pleistocene glaciation in the adjacent area is believed to have occurred in the Middle Pleistocene, correlated with the Samarovo Glacial Period (OIS 8), and evinced by the relics of moraines in the Northern Baikal Range (DUMITRASHKO 1956, POPOVA et al. 1982, REZANOV and KALMIKOV 1999). The most extensive glaciation occurred during the early Last Glacial period (OIS 4), when both the Baikal Mountains and the Eastern Sayan Mountains, bordering the Irkutsk Basin from the east and south, respectively, were covered by glaciers that expanded far into the extra-glacial zone (NEMCHINOV et al. 1999).

The region's present climate is strongly continental, reflecting its geographical location in central Asia and the geomorphic configuration of high mountain ranges that form an orographic, atmospheric barrier, which strengthens the influence of the Siberian Anticyclone. The maximum precipitation falls on the northern slopes of the surrounding mountains (700–800 mm per year), which are covered by dark coniferous (mostly pine) taiga forests. A relatively humid climate prevails along the margins of the Irkutsk Depression, particularly due to the warming effects of the Lake Baikal, with 350–450 mm precipitation per year, and with mixed southern taiga forests largely comprised of spruce, larch, and birch. The interior River valleys are more arid (250–300 mm per year), with open steppes and parkland communities. The average July temperature for the region is +14/+17 °C, while that for January is –20/–26 °C; the mean annual temperature fluctuates around –2 °C.

Quaternary climate change and landscape development

The Pleistocene climate history in the Pribaikal area is a continuation of the palaeoclimatic development that began in the late Tertiary, when intensified early Pliocene orogenic movements initiated the formation of the Baikal rift zone and the progressive uplift of the Eastern Sayan Mountains and the Baikal Range. The interval of the Pliocene/Pleistocene transition was a time of major cooling, as evidenced by the appearance of the first cryogenic features.

The Early and Middle Pleistocene climatic variations are evinced by a wide range of palaeosols (kashtanozems, chernozems, luvisols, brunisols, gleysols), indicating a mosaic vegetation pattern. Interglacial periods were fairly warm and humid, allowing the expansion of mixed taiga parkland forests. However, the progressive climatic deterioration is recorded by the presence of weakly developed initial soils, the solifluction of sediments in areas of increased topographic gradient, cryogenic deformation structures, and relic periglacial and glacial landforms in the surrounding mountains.

The Late Pleistocene climate variations caused major restructuring of the regional landscape, with deep frost bedrock weathering, sediment deposition, solifluction, and cryogenesis during cold stages, and pedogenic development during warm interstadial periods. Renewed tectonic activity contributed to intense river incision, leading to the formation of the present river valleys.

The last (Kazantsevo) interglacial period in the upper Angara region is represented by the Igetei Pedocomplex, which includes two chernozemic soils. In comparison with the present-day soils found in the area, the lower palaeosol (correlated with the OIS 5e substage) is distinguished by a much thicker (1–1.2 m) humic (Ah) horizon, suggesting warmer and more humid conditions with a higher input of biomass into the soil structure (MEDVEDEV et al. 1990, CHLACHULA et al. 2004). The upper chernozemic palaeosol (correlated with OIS 5c) is characterized by a thinner (0.5 m) humic layer with an increased degree of lessivage in comparison to the lower soil (see Plate II/1, 2). A broad variety of landscape settings is indicated by a wide range of fossil soils, including saline soils and grey forest soils. The pollen records, which include warm deciduous species such as oak and lime trees, show a fairly warm and humid climate, much less continental than today (BELOVA 1985).

The onset of the early-last glacial stage (the Murkhtinsk Horizon), correlated with OIS 4, is associated with the intense erosion of exposed land surfaces, leading to the transfer of large amounts of sediments, particularly fine sands from the major denudation areas along the margin of the Irkutsk Depression. Distinct deflation surfaces, in the form of heavily corroded gravelly beds (e.g., 3rd terrace of the Belaya River, the Sosnovyy Bor Site), or truncated interglacial pedocomplexes (the Ma-

karovo IV Site), have been identified in the upper Angara and Lena rivers and their tributary valleys (MEDVEDEV et al. 1990). During the following time interval, some loess and loess-like sediments were deposited as the result of moderate warming, followed by solifluction. Accumulation of massive colluvia (up to 20 m thick) towards the end of the early last glacial stage was apparently triggered by the re-activated regional neotectonic movements.

A major climatic amelioration occurred during the mid-last glacial (Karginsk) interval (OIS 3), with several stages of surface stabilization and soil development. The first half of the interpleniglacial interval (55–40 ka BP) was characterized by a cold and arid climate, as evidenced by deposition of loess and loess-like silty sediments intercalated by initial gleyed soil horizons. The later warm and humid phase (40–24 ka BP) is represented by the Osinsk Pedocomplex, which comprises two chernozemic soils, the lower of which approaches the degree of pedogenic development of the present-day chernozems.

The late-last glacial stage (the Sartan Horizon), chronostratigraphically divided into four phases, is the most well-known Pleistocene time interval in eastern Siberia due to the numerous associated Late Palaeolithic cultural records. The first phase (radiocarbon dated to 24–17 ka BP) is linked to marked climatic oscillations indicated by solifluction and cryoturbation of the latest Karginsk (OIS 3) soils, followed by loess deposition due to a major climatic cooling with the approach of the final glacial maximum. Climatic warming during the following phase (17–16 ka BP) is demonstrated by intensified gleying processes and the degradation of permafrost in the southernmost part of the territory. The initial regosols at the palaeolithic sites of Sosnovyy Bor (Horizon 5) and Krasnyy Yar III (Horizon 2) show evidence of environmental amelioration. A shift towards a cold arid climate during the following phase (16–14 ka BP) is linked with the accumulation of eolian sands and the appearance of cold-climate fauna characteristic of periglacial steppes. The deposition of loess with the formation of humic soil horizons in the upper part of the eolian deposit defines the final Pleistocene warm phase (14–10 ka BP).

The cold Late Pleistocene climatic intervals are indicated by several generations of cryogenic surface deformation, the most prominent of which are located at the contact of the Pleistocene/Holocene formations (correlated with Younger Dryas), and include up to 5 m deep ice-wedge casts filled by early postglacial sediments. Major polygons (5–7 m on average), with up to 3–4 m deep frost wedges, are found on top of the last interglacial palaeosols (particularly the OIS 5e chernozem). Reduced cryoturbation features are documented in earlier deposits. Apart of the frost-/ice-wedge casts, the most intense cryoturbation activity is associated with massive solifluction during the early-last glacial interval (MEDVEDEV et al. 1990).

Palaeontological evidence

Aside from the geological data, biotic (palynological and palaeontological) records provide the main source of information on the Late Quaternary climatic variations as manifested by the particular vegetation and fossil fauna species distribution.

The Late Pleistocene fauna assemblages from the Angara Basin show specific environmental adaptation to changing natural habitats. The typical and, in East Siberia, broadly distributed fossil fauna, including woolly rhinoceros (*Coelodonta antiquitatis*), mammoths (*Mammuthus primigenius*), bison (*Bison priscus*), horses (*Equus caballus*), kulans (*Equus /Hemionus/ hemionus*), giant deer (*Megaloceros giganteus*) and argalis (*Ovis ammon*), indicate a cold periglacial parkland-steppe habitat (VERESHAGIN and BARYSHNIKOV 1984, KALMIKOV 1990, MEDVEDEV et al. 1990).

The small mammalian (rodent) spectra at the Late Palaeolithic localities, with non-analogous communities of co-existing tundra-steppe and taiga species, indicate a mosaic type of landscape (KHENZYKHENOVA 1995, 1999). The taxonomic composition of the palaeontological record from the multistratified archaeological complex at Igetei, where abundant rodent remains (*Spermophilus* sp., *Cricetulus* sp., *Dicrostonyx* cf. *simplicior* FEJFAR and *Lagurus* cf. *lagurus*, etc.) have been found with isolated stone artifacts in a sandy layer below solifluction sediments dated at 24,400 ± 390 yr BP (GIN-5327), attest to a cold and arid tundra-steppe environment.

Specimens of *Mammuthus primigenius*, *Coelodonta antiquitatis*, *Equus* sp. *Cervus elaphus*, *Alces alces*, and other large periglacial fauna species have been recovered from the Late Palaeolithic sites at Buret' (with ¹⁴C date of 21,190 ± 100, SOAN 1680) and Krasnyy Yar (19,100 ± 100, GIN 5530). This palaeontological evidence is characteristic of a cold periglacial habitat (MEDVEDEV et al. 1990). The pollen record from the Buret' locality, which includes *Pinus cembra* (14 %), *P. sibirica* (10 %), *P. diploxylon* (10 %), *Betula* sp. (3 %), *Betula nana* (6 %), *Artemisia* (14 %), and green sphagnum mosses, indicates a tundra-parkland setting.

Five distinct micro-faunal horizons associated with cultural finds have been recorded in the last glacial loess and colluvial deposits at the Malta site in the Belaya River valley, which is known for the Late Palaeolithic art discovered there (OKLADNIKOV 1975, TSEITLIN 1979). The lower horizons (I–III), with ¹⁴C dates of 20,700–21,000 yr BP, yielded remains of *Lagurus lagurus* cf. *henseli* HINT. (70.4 % of the total assemblage), *Ochotona* cf. *pusilla* PALL., *Spermophilus undulatus* PALL., *Microtus gregalis* PALL., *M. oeconomus* PALL., and *M. cf. hyperboreus* VIN. (KHENZYKHENOVA 1999), all of which indicate a cold tundra-steppe habitat. This conclusion is corroborated by other palaeoenvironmental (palaeontological and palynological) data as well (LOGACHEV et al. 1964). The Pleistocene fauna (*Mammuthus primigenius* BLUM., *Coelodonta antiquitatus*

Table 1. Chronology of the principal palaeolithic sites in the Angara-upper Lena area, East Central Siberia

Oxygen Stage	Stratigraphy	Site	¹⁴ C age (yr BP)	Cultural record
OIS 2	Sartan Glacial	Oshurkovo	10,400 ± 500	<i>Early Mesolithic</i>
		Makarovo II	11,400 ± 500 (GIN 480) 11,860 ± 280 (GIN 480) 11,950 ± 50 (GIN 481)	Irkutsk, Kachuga, Baday cultural complexes (13,000–11,000 BP)
		Ust'-Belaya XIV	11,930 ± 230	
		Sosnovyy Bor	12,060 ± 120	
		Verkholskaya Gora	12,750 ± 180 12,540 ± 180 (MO 441)	<i>Final Palaeolithic</i>
		Malta		Verkholskaya Gora,
		Shishkino II	13,930 ± 220	Shishkino, Kurla, Baday,
		Kurla I	14,150 ± 960	Maina, Northern Angara
		Kurla III	13,160 ± 350 13,200 ± 1,200	cultural complexes (16,000–13,000 BP)
		Sosnovyy Bor III		
		Malta	14,720 ± 130	
		Ust'-Kova	14,750 ± 240	
		Krasnyy Yar I–III		
		Sosnovyy Bor IV–V		
		Malta	21,000 ± 21,700 ±	"Classical" Late <i>Palaeolithic complexes</i> (21,000–16,000 BP)
		Krasnyy Yar I	19,100 ± 100 (GIN 5530)	
		Buret'	21,190 ± 100 (SOAN 1680)	
	Igetei Hor. 4	21,260 ± 240 (LE 1590)	<i>Late Palaeolithic</i> (30,000–21,000 BP)	
		23,508 ± 250 (LE 1592)		
		23,760 ± 1100 (SOAN 405)		
		23,780 ± 600 (SOAN 1681)		
		24,400 ± 100 (GIN 4327)		
	Hor. 6	24,400 ± 400 (GIN 5327)		
OIS 3	Karginsk Interstadial Interval	Voenny Gospital	29,700 ± 500 (GIN 4440)	partly <i>in situ</i> in the late Karginsk soil horizons <i>early Late Palaeolithic</i> (40,000–30,000 BP) non-stratified loess deposits without distinct cultural horizons
		Ust'-Kova	28,050 ± 670 30,100 ± 150 32,865 ±	
		Igetei Log III	> 35,000	
		Ust'-Orda		
		Mamony	> 36,000	
		Afontova Gora VI	> 36,000	
		Malta	43,100 ± 2400	
		Gora Igetei		
		Manzyrka		
		Lokomotiv Georgievskoye		
OIS 4	Muruktinsk Glacial	Makarovo IV	> 50,000	<i>Middle Palaeolithic</i> (150,000–40,000 BP) corroded artefacts in slope deposits
		Gora Igetei		
		Georgievskoye		
		Sosnovyy Bor		
OIS 5	Kazantsev Interglacial	Gora Igetei		artefacts in the last interglacial pedocomplex
		Georgievskoye		
		Malta		
OIS 6	Tazov Glacial			<i>Early Palaeolithic</i> (ca. > 150,000 BP)
OIS 7	Shirta Interglacial	Igetei		artefacts in colluviated slope deposits and alluvia
OIS 8	Samarovo Glacial			

BLUM., *Equus caballus* L., *Rangifer tarrandus* L., *Cervus priscus* L., *Bison priscus* BOJ., *Ovis nivicola* ESCH., *Ovis* sp., *Felis spelaea* GOLD., *Canis lupus* L., *Vulpes vulpes* L., *Alopes lagopus* L., *Gulo gulo* L. and *Ursus arctos* L.) documents periglacial forest-tundra and forest-steppe landscapes around the Pleistocene locality (ERMOLOVA 1978, MEDVEDEV et al. 1990). The increased representation of forest species (27 %) in the rodent fauna assemblages (*Ochotona hyperborea* PALL., *Clethrionomys rutilus* PALL., *Myopus schisticolor* Liss.) in the overlying horizons suggests climatic amelioration and a shift towards a parkland-forest setting following the last glacial maximum (KHENZYKHENOVA 1999). The present Holocene rodent fauna is marked by the absence of taxa that are typical of steppe (*Ochotona pusilla* and *Lagurus lagurus*) and tundra (*Lemmus sibiricus*, *Dicrostonyx* and *M. ex gr. hyporboreus-middendorffii*) environments. The trend of environmental change, revealed in the faunal records from about 21,000 to 10,000 yr BP, shows a gradual transition from tundra-steppe and meadow-steppe to forest-steppe, corresponding to a change from a cool and dry climate to milder and more humid conditions in the upper Angara-Lena region.

Finally, apart of the Pleistocene macro- and micro-fauna, fish and bird taxa found at the archeological sites attest to a wide range of biotic variety in the Late and Final Palaeolithic habitats. The best example is from the sediment infillings of frost wedge casts, dated to $12,540 \pm 180$ (MO 441), from Verkholenskaya Gora, which include several species of fish (LOGACHEV et al. 1982).

Geoarchaeological evidence

Geographical distribution

There are more than two hundred Pleistocene-age (palaeolithic) sites in the Pribaikal (upper Angara and Lena) region. All main occurrences are found near the confluences of the Angara River with its main tributaries (the Irkut, Kitoy, Belaya, Ungi, Ida, Oka and Idim River) and some smaller rivers (Ushakovka, Kuda, Ida, Osa). These sites have been identified particularly in places where large-scale erosion has increased exposure along the Angara River following the construction of the Bratsk dam (Figure 1). The river valley is 1–8 km wide in the upper reaches, broadening to 9–15 km farther north. The preserved river terraces, which extend 35–45 m (V) and 50–60 m (VI) above the river, date to the Early and Middle Pleistocene, while the more recent terraces (Late Pleistocene) are currently flooded by the Bratsk Lake (TSEITLIN 1975, 1979).

The area of the principal archaeological investigation is the southern Angara River basin, which extends ca. 300 km northward along the Angara River from its outlet at Lake Baikal to its confluence with the Uda River. Lacustrine erosion caused a lateral slope retreat of

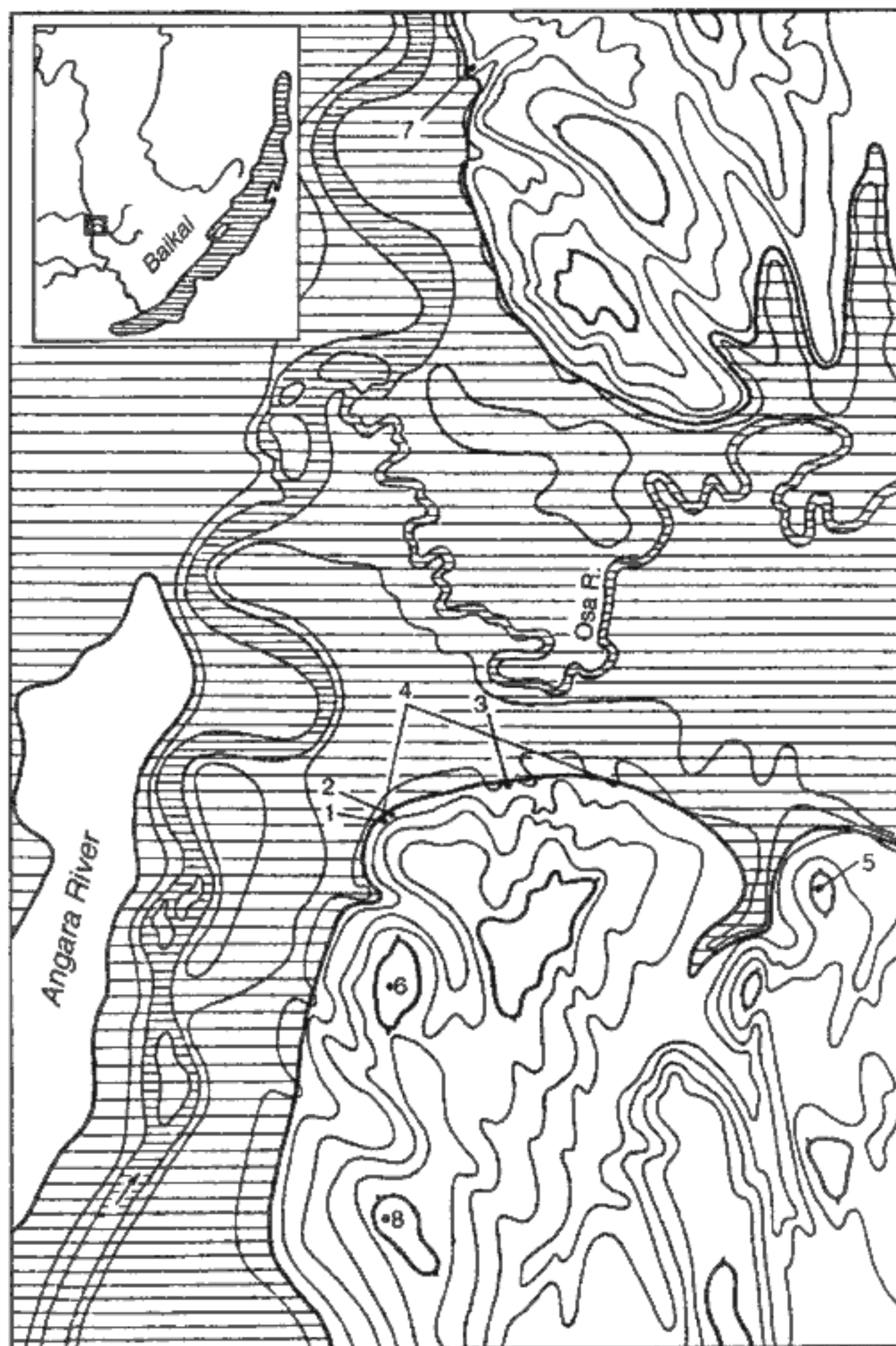
200–300 m along the original valley side, with the present river level raised by 28–30 m above the former floodplain. The thickness of the Quaternary sequence varies with degree of preservation and geomorphic disposition from 2 to 20 m. The most complete, 5–20 m high sections, which comprise a complex series of Quaternary deposits, have been mapped at Igetei near the opening of the Osa River valley (known for its high density of palaeolithic sites) – Igetei, Tara Khay, Khadekhau, Krasnyy Yar, Mel'khytuy, etc. (Figure 2).

The palaeolithic sites in the upper Lena region are concentrated in the northern part of the Baikal Depression and on the adjacent Upper Lena Plateau. The Makarovo IV Site is one of the earliest and most prolific in East-Central Siberia; it is buried in lateral alluvial fan facies (about 3 m thick), on top of colluvial loess deposits (AKSENOV 1981, VOROBYOVA 1987). Other cultural sites occur along the smaller tributary river valleys of the broader Angara Basin.

Geological setting

The palaeolithic sites can be classed into two categories based on their geological settings: exposed and stratified. Among the more than 180 stratified sites, the locations that allow close spatial and chronological correlation are of major significance. The first group includes sections of sub-aerial deposits overlying former river terraces and adjacent slopes. The most representative geoarchaeological complexes occur at Igetei and Krasnyy Yar in the Angara River valley, Malta in the Belaya River valley, Makarovo III–V and Shishkino VIII in the Lena River valley, and Mezensk and Strizhovaya Gora in the Kana River valley (MEDVEDEV et al. 1990; Figure 1). The cultural records found at these sites are from similar stratigraphic positions, which reflects the similarities in the overall stratigraphy of the Quaternary deposits over a broader area. It is expected that a number of other early sites that would allow close chronostratigraphic correlation may be buried at analogous levels in the loessic and sandy sediments.

The second group includes sections of well-stratified, though diverse, geological deposits, displaying rhythmic intervals of sedimentation. The archaeological sites of this group are found in alluvial deposits (e.g., Ust'-Belaya, Gorelyy Les, Kazachka), stratified slope deposit facies (e.g., Sagan-Nuge, Ulan Khada, Tyshkine, Makarovo II), and eolian deposits (e.g., Sosnovyy Bor, Baday V). The cyclic reactivation of sedimentary processes is evinced by an increased number of archeological strata intercalated between sterile layers. The more complex geological structure of this group of sites, as compared to those of the exposed group, suggests unstable, fluctuating, and locally diverse environmental conditions. The effects of regional palaeoclimatic factors are also present, such as the distinct but widely distributed stratigraphic markers of cryogenesis, solifluction,



2. Schematic topographical map of the Angaro-Osinsk Depression, with the locations of the investigated paleolithic sites on the Bratsk reservoir lake-shore.

1 – Igeteiskiy Log I, 2 – Gora Igetei, 3 – Igeteiskiy Log III, 4 – Igetei Beach, 5 – Malyy Tarkhatay, 6 – Gora Lysaya, 7 – Krasnyy Yar, 8 – Gora Stepanova.

and other permafrost deformation features, and of (incipient) pedogenic and loess sedimentation horizons.

Aside from the two groups described above, a third group can be defined as representing cave sites. Despite the relatively high number of caves in the investigated territory, however, none of them can presently be considered as representative sites or type sections because of the absence of long, well-stratified, and dated geological records containing archeological remains analogous to those of the open-air localities.

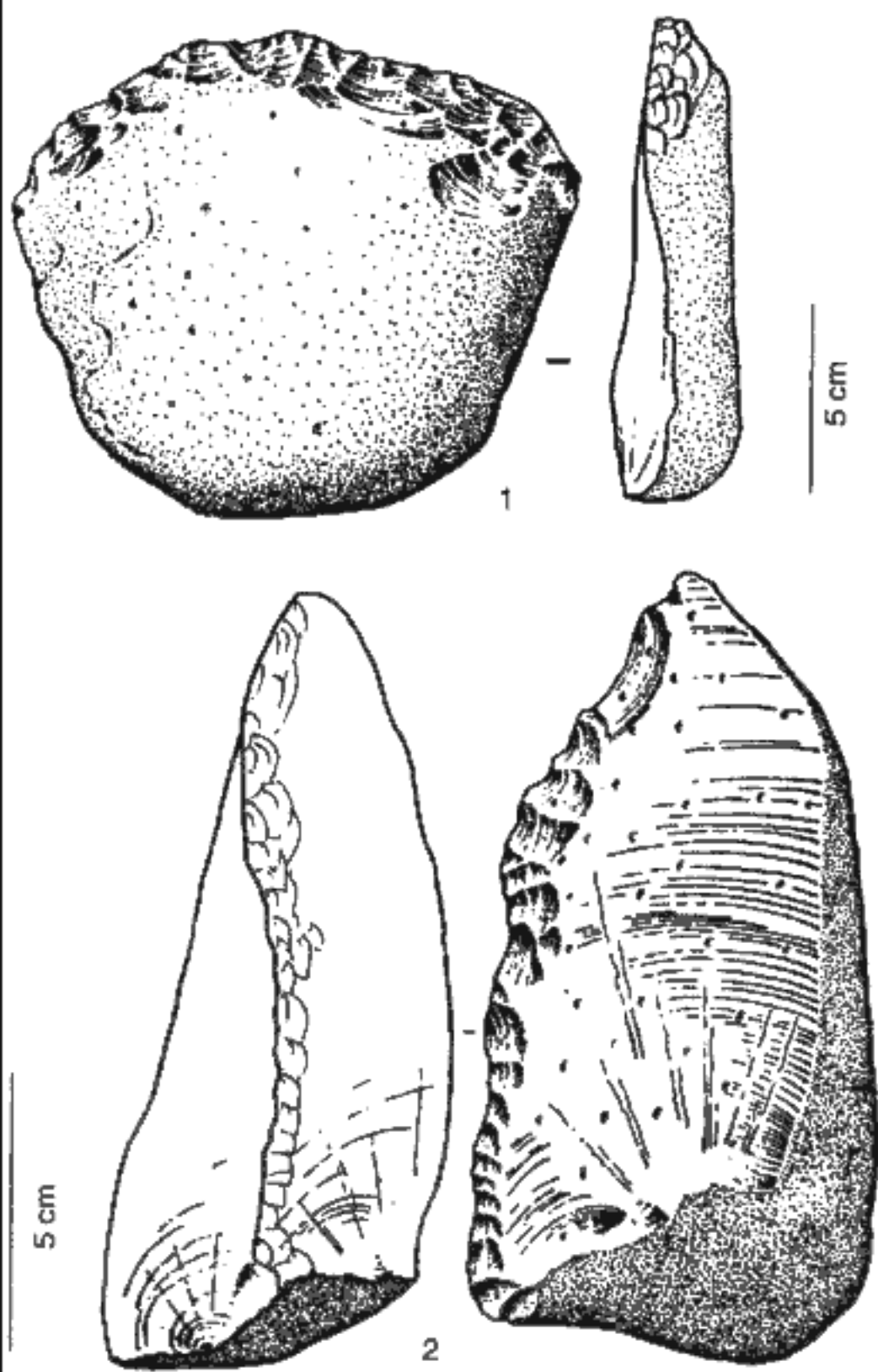
Chronology

The recorded archeological finds can be classified into the following six chronological stages based on their geological position, specific surface texture, stone tool flaking characteristics, and radiocarbon age assessment: 1) the Early/(early) Middle Palaeolithic, associated with the pre-Kazantsevo (> 130 ka BP) deposits; 2) the Mid-

dle Palaeolithic (Mousterian?) from the early-last glacial eolian layers; 3) the early Late Palaeolithic (42/40–30 ka BP) from the mid-last glacial soil horizons (more than 50 sites); 4) the Late Palaeolithic from the late mid- and early-last glacial sub-aerial formation, particularly the intercalated gleyed soil horizons (30–17/16 ka BP); 5) the final Palaeolithic (17/16–12 ka BP) with >10 occupation sites; and 6) the Mesolithic (12–8 ka BP) with > 60 pre-Ceramic Final Pleistocene and early Holocene localities.

Based on degree of corrosion, the highly wind-abraded artifacts are associated with the early-last glacial (Muruktinsk) sandy deposits, the slightly corroded artifacts with the mid-last glacial (Karginisk) loess units, while those with no signs of eolian abrasion are from the late-last glacial (Sartan) colluvial deposits. In the loess region of the upper Angara and Lena River basins and their tributary valleys, about 11 cultural horizons have been recorded within the Late Quaternary formations.

According to the present data, the earliest definite



3. Igetei Site I–II. Retouched quartzite flakes (the Middle Pleistocene series).

Pleistocene cultural sites are associated with old alluvial formations of buried river divide surfaces, exposed locally during recent surface disturbances (mostly caused by the construction of the large river dams). The cultural record chronostratigraphically assigned to the Middle Pleistocene (Igetei, Gora Dolgaya, Gora Glinianaya, Gora Olonskaya, Krivolukshoye) is represented by simple stone artifacts. These have been fashioned from quartz or quartzite cobbles, by a direct striking (clactonian, levalloisian) technique, into a variety of rudimentary forms typical of the Early and Middle Palaeolithic complexes (i.e., choppers, bifaces, scrapers on flakes, prepared cores, etc.; Plate I/2, Figure 3). The flaked surfaces of many of these artifacts have become strongly abraded by subsequent eolian activity. Outside the primary palaeorelief areas in the active geomorphic zones, analogous artifacts often become re-deposited in various Late Pleistocene sediments by subsequent gravity-flow and solifluction processes. Such artifacts may thus become dislocated > 2 km from their original locations.

The earliest archeological records found *in situ* have been documented in the late Quaternary (early Late Pleistocene) formations from the upper part of the last interglacial (OIS 5) pedocomplex in the upper Angara River basin (Gora Igetey, Georgievskoye, Malta; Plate

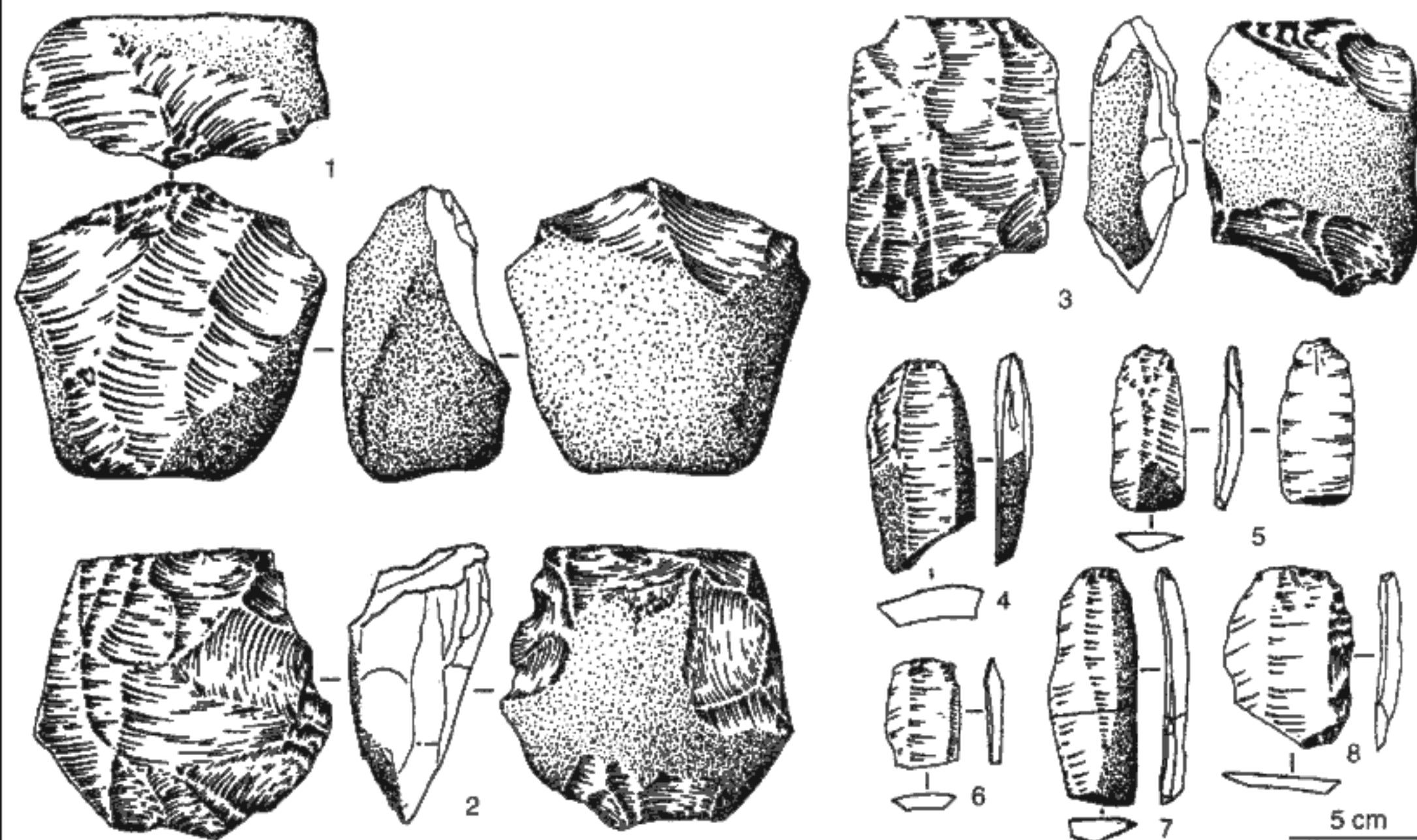
II/1, 2). The stone artifacts, partly affected by eolian activity, were crafted exclusively from local quartzite cobbles from the Middle Pleistocene terraces. Unifacial flaking on flat, partly prepared cobble cores was the primary technique; some of the flakes generated from this process were subsequently retouched into a variety of scrapers, including *déjetés* forms.

The more recent Middle Palaeolithic finds dated to the early-last glacial stage (OIS 4) are chronologically heterogeneous, being located in less distinct stratigraphic contexts and geological complexes (Gora Igetey, Tarakhay, Georgievskoye, Mel'khetyy, etc.). The assemblages from the well-defined Makarovo Complex (Makarovo IV, Sosnoyy Bor, VI, Gora Igetei) are, however, notable exceptions. The associated palaeolithic artifacts have been produced from quartz, quartzite, radiolarite, and argillite. They are further characterized by uniformly flaked blades, including the progressive early Late Palaeolithic forms that were subsequently bilaterally retouched or otherwise modified into end scrapers, burins, and notched/denticulate tools (Figures 4 and 5). All artifacts display eolian abrasion.

At the present time, geoarchaeological finds of the middle last glacial (Karginsk) stage (OIS 3) are inadequately known due to the poor preservation of the geological deposits of this time interval. This poor preservation is the result of intense cryogenetic and solifluction processes, which persisted until the beginning of the late-last glacial (Sartan) stage (OIS 2). Geoarchaeological records from the early part of the interstadial (interpleniglacial) interval are rare (Gora Igetei, Georgievskoye), whereas the more recent deposits (dated to ca. 40–25 ka BP) are relatively numerous and well documented. The principal sites of the latter type include the famous Ust'-Kova Site in the lower Angara region, the Mezinsk Site in the Kana River valley, the Mamony Site in the Irkutsk Depression, the Voenny Gospital Site in the upper Angara River valley (AKSENOV and MEDVEDEV 1968, VOROBYOVA and MEDVEDEV 1985, MEDVEDEV et al. 1990; Figures 6 and 7).

The cultural evidence from the late-last glacial (Sartan) stage (OIS 2) is more representative than that of the previous stages, due to the appearance of typical Late Palaeolithic artifact assemblages in colluvial last glacial slope or loess sediments. The highest density of finds occurs in the initial (early Sartan) interval, associated with horizons of intense solifluction. Apart of these findings, isolated and strongly weathered artifacts, derived secondarily from the Middle Pleistocene terraces and subsequently cryogenically mixed with more recent archaeological assemblages, are also present (Gora Igetei, Igeteiskiy Log I and III, Malta 7, Krasnyy Yar III, Shishkino).

The "classic" Late Palaeolithic is associated with loess deposits and their facial derivatives, which accumulated around the last glacial maximum (21–18 ka BP). The most well studied and representative sites with rich cultural inventories are those at Malta, Buret', Krasnyy



4. Makarovo IV. The Middle Palaeolithic stone industry from the early-last glacial sandy deposits. 1-3 cores, 4-8 blades.

Yar I and Ust'-Kova in the Angara region (OKLADNIKOV 1975, MEDVEDEV et al. 1990). This geoarchaeological complex represents a climax in Siberian palaeolithic development, with advanced blade-oriented reduction techniques, by which a variety of lithic raw materials of a superior quality were processed (quartzite, silex, radiolarite, argillite, diorite, etc.). Aesthetic and religious developments are documented by the appearance of sculptures and other forms of palaeolithic artwork, made from mammoth ivory and bones.

The palaeolithic complexes of the late Sartan stage (18-10 ka BP) contain the highest number of the Pleistocene occupation sites. The corresponding cultural remains are uniformly defined by the appearance of micro-blade stone processing, and related bone-working techniques. These cultural records of the Angara region were previously referred to as "early Mesolithic," and were morphologically classified to the Badayskaya and Verkholskaya cultures (AKSENOV and MEDVEDEV 1968). Nevertheless, the apparent differences in the regional stone industries would seem to reflect a misbalance of data over the large territory, rather than a local stylistic development (Figures 8 and 9). These Central and East Siberian micro-lithic assemblages have close analogues in the Russian Far East, Korea, Japan, and in NW North America.

The typical early Holocene Mesolithic sites (10,000-8,000 yr BP) of eastern Siberia, well documented along the Lake Baikal coast and in the adjacent river valleys (OKLADNIKOV 1975), show minor differences in technological development from the Final Pleistocene micro-blade traditions. Their relatively re-

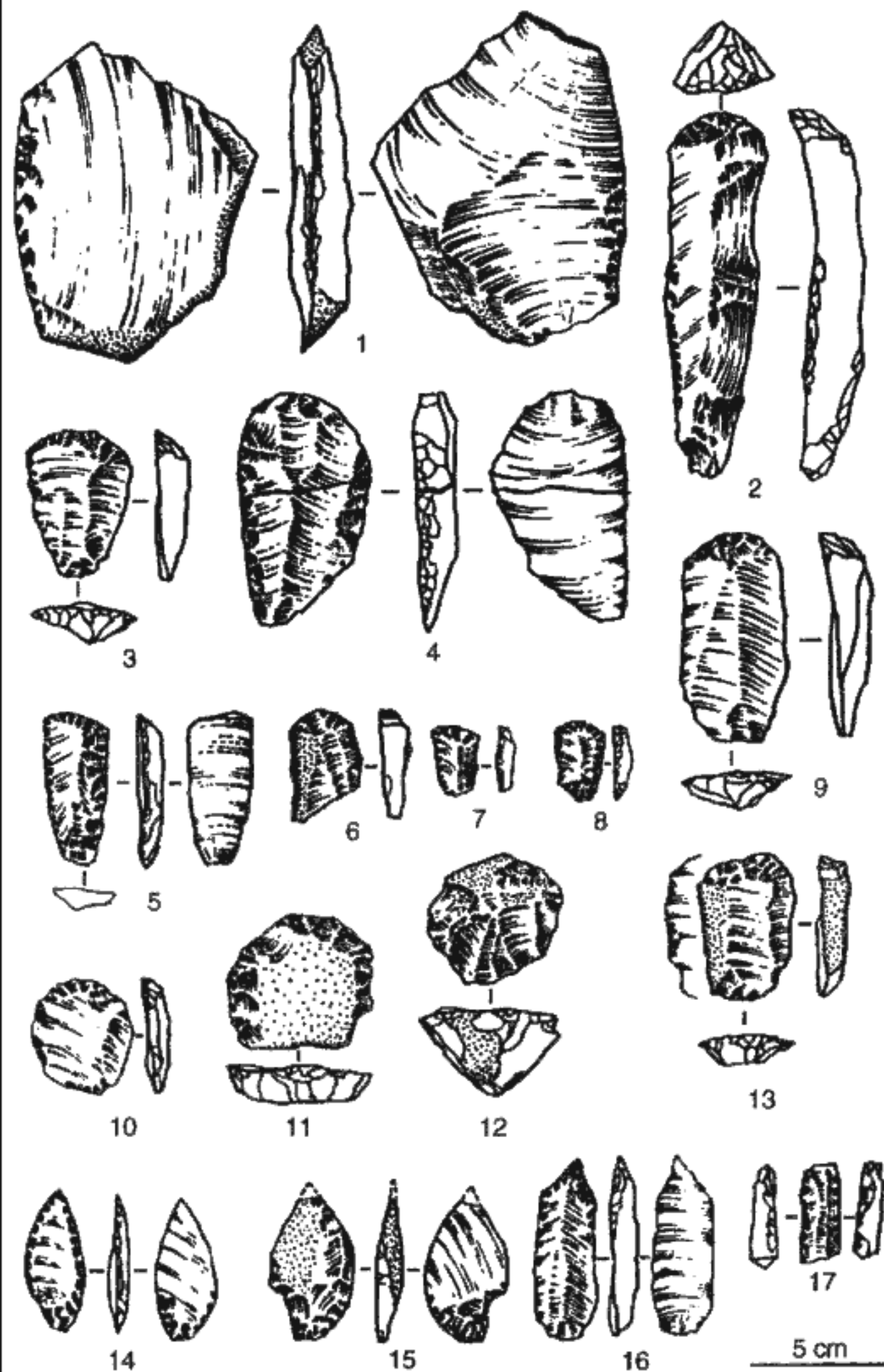
cent age has been determined principally by the identification of taxonomically modern fauna, fragments of pottery, and by corresponding radiocarbon dates. Closer cultural and chronostratigraphic classification of the archaeological records is only possible with high-resolution geological sections that underwent increased sedimentation throughout the time of their formation (Berloga, Ityrkhey, Ust'-Belaya, Strizovaya Gora, Bol'shoy Yar and some other sites). Finally, the later (middle and late Holocene) cultural records are chronostratigraphically well determined by their narrow time span, and principally by the stylistic differences within their archaeological assemblages (pottery, bone and metal artifacts), rather than by their geological context.

The Igetei locality

The Igetei locality has been investigated since the late 1980s. It contains a rich multi-stratified archaeological complex with several palaeolithic levels, and has provided the most important information on early human occupation, as well as the Pleistocene environments and climate history in southern East Siberia during the Late Quaternary (VOROBYOVA and MEDVEDEV 1985, MEDVEDEV et al. 1990, GAI and ANTOSCHENKO-OLENEV 1993).

Site geology

The Igetei locality is the key Late Pleistocene chronostratigraphic site in the upper Angara region. It lies at the



5. Makarovo IV. The Middle/early Upper Palaeolithic stone industry from the early-last glacial sandy deposits.

1 - side-scraper; 2, 3, 5-12, 15 - end-scrapers; 4, 16, 17 - retouched blades; 14, 15 - points.

foot of an elevated platform, which is a relic of an old Neogene weathering surface (150-170 m asl.; Figure 2). Multi-stratified reddish-brown clays at the base of the exposed sections (Plate I/1) represent re-deposited, unconsolidated Lower Cambrian deposits derived from the upper relief elevations, and characterized by a high amount of hematite pigment bound to the clay fraction. The uppermost dark brown layers may be geologically more recent (Pliocene). Large cryogenic polygons, 20-25 m in diameter and up to 2 m deep, found on the elevated Tertiary platform attest to dramatic drops in temperature during the Pleistocene, and the approaching high Arctic conditions.

The Quaternary deposits are 5-12 m thick on average. They are comprised of eolian and solifluction sediments, inter-bedded by fossil soils that were partly re-deposited as pedosediments, and cover the Neogene

formation. The more recent (last glacial) sub-aerial deposits are partly destroyed by slope erosion and former solifluction processes. The buried palaeosols are characterized by a high fine sand fraction, suggesting intense wind activity, and clastic sediments derived from the local Lower Cambrian sandstones. The mineralogical composition of the silty-sandy eolian sediments is dominated by quartz (55-75 %) and feldspar (10-20 %), with some gneiss fragments (2-8 %) and other minerals. The humus content in the palaeosols is 0.7-2.4 %, and 0.3-0.5 % in the loess.

Four main stratigraphic boundaries in the Pleistocene sections have been recognized and delimited by: 1) the contact between the Final Pleistocene and Holocene deposits marked by major cryoturbation; 2) the early-last glacial (Sartan) solifluction horizon associated with the Late Palaeolithic records, radiocarbon dated to $23,700 \pm$



6. Principal Late Pleistocene geoarchaeological sites in the Irkutsk area.

1 – Voenny Hospital', 2 – Arembovskogo Site, 3 – Verkholskaya Gora I-II, 4 – Ushkanka, 5 – Pereselencheskiy Punkt, 6 – Lokomotiv, 7 – Tsar'-Devitsa, 8, 9 – Lisikha.

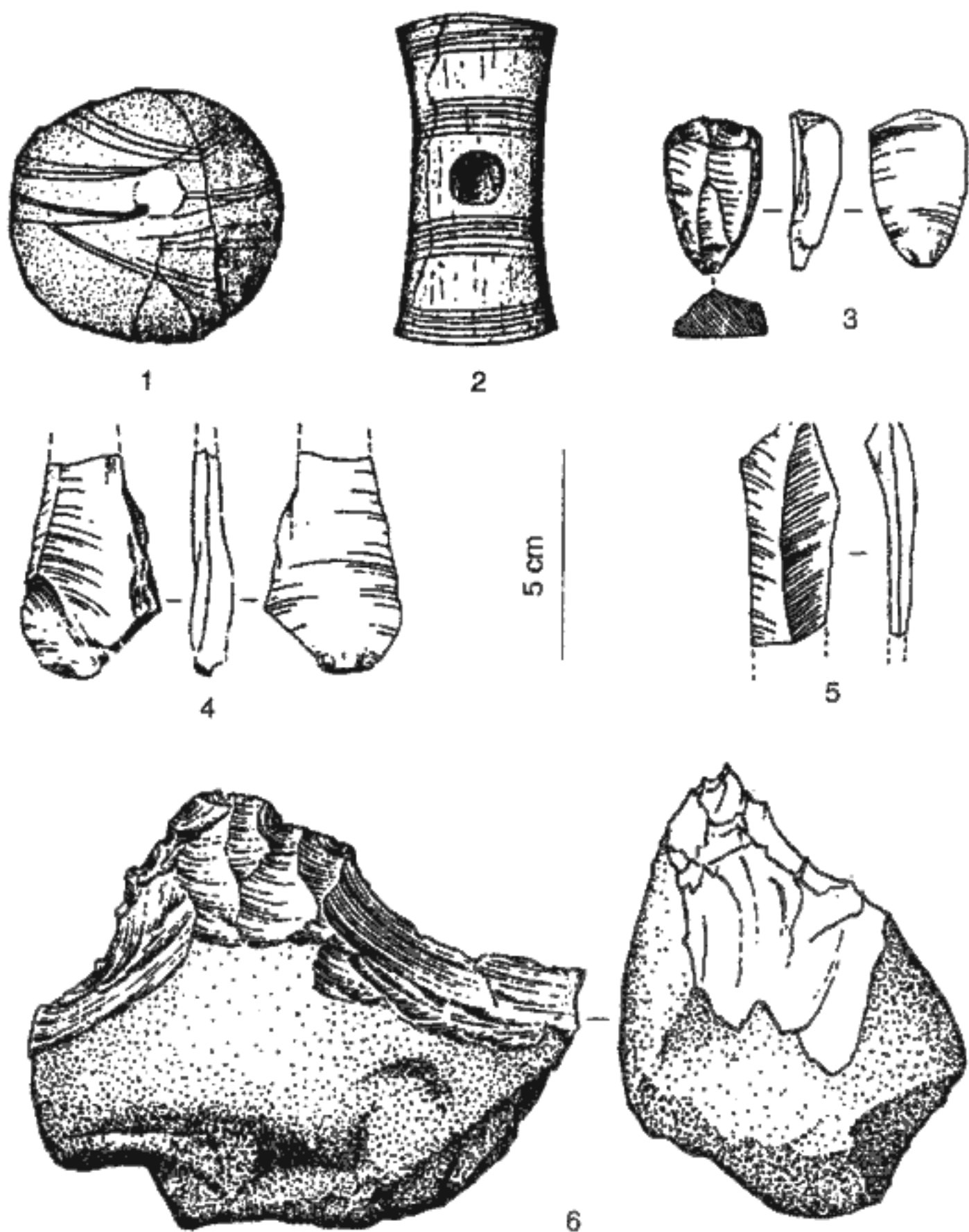
1100 (SOAN 405) and $23,780 \pm 600$ BP (SOAN 1681) in the upper part, and to $24,400 \pm 400$ BP (GIN 5327) in the lower part; 3) the Karginsk (mid-last glacial) cryoturbated chernozem, ^{14}C dated to around 30 ka BP; and 4) the Kazantsevo (last interglacial) pedocomplex, buried 5-8 m below the present surface. The site chronology has been fixed by several ^{14}C dates (MEDVEDEV et al. 1990, ORLOVA 1995), the associated Late Pleistocene fossil fauna records (e.g., *Equus* sp., *Cervus elaphus*, *Coelodonta antiquitatis*, *Mamuthus primigenius*, *Lagurus lagurus*), and the diagnostic Middle and Late Palaeolithic stone industries.

Pleistocene environments

The geological record of the Igetei sections attests to complex environmental variations during the Late Pleistocene. The cyclicity of the pre-Late Quaternary climate change is shown by five levels of buried, but poorly preserved and largely colluviated Early/Middle Pleistocene palaeosols (steppe chernozems or brown forest soils).

Climatic conditions warmer than those during the Late Pleistocene are indicated by a reduced amount of sands in the clay-rich sediment composition, as well as by less developed cryogenic features, and the associated thermophilous malacofauna (*Vallonia pulchella*). Warm and relatively humid natural conditions prevailed during the last interglacial period. This warmer period is represented by the 2–2.5 m thick Igetei Pedocomplex, which includes two chernozemic palaeosols, the lower of which correlates to the climatic optimum (OIS 5e), and is distinguished by a humic horizon up to 1.2 m thick. The thickness of the pedocomplex has been partly reduced due to the subsequent intense solifluction processes of the early-last glacial interval (Plate II/1).

The early-last glacial (OIS 4) climatic variations are indicated by the rhythmic accumulation of up to 8 m of eolian sands, inter-bedded with colluviated silty sediments. Pollen records indicate a cold and dry climate within a periglacial forest-tundra with a high proportion (90 %) of arboreal taxa, dominated by pine (*Pinus* sp. 40–80 %, *Pinus sibirica* 10–30 %, *Pinus cembra* 9–18 %) and some birch (*Betula nana* 2–8 %). A warming phase



7. Voenny Gospital' Site.

1-2 mammoth ivory artifacts, 3-6 - lithic industry from the mid-last glacial (Late Palaeolithic) cultural horizons (according to MEDVEDEV et al. 1990).

in the second half of the glacial stage, during which loess deposition and subsequent pedogenic alteration in the form of embryonic soils occurred, was eventually succeeded by a final phase of a climate deterioration. Slope gravitation processes were thus reactivated, which led to the accumulation of up to 3 m of colluvia in conjunction with renewed tectonic activity.

During the mid-last glacial interval, the Karginsk interstadial (OIS 3), an early cold and arid phase of loess sedimentation (ca. 55-40 ka BP), was followed by a later warm and humid pedogenic phase (40-24 ka BP). This transition caused a major shift in the distribution of vegetation zones, with the northern expansion of mixed taiga forests and the establishment of a climate similar to, and possibly more humid than, that of today. The termination of the warm climatic conditions is fixed by a date of 24,400 ± 400 yr BP (GIN 5327), from the uppermost solifluction horizon above the Osinsk Pedocomplex (MEDVEDEV et al. 1990).

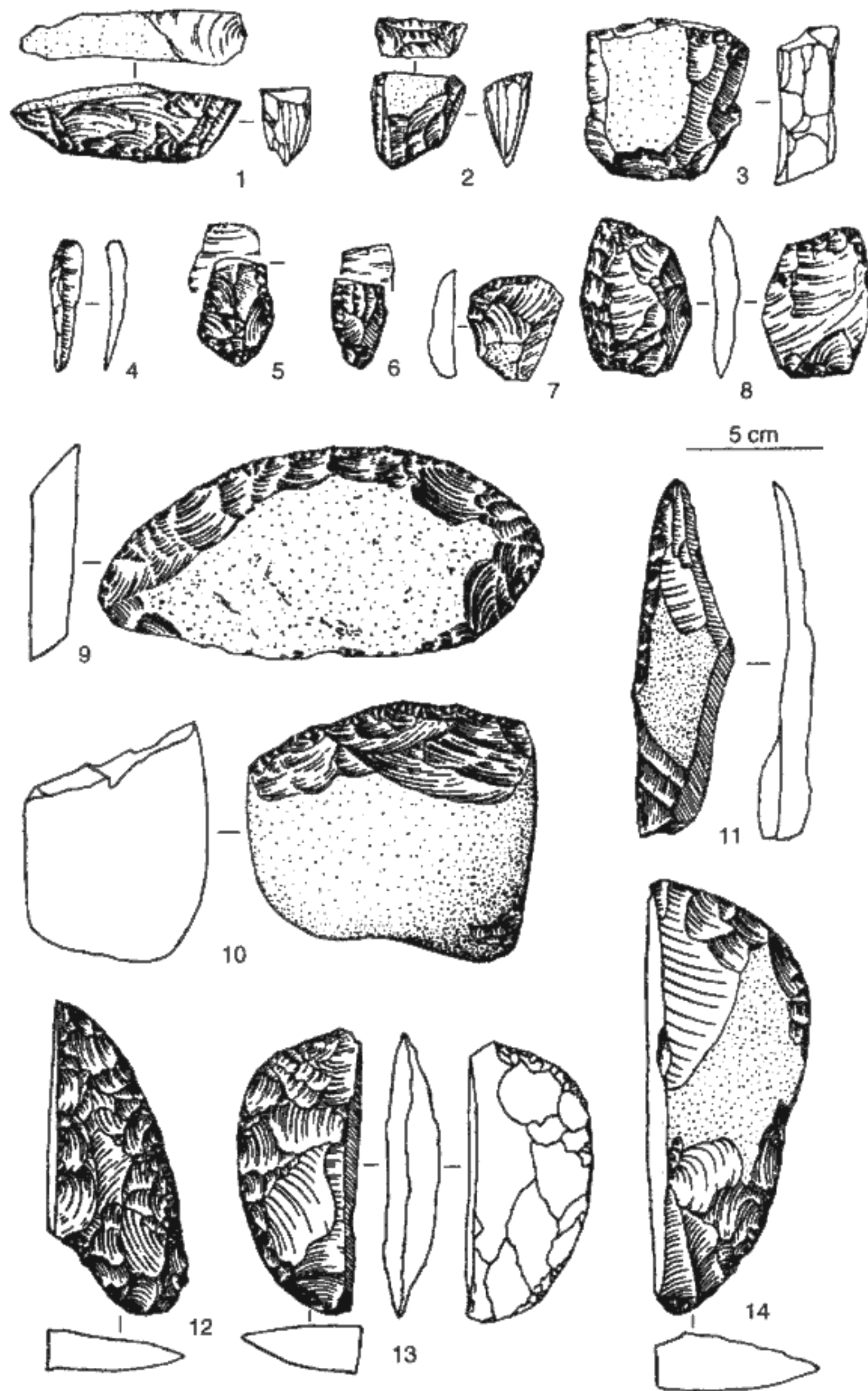
Climatic variations during the early-last glacial (Sartan) stage (OIS 2) in the Igetei sections are demonstrated by three distinct stratigraphic horizons, characterized by intense solifluction, reactivated loess deposition (0.3-0.5 m), and increased sand accumulation (up to 3 m

thick), respectively. The latter unit testifies to the marked intensity of eolian processes around the last glacial maximum.

Site archaeology

The Igetei locality has produced several early cultural assemblages classified as Middle and Late Palaeolithic (AKSENOV and MEDVEDEV 1968, VOROBYOVA and MEDVEDEV 1985, MEDVEDEV et al. 1990). The Late Palaeolithic records (Igetei I) come from the silty sand layers below a solifluction horizon which has been radiocarbon dated, from charcoal specimens, at 23,760 ± 1100 yr BP (SOAN 405), 21,260 ± 240 yr BP (LE 1590), and 23,508 ± 250 yr BP (LE 1592). Based on a bone sample from the upper archaeological unit, ¹⁴C dated at 24,400 ± 100 BP (GIN 4327), the palaeolithic occupation is estimated to have existed between 30,000-25,000 yr BP. The associated lithic industry, which utilized quartzite and siltstone, represents a specific local tradition with progressive prismatic cores and archaic "pebble tools".

The Middle Palaeolithic finds, distinguished by eolian corrosion, were excavated from the sandy sedi-



8. Verkholsenskaya Gora Site (Horizon III). Final Palaeolithic/Mesolithic stone industry (according to MEDVEDEV et al. 1990).

1-3, 6 - microblade cores; 4, 10 - blades; 7 - end-scrapers; 5, 8, 9 - side-scrapers; 11 - chopper; 12-14 - knives.

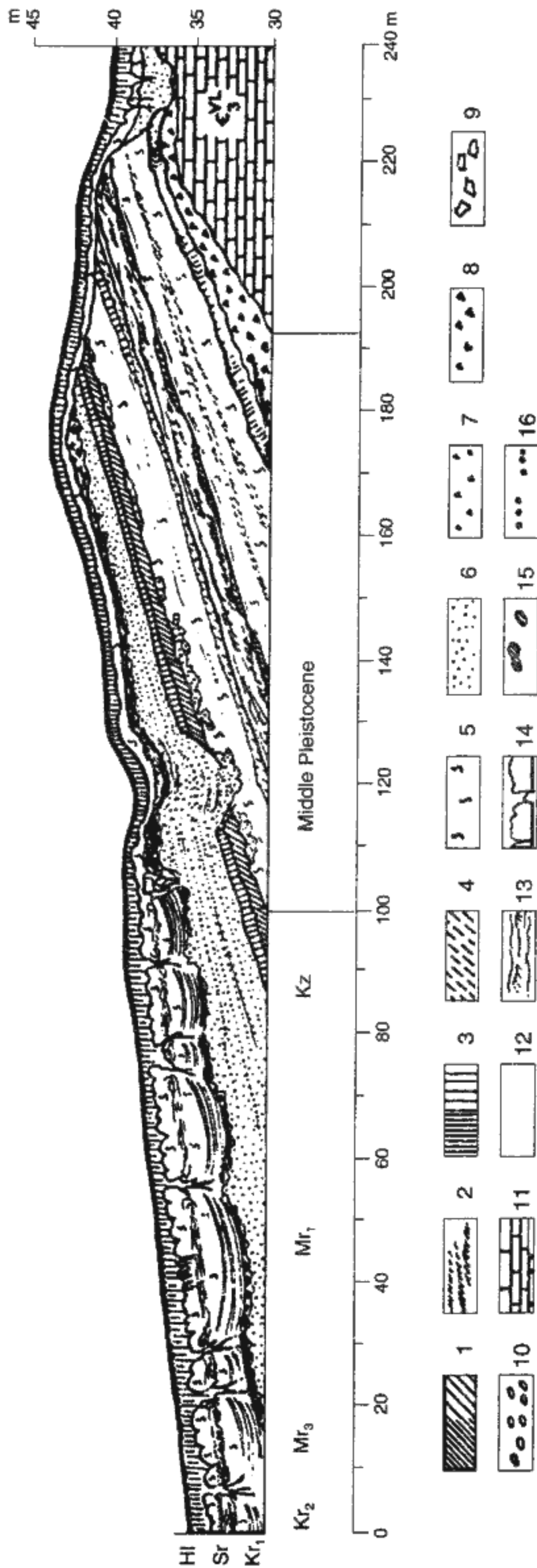
ments above the last interglacial pedocomplex (Igetei III) and the overlying colluviated silty sandy strata. The earliest cultural artifacts, assigned to the Early/early Middle Palaeolithic, are referred to Acheulian-Mousterian tradition, characterized by bifaces, choppers, retouched side scrapers, etc. These have been recovered from the colluviated Middle Pleistocene layers (Plate I/2, Figure 3). In view of the strong wind abrasion textures on individual artifacts, presumably induced during the penultimate (Tazov) glacial period, the age of the earliest cultural assemblage is estimated to be around

200 ka BP (MEDVEDEV et al. 1990, MEDVEDEV and VO-ROBYOVA 1987).

Pleistocene environments and palaeolithic population in the Angara Basin

According to the present evidence, the initial human inhabitation of the Angara Basin is believed to have occurred during the late Middle Pleistocene interglacial

IGETEI SECTION



10. Schematic stratigraphic profile of the Igetei sections. 1 - intact Ah palaeosol horizons, 2 - fragmented (colluviated) Ah palaeosol horizons, 3 - brown palaeosol B horizons, 4 - gleyed horizons, 5 - loess, 6 - sands, 7, 8 - sandy-gravel detritus, 9, 10 - gravels, 11 - bedrock, 12 - reddish (Tertiary) deposits, 13 - solifluction deformations, 14 - frost-wedge casts, 15 - krotovinas, 16 - charcoal; Kz - Kazantsevo/Igeteiskiy pedocomplex (last interglacial, OIS 5e, 5c), Mr - Murutinsk, early last glacial loess (OIS 4), Kr - Karginsk, mid-last glacial pedocomplex (OIS 3), Sr - Sartan, late-last glacial loess (OIS 2), HI - Holocene soil (OIS 1; modified according to MEDVEDEV et al. 1990).

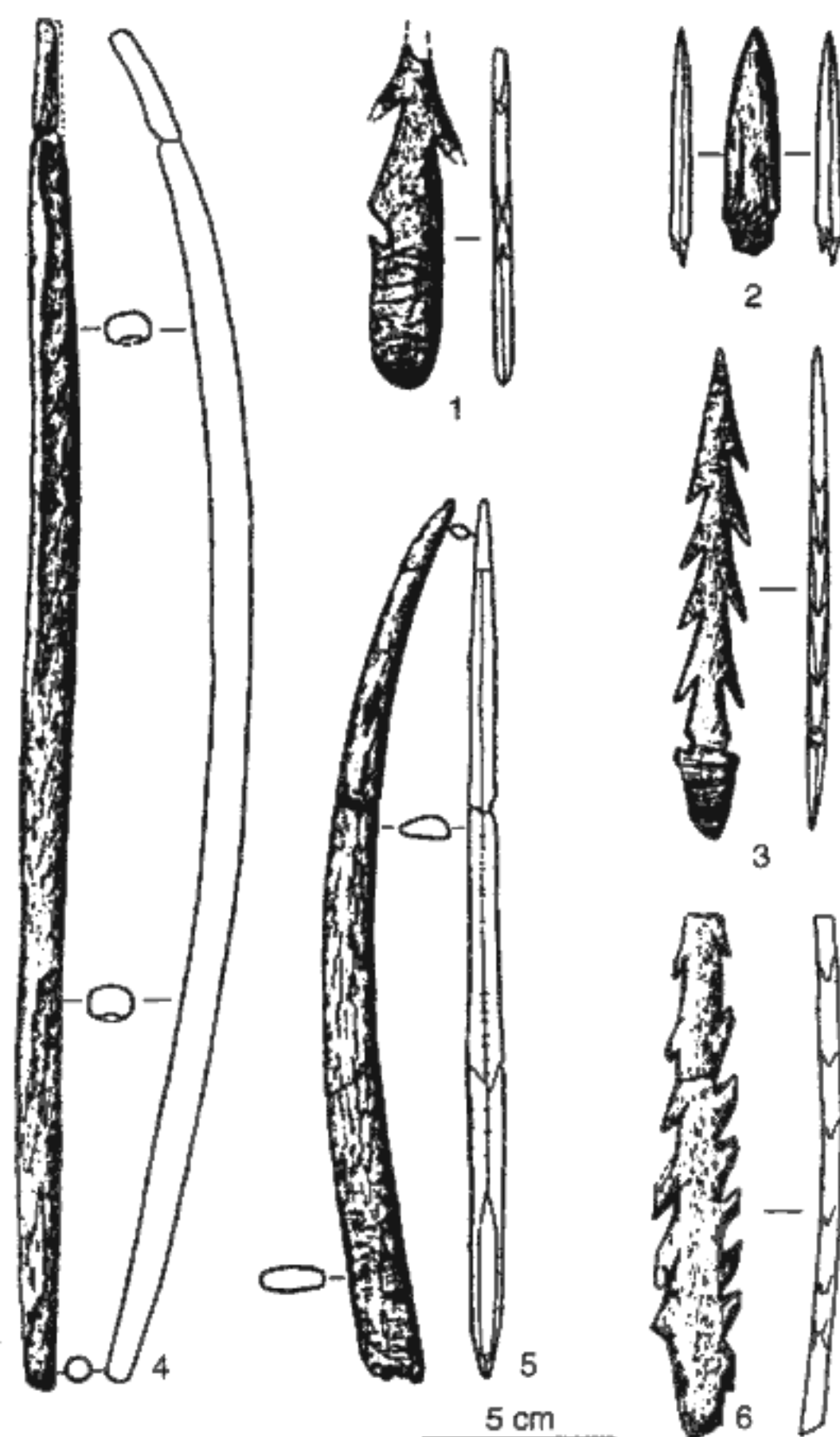
intervals (Tobolsk/Shirta). This time estimate is consistent with the palaeolithic records, and is distinguished by the "pebble tool" industries from other parts of Siberia (particularly from the Yenisei and Lena regions; MOCHANOV et al. 1988, WATERS et al. 1995, CHLACHULA et al. 1994, DROZDOV et al. 1990, 1999, CHLACHULA 2001b).

Pollen data from the Tobolsk Interglacial interval (OIS 9) indicates a precipitation increase of up to 50 % compared to the present time, and an expansion of broadleaved arboreal species (*Quercus*, *Fagus*, *Ulmus*, *Corylus*, *Pterocarya*, *Juglans* and *Tilia amurensis*) and *Tsuga* within the prevailing pine-birch forests (REZANOV 1988, REZANOV and KALMIKOV 1999). Temperate and drier conditions prevailed during the following late Middle Pleistocene Shirta Interglacial interval (OIS 7), characterized by mixed forests dominated by *Pinus*, *Picea*, *Alnus*, *Salix* and *Betula*. Both periods were undoubtedly favorable to early human occupation, particularly in more humid River valleys.

Due to low winter temperatures, human survival in southern Siberia during the late Middle Pleistocene Samarovo (OIS 8) and Tazov (OIS 6) glacial stages must have depended on the knowledge of fire-making. Climatic cooling, leading to expansion of mixed steppe and pine-larch parklands, characterized the onset of the Samarovo (OIS 8) glacial period. A drop of temperature and a progressive increase in aridity during the Tazov Glacial stage (OIS 6) hastened the successive degradation of forests and the extension of open periglacial, tundra landscapes in the broader Baikal area (NEMCHINOV et al. 1999). The marked final Middle Pleistocene environmental deterioration is indicated by the records of cold-adapted fossil fauna from gravelly river terrace formations. This fauna includes more progressive forms typical of open periglacial landscapes, such as *Mammothus primigenius*, *Coelodonta cf. antiquitatis*, *Cervus elaphus* and *Bison priscus*, and glacial landscape relics in the northern Baikal and Eastern Sayan Mountains (KALMIKOV 1990, NEMCHINOV et al. 1999, REZANOV and NEMCHINOV 1999).

The return to a warmer, temperate climatic system during the last interglacial interval (OIS 5) promoted the expansion of a pine-birch forest, which also included some thermophilous taxa of a broad-leaved flora (*Tsuga*, *Corylus*). Chernozemic palaeosols at Malta and Igetei, correlated with OIS 5e and 5c, respectively, and containing Middle Palaeolithic artifacts, attest to warm and temperate conditions within parkland-steppe settings.

Marked cooling, increased aridity, and strong eolian activity that contributed to the accumulation of extensive sandy deposits during the early last glacial interval (OIS 4), are suggested by the intense abrasion of stone tools. It is presumed that the sources of the sands, which cover elevations of 80–100 m, were the drying riverbeds of the major river valleys (REZANOV and NEMCHINOV 1999). The decrease in annual temperatures and the action of strong winds stimulated the drifting of sandy sur-



9. Verkholenskaya Gora Site (Horizon III). Mesolithic bone harpoons (according to MEDVEDEV et al. 1990).

faces and the accumulation of fine, eolian dust on lee slopes in the Angara Basin, thus forming a loess-like series. Palynological data indicate an invasion of sparse pine-birch vegetation dominated by grasses, pointing to a cold and humid climate. A Mousterian occupation, dating to this environmentally harsh interval, is recorded at the Igetei Site III (MEDVEDEV et al. 1990). The succeeding climatic fluctuations towards the end of the early-last glacial stage triggered major solifluction, deriving masses of mixed (pre-)Quaternary deposits from the higher relief platforms, and depositing them in the river valleys (the Igetei and Tarakhai sections). The subsequent cooling is linked to cryoturbation associated with the Middle/early Late Palaeolithic occupation surfaces (Makarovo IV, Sosnovyy Bor, horizon 6).

Major climatic amelioration during the mid-last glacial (Karginisk) interval is demonstrated by several stages of surface stabilization and pedogenic development. Favorable conditions, though more arid than during the last interglacial optimum, led to the expansion of taiga forests and mixed pine-birch parklands. Thermo-

philous taxa (*Quercus*, *Fagus*, *Ulmus*, *Juglans* and *Corylus*), distributed throughout more humid river valleys, testify to a mosaic of occupied habitats. A detailed pollen record exists from the principal occupation site, Voennyi Gospital Site in Irkutsk, which was the first palaeolithic site discovered in Russia in the late 19th Century. This pollen record shows a more humid and relatively warm climate, similar to that of the present. Large fossil fauna (*Mammuthus primigenius*, *Equus caballus*, *Rangifer tarandus*, *Bison priscus* and other species) were intensely hunted by early people, as shown by a number of used bone fragments as well as ivory carvings and bone pendants. The climatic warming caused the transgression of Lake Baikal, which triggered the deposition of alluvial sediments in the river valleys and estuarine deltas at the mouths of the lake's tributaries. A Late Palaeolithic archaeological layer (ESR 34600 ± 3400 yr BP) was found in the middle part of the Karginsk sandy formation (REZANOV and KALMIKOV 1999).

Progressive cooling during the early last glacial stage (Sartan) is indicated by solifluction followed by loess sedimentation. The Baikal Highlands experienced the most extensive glaciation (20–18 ka BP), with mountain glaciers advancing far down into the valleys (REZANOV and KALMIKOV 1999). This time interval, during which vast tundra-steppe covered most of the territory occupied by Late Palaeolithic people, is represented by some of the most well known Siberian palaeolithic sites (Malta, Buret'; OKLADNIKOV 1975, LOGACHEV et al. 1964, TSEITLIN 1979). Severe climatic conditions with sparse vegetation and progressive loess accumulation around the last glacial maximum caused a major decline in the palaeolithic population density in this region. Nevertheless, adaptation to extreme periglacial environments has been documented at the Krasny Yar Site (Horizon 6), where the bones of hunted animals and fossil coal were used as fuels (MEDVEDEV et al. 1990). A periglacial fauna (*Equus caballus*, *E. hemionus*, *Coelodonta antiquitatis*, *Bison priscus occidentalis*, *Cervus elaphus*, *Mammuthus primigenius*, *Megaloceros giganteus*, *Saiga tatarica*, *Alces alces* and other species) attests to a cold tundra steppe environment, widely dispersed throughout the Angara Basin and the Lake Baikal region.

Gradual climatic warming, following the last glacial maximum, facilitated the re-colonization of the eastern Central Siberian region. This allowed a marked increase of the local population by the end of the Pleistocene, represented by early Mesolithic hunters and gatherers.

Summary

The geological, biotic, and early cultural records from the broader Pribaikal area (the upper Angara and Lena River basins) provide evidence of strongly fluctuating Pleistocene climates and the related evolutionary transformations in the local ecosystems. In particular, the loess-palaeosol sections with multi-stratified archaeo-

logical complexes produce the key information on early human occupation, as well as on palaeogeography and climate history in east Central Siberia during the late Quaternary. Tectonic activity promoted large-scale gravity flow processes, resulting in diverse geomorphic zones and geological settings. The associated geoarchaeological sites bear witness to complex landscape development and related natural processes.

Analytical studies of the technological, morphological, and functional attributes of the palaeolithic stone industries indicate a certain developmental similarity with those of European cultures, beginning with the Middle Pleistocene. The principal study objectives of current geoarchaeological research in the Angara-upper Lena sector of Siberia include reconstructing the evolutionary pathways and processes of the natural and social environments, assessing the specific material and technological conditions of Pleistocene human communities, and documenting the climatic events stored in the geological record.

Acknowledgements

The Quaternary geology and geoarchaeology investigations in the upper Angara area (1997–1998) were supported by Irkutsk University, the National Geographic Society, and the Royal Society of London; the latest studies by the NATO Science Programme.

Translated by the first author

Recommended for print by S. Vencel

References

- AKSENOV, M. R. (1981): Investigations of archaeological sites in the Upper Lena region. *Archaeological Discoveries in 1980*. – Nauka, Moskva, 162–193 (in Russian).
- AKSENOV, M. R. – MEDVEDEV, G. I. (1968): New data on the preneolithic period of the Angara region. – *Arctic Anthropology* 5/1, 213–223.
- ANTOSHENKO-OLENEV, I. V. (1982): The History of the Natural Environment and Tectonic Movement in the Late Cenozoic of the Western Zabaikalye. – Nauka, Novosibirsk, 158 p. (in Russian).
- BAZAROV, D. B. (1986): Pribaikal and West Transbaikalian Cenozoic. – Nauka, Novosibirsk, 190 p. (in Russian).
- BELOVA, V. A. (1985): Vegetation and Climate of the Late Cenozoic in Eastern Siberia. – Nauka, Novosibirsk, 160 p. (in Russian).
- CHLACHULA, J. (2001a): Pleistocene climates, natural environments and palaeolithic occupation of the Baikal area, East Central Siberia. – *Quaternary International*, 80–81, 69–92.
- (2001b): Pleistocene climates, natural environments and palaeolithic occupation of the Yenisei area, South Central Siberia. – *Quaternary International*, 80–81, 101–130.

- CHLACHULA, J. – DROZDOV, N. I. – CHEKHA, V. P. (1994): Early Palaeolithic in the Minusinsk Basin, Upper Yenisei River region, southern Siberia. In: *Current Research in the Pleistocene, Special Volume Beringia* (R. BONNICHSEN, Ed.). – University of Oregon Press, Corvallis, 128–130.
- CHLACHULA, J. – DROZDOV, N. I. – OVODOV, N. D. (2003): Last interglacial peopling of Siberia: the Middle Palaeolithic site Ust'-Izhul', the Upper Yenisei area. *Boreas* 32, 506–520.
- CHLACHULA, J. – KEMP, R. A. – JESSEN, C. A. – PALMER, A. P. – TOMS, P. S. (2004): Landscape development in response to climate change in the Oxygen Isotope Stage 5 in the southern Siberian loess region. – *Boreas* 2004/2.
- DEREVIANKO, A. P. – DROZDOV, N. I. – CHEKHA, V. P. (1992): *Archaeology, Geology and Palaeogeography of Archaeological Sites of South Central Siberia (the Northern Minusinsk Basin, the Kuznetskiy Alatau and the Eastern Sayan)*. – Excursion Guide of International Symposium "Palaeoecology and Settlement of Early Man in Northern Asia and America." SB RAS, Krasnoyarsk (in Russian).
- DROZDOV, N. I. – CHEKHA, V. P. – LAUKHIN S. A. – KOL'TSOVA, V. G. – AKIMOVA, E. V. – ERMOLAEV, A. V. – LEONT'EV, V. O. – VASIL'EV, S. A. – YAMSKIKH, A. E. – DEMIDENKO, G. A. – ARTEM'EV, E. V. – VIKULOV, A. A. – BOKAREV, A. A. – FORONOVA, I. V. – SIDORAS, S. D. (1990): *Chronostratigraphy of Palaeolithic Sites of Central Siberia (the Yenisey Basin)*. – Excursion Guide of International Symposium "Chronostratigraphy of Palaeolithic of North, Central, Eastern Asia and America." SB RAS, Novosibirsk (in Russian).
- DROZDOV, N. I. – CHLACHULA, J. – CHEKHA, V. P. (1999): Pleistocene environments and Palaeolithic occupation of the Northern Minusinsk Basin, southern Krasnoyarsk Region. In: *Quaternary of Siberia. Quaternary Geology, Palaeogeography and Palaeolithic Archaeology* (J. CHLACHULA – R. A. KEMP – J. TYRÁČEK Eds). – *Sbor. geol. Věd, Antropozoikum*, 23, 141–155.
- DUMITRASHKO, N. V. (1956): Problems of the origin of Lake Baikal and the glaciation of the Baikal Range. – *Proceedings of the Geographical Institute* 68, 129–146 (in Russian).
- ERMOLOVA, N. M. (1978). *Theriofauna of the Angara River valley in Late Anthropogene*. – Nauka, Novosibirsk, 178 p. (in Russian).
- GAI, P. – ANTOSHENKO-OLENEV, I. V. (1993): *The Palaeolithic Prehistory of the Baikal Siberia*. – *The Review of Archaeology* 14/1, 1–8.
- KALMIKOV, N. P. (1990): Large mammalian fauna of the Pribaikal and West Transbaikalian Pleistocene. – *Proceedings of the Buryat Scientific Centre, Ulan-Ude*, 116 p. (in Russian).
- KHENZYKHENOVA, F. I. (1995): Palaeolithic Micromammalia in the Baikal region. – *Abstracts of The First International Mammoth Symposium, St. Petersburg*, 678.
- (1999): Pleistocene disharmonious faunas of the Baikal region (Russia, Siberia) and their implication for palaeogeography. In: *Quaternary of Siberia. Quaternary Geology, Palaeogeography and Palaeolithic Archaeology* (J. CHLACHULA – R. A. KEMP – J. TYRÁČEK Eds). – *Sbor. geol. Věd, Antropozoikum* 23, 119–124.
- KONONOV, E. E. – MATS, V. D. (1986): History of the Lake Baikal water discharge. – *Geological Survey* 6/C, 91–98 (in Russian).
- LOGACHEV, N. A. – AKSENOV, M. R. – MEDVEDEV, G. I. – SAVELIEV, N. A. – SVININ, V. V. – VOROBYOVA, G. A. (1982): *The INQUA XIth Congress Guidebook for Excursions A-13*. – Irkutsk State Univ. Press, Irkutsk, 55 p.
- LOGACHEV, N. A. – LOMONOSOVA, T. K. – KLIMANOVA, V. M. (1964): *Cenozoic Deposits of the Irkutsk Amphitheater*. – Nauka, Moskva, 195 p. (in Russian).
- MATS, V. D. – POKATILOV, A. D. – POPOVA, S. M. (1982): *Pliocene and Pleistocene of Central Baikal*. – Nauka, Novosibirsk, 192 p. (in Russian).
- MEDVEDEV, G. I. – SAVELIEV, N. A. – SVININ, V. V. (1990): *Stratigraphy, Palaeogeography and Archaeology of Southern Central Siberia*. – AN SSSR, Siberian Branch, Irkutsk, 164 p. (in Russian).
- MEDVEDEV, G. I. – VOROBYOVA, G. A. (1987): Igetei – a key Late Pleistocene section with subaerial deposits and archaeological cultures in southern Siberia. In: *Geology of Cenozoic in southern Eastern Siberia*. – *Conference Proceedings, Irkutsk State University Press, Irkutsk*, 20 (in Russian).
- NEMCHINOV, V. G. – BUDAEV, R. T. – REZANOV, I. N. (1999): Pleistocene glaciations of the eastern Sayan Mts. In: *Quaternary of Siberia. Quaternary Geology, Palaeogeography and Palaeolithic Archaeology* (J. CHLACHULA – R. A. KEMP – J. TYRÁČEK Eds). – *Sbor. geol. Věd, Antropozoikum* 23, 11–15.
- OKLADNIKOV, A. P. (1975): On study of the palaeolithic occupation around the Lake Baikal: "the quartzite Palaeolithic". – *Archaeology of Northern and Central Asia*. Nauka, Novosibirsk, 11–21 (in Russian).
- ORLOVA, L. A. (1995): Radiocarbon dating of the archaeological sites in Siberia and the Russian Far East. In: *Natural Science Methods in Archaeological Reconstructions* (A. P. DEREVIANKO – U. KHOLUSHKIN Eds). – Institute of Archaeology and Ethnography, Novosibirsk, 207–232 (in Russian).
- REZANOV, I. N. (1988): *Cenozoic Deposits and Morphostructure of East Pribaikal*. – Nauka, Novosibirsk, 128 p. (in Russian).
- (1994): On the correlation of the Neogene series of North-Eastern Pribaikal. The Lake Baikal and the surrounding mountains. – *Proceedings of the Institute of the Earth Crust, Irkutsk*, 80–82 (in Russian).
- REZANOV, I. N. – KALMIKOV, N. P. (1999): Palaeogeography of the Pribaikal and Transbaikalian Quaternary. In: *Quaternary of Siberia. Quaternary Geology, Palaeogeography and Palaeolithic Archaeology* (J. CHLACHULA – R. A. KEMP – J. TYRÁČEK Eds). – *Sbor. geol. Věd, Antropozoikum* 23, 43–48.

- REZANOV, I. N. – NEMCHINOV, V. G. (1991): On the palaeogeography of the Eastern Sayan Pleistocene (The Oka Mountain region). In: The Problems of Pribaikal and Transbaikal Cenozoic Geology. – The Buryat Scientific Centre, Ulan-Ude, 24–32 (in Russian).
- TSEITLIN, S. M. (1975). On chronology of palaeolithic sites on the high terraces on the right bank of the Angara River. – Ancient History of Nations of southern Eastern Siberia 3, 37–43 (in Russian).
- (1979): Geology of Palaeolithic of Northern Asia. – Nauka, Moskva, 286 p. (in Russian).
- VERESHAGIN, N. K. – BARYSHNIKOV, G. F. (1984): The Quaternary mammalian extinctions in Northern Eurasia. In: Quaternary Extinctions, a Prehistoric Revo-

- lution (P. S. MARTIN – R. G. KLEIN Eds). – Tuscon, University of Arizona Press, 483–516.
- VOROBYOVA, G. A. (1987): Geology of the archaeological site Makarovo IV. In: Anthropological and Archaeological Problems of the Stone Age of Eurasia. Conference Abstracts. – Irkutsk State University Press, Irkutsk, 21–24 (in Russian).
- VOROBYOVA, G. A. – MEDVEDEV, G. I. (1985): Late Pleistocene sub-aerial deposits and stratigraphy of palaeolithic sites in the southern Angara region. In: Geology and Palaeogeography of Siberia and the Russian Far East. – Irkutsk State University Press, Irkutsk, 71–84 (in Russian).

Pleistocenní klima a paleolit v údolí Angary ve východní části střední Sibiře

(Résumé anglického textu)

JIŘÍ CHLACHULA – GERMAN I. MEDVEDEV – GALINA A. VOROBYOVA

Předloženo 24. ledna 2003

Systematický geoarcheologický výzkum v oblasti horního toku Angary dokládá opakované paleolitické osídlení s nejstaršími nálezy datovanými do pozdní fáze středního pleistocénu. Multidisciplinární kontextová kvartérní studia poskytla kromě kulturně-historických implikací také důležité informace o dlouhodobých klimatických změnách a paleoenvironmentálním vývoji na střední Sibiři. Klimatické variace měly zásadní dopad na intenzitu a geografické rozšíření místního paleolitického osídlení s výrazným ústupem v chladných obdobích. Rekonstrukce evolučních směrů a procesů přírodního prostředí a specifické materiálně-technologické podmínky raně až pozdně paleolitických komunit jsou klíčovými oblastmi současného geoarcheologického studia.

Vysvětlivky k tabulce a obrázkům

Tabulka 1. Chronologie nejdůležitějších paleolitických lokalit oblasti Angary–Horní Leny ve východní části střední Sibiře.

1. Geografická mapa centrální Sibiře s polygony nejdůležitějších paleolitických lokalit v údolí řeky Angary, sousední části jezera Bajkalu a údolí Jeniseje. 1 – kanský, 2 – kovinský, 3 – ilimský, 4 – balyšovský, 5 – zajarský, 6 – angaro-okinský, 7 – tulunský, 8 – centrálně okinský, 9 – angaro-okinský, 10 – kačurgský, 11 – severobajkalský, 12 – mišelevský, 13 – angaro-idinský, 14 – maltinsko-burešský, 15 – olchenský, 16 – zangisanský, 17 – irkutský, 18 – nižněselengijský.

2. Schematická topografická mapa Angaro-osinské pánve se zkoumanými paleolitickými nalezišti podél bratského jezera. Igetejskij Log I, 2 – Gora Igetei, 3 – Igetejskij Log III, 4 – pláž Igetei, 5 – Malij Tarchataj, 6 – Gora Lysaja, 7 – Krasnyj Jar, 8 – Gora Stepanova.

3. Igetei I–II. Retušované kvarcitové úštěpy (střední pleistocén).

4. Makarovo IV. Středně paleolitická kamenná industrie z eolicých sedimentů rané fáze poslední doby ledové (OIS 4). 1–3 – jádra, 4–8 – čepele.

5. Makarovo IV. Středně paleolitická kamenná industrie z eolicých sedimentů rané fáze poslední doby ledové (OIS 4).

6. Klíčové pozdně pleistocenní geoarcheologické lokality Irkutské oblasti. 1 – Vojennyj Hospital, 2 – Arembovskogo, 3 – Vercholenskaja Gora I–II, 4 – Uškanka, 5 – Pereselenčeskij Punkt, 6 – Lokomotiv, 7 – Car-Devica, 8, 9 – Lisicha.

7. Vojennyj Hospital. 1, 2 – artefakty ze slonoviny, 3–6 – pozdně paleolitická kamenná industrie (Karga interstadiál; MEDVEDEV et al. 1990).

8. Vercholenskaja Gora (Horizont III). Pozdně paleolitická/mezolitická kamenná industrie (MEDVEDEV et al. 1990).

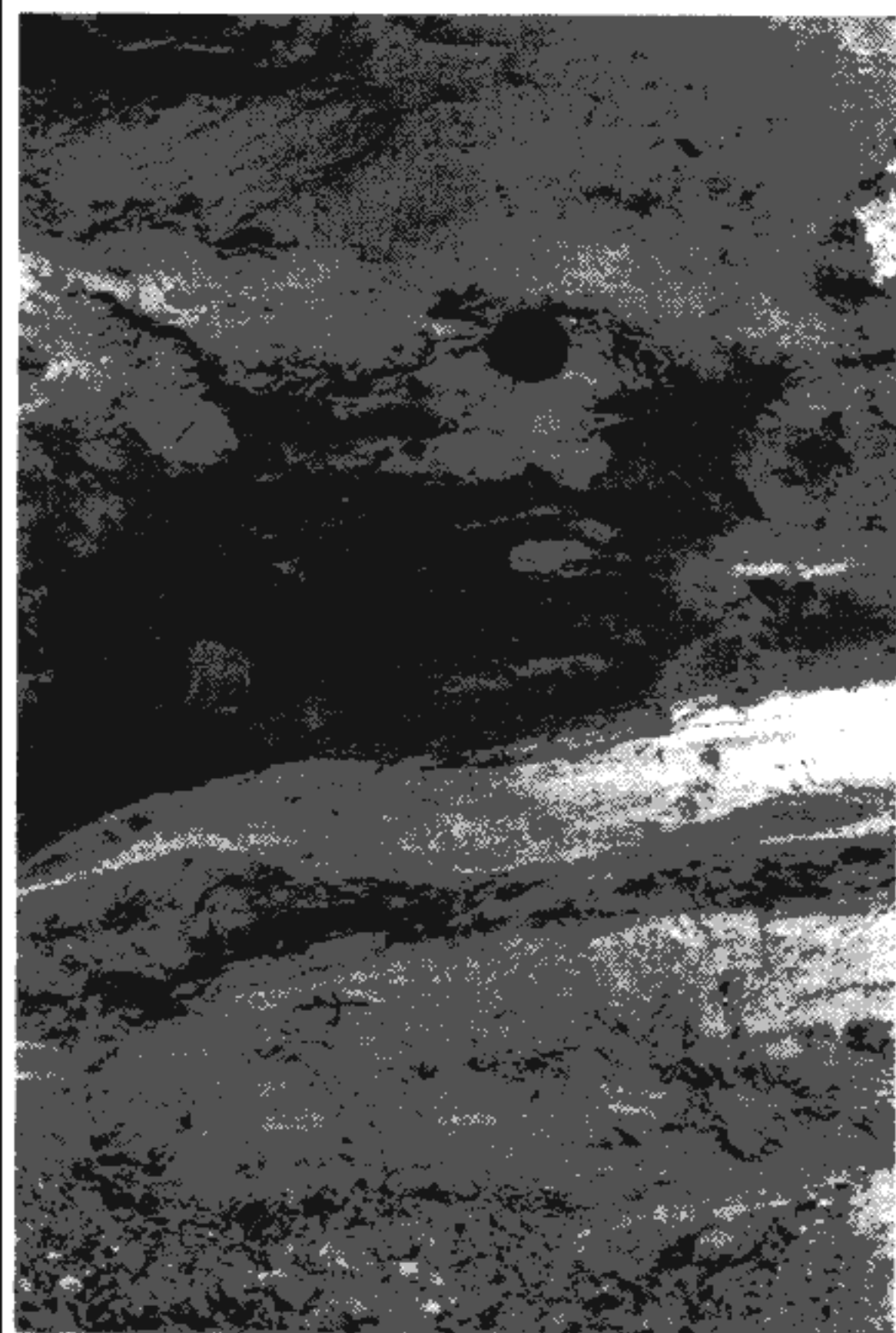
9. Vercholenskaja Gora (Horizont III). Mezolitické kostěné harpuny (MEDVEDEV et al. 1990).

10. Schematický stratigrafický profil profilu Igetei. 1 – intaktní půdní horizont Ah, 2 – svahově splavený horizont Ah, 3 – fosilní půdní horizont B, 4 – glejový horizont, 5 – spraš, 6 – písčiny, 7, 8 – štěrko-pískové sedimenty, 9, 10 – štěrky, 11 – podloží, 12 – terciární sedimenty, 13 – soliflukční deformace, 14 – mrazové pseudomorfózy, 15 – krotoviny, 16 – uhlíky. Kz – pedokomplex Kazancevo/Igetei (poslední interglaciál, OIS 5e, 5c), Mr – Murrakta glaciál (OIS 4), spraš, Kr – Karga interstadiál (OIS 3), pedokomplex, Sr – Sartan glaciál (OIS 2), spraš, Hl – holocenní (OIS 1) půda (upraveno podle MEDVEDEVA et al. 1990).



1. General view of the Igetei (Late Quaternary) sections exposed by erosion on the left bank of the Angara River.

2. Igetei Site I. Middle Palaeolithic artifacts, with fossil faunal remains eroded from the Pleistocene sections, are abundantly scattered on the present beach of Bratsk Lake (the dammed Angara River).



1. A partly colluviated last interglacial pedocomplex at Igetei, with the lower steppe chernozem (correlated with OIS 5e) characterized by a high humus content, charcoal, and numerous krotovinas, overlain by the OIS 5c forest-steppe soil.

2. The last interglacial (OIS 5) pedocomplex at the Malta site, the Belaya River valley, with the OIS 5e chernozem at the base of the section secondarily distorted by frost-wedge casts. Isolated Middle Palaeolithic stone artifacts were found in the upper part of the paleosol (excavation by G. I. Medvedev, 1998).

All photographs by J. Chlachula



Vysvětlivky k přílohám

Příloha I

1. Celkový pohled na pozdně kvartérní profily u lokality Igetei, vytvořené říční erozí na levém břehu Angary.

2. Lokalita Igetei I. Artefakty středního paleolitu s fosilní faunou, exponované erozivní činností přehrazené řeky Angary (bratské přehradní nádrže).

Příloha II

1. Pedokomplex posledního interglaciálu (igetejský profil) se

spodní stepní černozemí (korelovanou s OIS 5e) a svrchní (lesně-stepní) hnědozemní půdou (OIS 5c).

2. Pedokomplex posledního interglaciálu (OIS 5) u lokality Malta (údolí řeky Belaja) s černozemí korelující s klimatickým optimumem (OIS 5e), sekundárně rozrušenou mrazovými pseudomorfózami posledního (?) glaciálu. Ojedinělé artefakty pocházejí ze svrchní části půdy.

Foto J. Chlachula



**SBORNÍK GEOLOGICKÝCH VĚD
JOURNAL OF GEOLOGICAL SCIENCES**

ANTROPOZOIKUM • ANTHROPOZOIC

25

Published by the Czech Geological Survey
Prague 2004
Scientific editor RNDr. Jaroslav Tyráček, CSc.
Editor Mgr. Vlasta Čechová
Cover and layout Hana Pěvrátilová
Computer typeset Mgr. Jana Kušková
Printed by the Czech Geological Survey,
Klárov 3, 118 21 Praha 1, Czech Republic
First edition, 50 pages, 2 plates
03/9 446-402-04

ISBN 80-7075-613-6
ISSN 0036-5270